1971

A Finite Element Model for Two-Dimensional Steady Flow Through Contractions in Natural Channels.

John Thomas Franques Jr
Louisiana State University and Agricultural & Mechanical College

A FINITE ELEMENT MODEL FOR TWO-DIMENSIONAL STEADY FLOW THROUGH CONTRACTIONS IN NATURAL CHANNELS

A Dissertation

Submitted to the Graduate Faculty of the
Louisiana State University and
Agricultural and Mechanical College
in partial fulfillment of the
requirements for the degree of
Doctor of Philosophy

in

The Department of Civil Engineering

by
John Thomas Franques, Jr.
B.S., Louisiana State University, 1965
M.S., Louisiana State University, 1968
December 1971

ACKNOWLEDGEMENTS

The research leading to this dissertation was sponsored by the U.S. Geological Survey, Water Resources Division, under its dissertation support program. Dr. R. A. Baltzer, Arlington, Virginia, served as the Division Scientific advisor. The helpful suggestions of Dr. Baltzer as well as those of the many USGS scientific personnel who helped and encouraged me are deeply appreciated.

The advice and guidance of members of my committee are deeply appreciated. Weekly conferences with Dr. D. W. Yannitell, Co-chairman and research advisor, were particularly helpful.

The programming assistance of Mrs. Janet Borg and the typing and clerical assistance of Mrs. Bobbie Vernon both of the U.S. Geological Survey in Baton Rouge, Louisiana are greatfully acknowledged.

The dissertation could not have been completed without the patience, moral support, and specialty typing of my wife, Patricia.

CONTENTS

TABLES

FIGURES

ABSTRACT

A numerical model is formulated for studying the effects of contractions in natural channels on flood profiles. It is based on Zienkiewicz's finite element technique for solving field problems.

Energy losses at contractions must be evaluated in order to compute water-surface profiles in natural channels. Currently used techniques for computing water-surface profiles rely on empirical formulae for evaluating contraction losses.

The U.S. Geological Survey (USGS) and the Bureau of Public Roads (BPR) have conducted laboratory hydraulic model studies to develop a method for predicting energy losses at contractions. But small scale hydraulic models cannot be designed to achieve dynamic similarity with the flood flow prototypes they represent. Since full scale hydraulic models have not been found economically feasible, numerical modeling seems to be the best approach to the problem.

Recent field measurements made by the USGS in Mississippi verify that the backwater at bridges in wide valleys can be much greater than would be predicted by techniques currently used by the BPR and by the USGS.

The physical flow is here approximated by the steady two-dimensional motion of a turbulent boundary layer. Viscous stresses are replaced by a friction body force which is related to velocity, depth of flow, and hydraulic

roughness by uniform flow formulae. Study is limited to flows of subcritical velocity.

The flow distribution is governed by the following differential equation which expresses equilibrium of torques due to friction forces $\underline{F}$: curl $\underline{F} \simeq 0$. The equation is non-linear since uniform flow formulae such as the Manning equation or the Chezy equation relate friction stress to the square of velocity. The equation can be expressed in terms of a stream function in a form similar to the general linear "quasi-harmonic" partial differential equation; that differential equation also governs the deflections of the elastic membrane. Approximate solutions are found by a successive-approximations algorithm which uses the finite element technique for solving the membrane equation.

Once the flow distribution is determined, the Bernoulli equation can be used to compute water-surface profiles along the computed two-dimensional streamlines. For the steady two-dimensional subcritical gradually varied flow of a turbulent boundary layer, the Bernoulli equation on a two-dimensional streamline is an integral identity of the two-dimensional Euler momentum equation. It can be applied to two-dimensional streamlines that pass through the contraction. The Bernoulli equation is solved numerically for water levels on the computed two-dimensional streamlines by an algorithm based on the step backwater procedure.

Separation of the flow at the abutment of the embankment and its reattachment downstream is studied as a free

boundary problem. A necessary condition for the existance of such separation is that the velocity head at the abutment exceed the head loss due to friction along the free streamline.

The solution algorithms have been applied to a bridge site in Mississippi where the USGS has surveyed high-water marks after two floods. Comparison of the observed water levels with the computed water levels supports the hypothesis that head losses at contractions can be related to friction stress along the computed streamlines. Close agreement was obtained between computed results and field observations with regard to the difference in water level across the approach embankments of the bridge. The surveyed high-water marks also support the validity of the necessary condition for separation. The finite element model is also capable of computing the above normal water levels downstream from contractions that characterize the Mississippi data.

1. INTRODUCTION

1.1 General

The problem of computing the effects of a contraction (including backwater) on water-surface elevations and flow distributions has been the subject of repeated investigation. The Bureau of Public Roads (BPR) has sponsored laboratory investigations as well as data collection programs (BPR, 1970) in an effort to develop techniques for predicting the effects of highway embankments on flood profiles. The U.S. Geological Survey (USGS) has conducted both laboratory investigations and data collection programs of their own and in cooperation with the BPR to develop such techniques (BPR, 1970) (Kindsvater, Carter, and Tracy, 1953). The USGS has the additional interest of obtaining a technique for computing peak discharges at contractions where the peak water-surface elevations are known from high-water marks.

Current techniques for computing water-surface profiles are based on one-dimensional mathematical models. Empirical formulae are usually used to predict the effects of contractions. These formulae are usually based on an analogy between the contraction and a slot orifice or other type of weir (Albertson, et. al. 1950) and/or laboratory hydraulic model studies (Kindsvater and Carter, 1955).

Water-surface profiles near contractions are of importance in evaluating the effects of highway construction on the flood flows it might obstruct. Highway grades must be

designed, and owners of land inundated as a result of the construction may have legal claims to compensation for damages caused them.

Eichert (1970) has surveyed computer programs available for computing water-surface profiles in natural channels; his survey covers leading Federal and State agencies in the water resources field and several universities. The Federal agencies include the U.S. Army Corps of Engineers, the USGS and the BPR. All of the programs which he compares are based on one-dimensional mathematical models and all rely on empirical formulae for computing fall at contractions. The empirical formulae are based primarily on laboratory hydraulic model studies.

Empirical formulae based on hydraulic model studies rely on dynamic similarity between the hydraulic models and the flood flow prototypes they represent. Reynolds' law of dynamic similarity postulates that "two flows can be considered dynamically similar if (1) they have geometrically similar boundaries, and at the same time, (2) the forces acting on the fluid particles at all corresponding positions of the two flow fields have a constant ratio " (Pao, 1967, p. 301).

The Reynolds number N_R is the ratio of inertia to viscous forces acting on a fluid element. It is defined as

$$N_R = \frac{VL}{\nu}$$

where V is the mean velocity in the channel, L is a

characteristic length (usually the hydraulic radius or hydraulic depth for open-channel flows), and ν is the kinematic viscosity (Chow, 1959, p. 7).

In open-channel flow the effect of gravity forces is very important since gravity is usually the principal force causing motion. The Froude number N_F is the ratio of inertia to gravity forces acting on a fluid element. It is defined as

$$N_F = \frac{V}{\sqrt{gL}}$$

where V and L are the mean velocity and characteristic length as defined for the Reynolds number above, and g is the acceleration of gravity.

Dynamic similarity can be achieved only if the Froude number and the Reynolds number are the same for both the flows in the models and the flows in the prototypes they represent. But it is usually not possible to design such small scale hydraulic models particularly if water is to be the fluid for both the models and the prototypes; the kinematic viscosity cannot be scaled. Inspection of the expressions for Froude number and Reynolds number reveal this, since the Reynolds number N_R is linearly related to the characteristic length L and the Froude number N_F is inversely related to the square root of the characteristic length. This nonlinear relationship among Reynolds number N_R, Froude number N_F, and geometry precludes the

possibility of satisfying both the geometric similarity and the constant ratio of forces acting on the fluid elements that is required by Reynolds' law for dynamic similarity. Only if the hydraulic model is built to the same scale as the prototype will dynamic similarity be possible; and full scale hydraulic models have not yet been found economically feasible.

In general, flood flows are characterized by very high Reynolds numbers and low Froude numbers. Many investigators using hydraulic models have chosen to design their models to match the Froude numbers of the prototype flood flows. The resulting Reynolds numbers of the model flows are too low and the effects of viscosity are thus exaggerated.

In the alluvial valleys of the southern states, channel gradients are very mild and the channels meander across very wide flood plains. The flow on the flood plains can represent the major part of the flow for the channel systems. Highway bridge approach embankments are frequently placed so that they greatly constrict the flows on the flood plains. The flood plains in some cases are one mile wide and the bridge openings are frequently over five hundred feet wide. Hydraulic modeling for such field prototypes would require extreme scale factors. The dynamic similarity between such model flows and the flood flow prototypes would be greatly distorted.

Recent field measurements by the USGS in Mississippi verify that under such conditions the backwater effects of contractions can be much greater than can be predicted by conventional techniques. The backwater at Tallahala Creek at State Highway 528 near Bay Springs, Mississippi, during a recent flood was approximately five times as great as the backwater that would be predicted by the USGS technique (USGS, 1955) or the BPR technique (BPR, 1970).

A mathematical model and numerical solution algorithm based on the finite element method are formulated here; they extend the relationships that have been developed and verified for one-dimensional open-channel flow to explain the relationships governing two-dimensional flow in bridge waterways.

The model is intended for use in the analysis of data currently being collected by the U.S. Geological Survey for State Highway Departments in Louisiana, Mississippi, and Alabama in cooperation with the BPR. The USGS has sponsored research on this model under its dissertation support program.

Once the relationships postulated in the model have been verified and calibrated by comparison with surveyed field data collected under the data collection program the model should be very useful for hydraulic design in bridge waterways. Sufficient data is not now available, however, to complete the verification and calibration phase of developing the model.

1.2 Open-Channel Hydraulics

1.2.1 Prismatic Channels

Consider a prismatic channel (unvarying cross-section, constant bottom slope S_o, and linear channel centerline). The total energy per unit weight of water in any streamtube including the free surface through a point (a) on a channel section can be expressed as the total head H in feet of water (Chow, 1959, p. 39):

$$H_a = Z_a + d_a + \frac{V_a^2}{2g} \tag{1.1}$$

where Z_a is the elevation of point (a) above the datum plane. d_a is the depth of point (a) below the water surface measured normal to the datum plane, and $V_a^2/2g$ is the velocity head in the streamtube passing through (a) (see figure 1.1). The total head is frequently computed for the streamline on the free surface using a mean velocity V computed by dividing the total discharge Q by the cross sectional area of the channel beneath the water surface A ; for the free surface $d_a = 0$. The first two terms on the right are measures of potential energy and the third (velocity head) is a measure of kinetic energy. The total energy can be plotted on the channel profile giving a total energy line as shown in figure 1.1. The energy gradient S is defined as the slope of the total energy line. Such a slope indicates a dissipation of energy from the channel system usually due to friction at the channel bottom; for this reason it is sometimes referred to as the friction slope S_f.

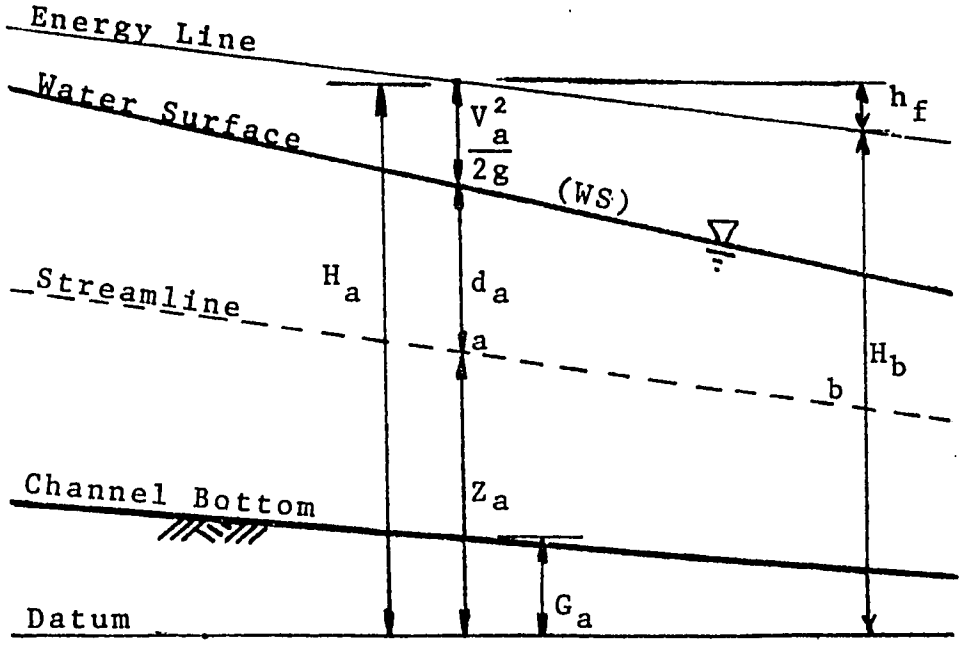

Profile

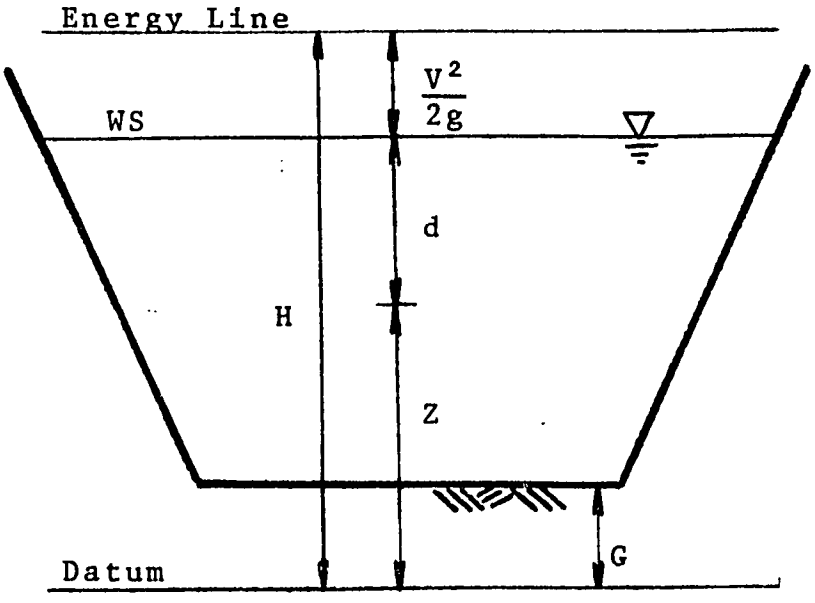

Figure 1.1 -- Schematic Diagram of Free Surface Flow in Prismatic Channel

The head loss due to friction from point (a) to a point (b) is indicated by h_f.

If the slope of the channel bottom S_o, the slope of the water surface S_w, and the energy gradient S, are all equal ($S = S_o = S_w$) then the flow is said to be uniform. Under these conditions an equilibrium has been reached between the rate of dissipation of energy through friction at the channel bottom G and the rate of decrease of potential energy as the fluid moves downstream to lower elevations.

If the water-surface slope S_w, channel-bottom slope S_o, and energy gradient S, are not all equal, then the free-surface flow is described as gradually varying or rapidly varying depending on the magnitude of acceleration components normal to the ground plane. If the acceleration components normal to the ground plane are such that the pressure distribution remains approximately hydrostatic then the flow is gradually varying, otherwise it is classified as rapidly varying. The theory of gradually varied flow is based on the assumption that the energy gradient S of the gradually varied flow at some point in the channel is the same as that of a uniform flow having the same velocity, hydraulic roughness, and hydraulic radius (Chow, 1959, p. 212). Steady flow is assumed throughout the above definitions.

Uniform flow may be subcritical, critical, or supercritical depending on the steepness of the channel bottom. If the slope of the channel bottom is such that uniform

flow will be subcritical, the slope of the channel bottom is said to be mild. Critical and steep refer to channel slopes for which the uniform flow will be critical or supercritical respectively.

1.2.2 Contractions

1.2.2.1 General

Consider now the problem of constricting the flow in a mild channel at some cross section. Such contractions are usually observed to cause a rise in water surface immediately upstream from the contraction. Backwater is defined as the maximum difference between the increased water-surface elevation and the normal water-surface elevation (BPR, 1970, p. 2). The flow upstream from the contraction will be gradually varied; it will approach uniform flow at some distant point upstream. The flow profile upstream is known as the backwater curve or M1 curve. It occurs when the water surface at the downstream end of a long prismatic channel of mild slope is raised above its normal depth (Chow, 1959, p. 228).

1.2.2.2 Measurement of Backwater and Fall at Contractions

Figure 1.2 illustrates the configuration of backwater. Field measurements made by the USGS on bridges where the flood plains on each side of the main channel were no greater than twice the bridge length b and hydraulic roughness was relatively low indicate that the elevation of the water surface throughout areas ABCD and AEFG will be essentially the same as at point A (BPR, 1970, p. 25).

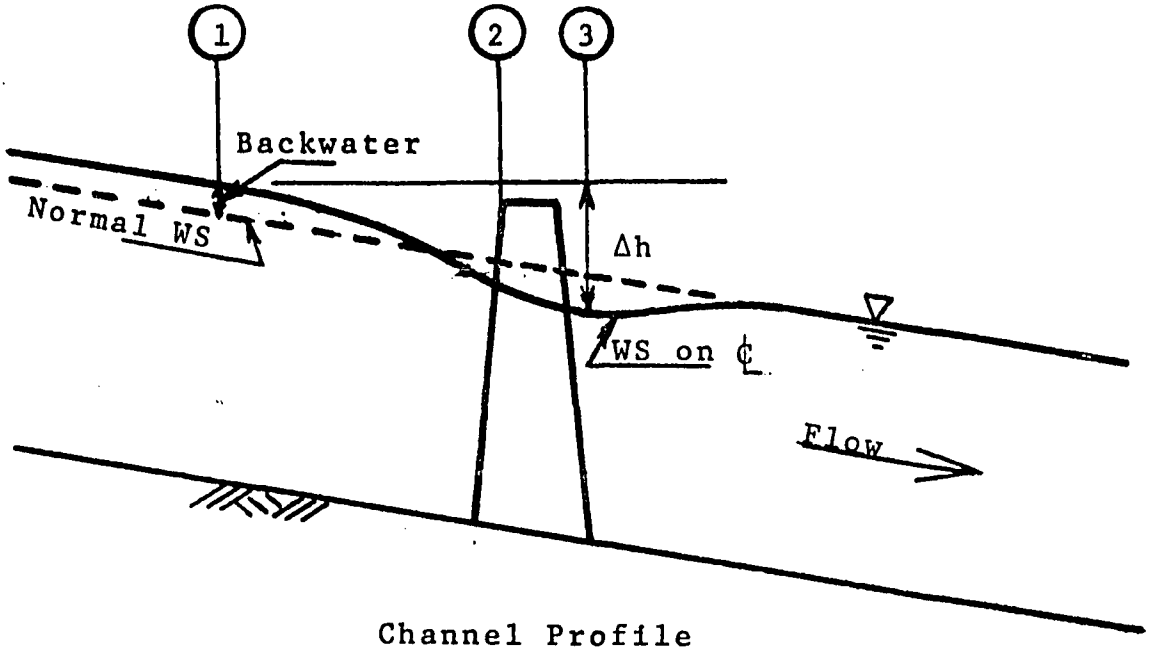

Channel Profile

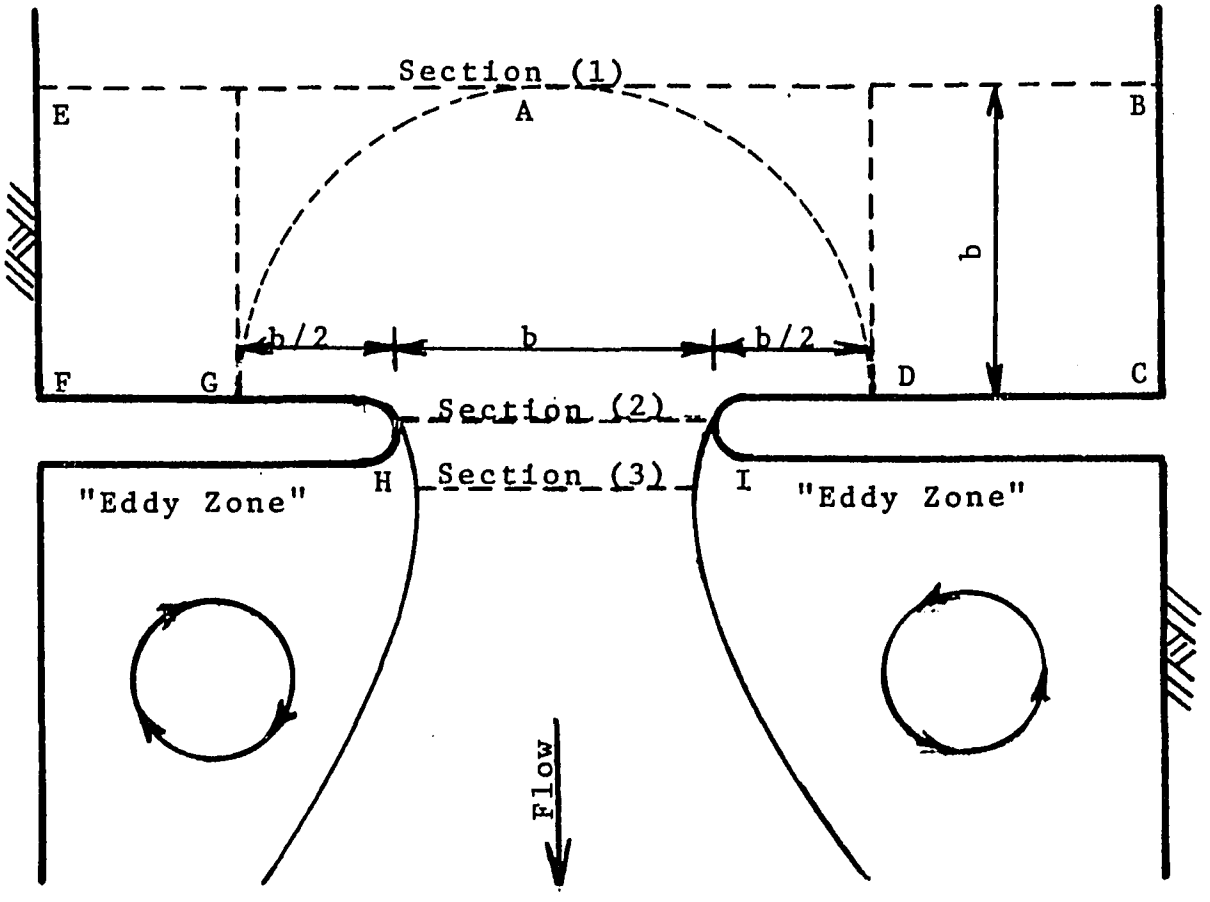

Figure 1.2 -- Configuration of Backwater

At section (1) the difference between the actual water surface elevation and the normal water-surface elevation is maximum. That difference was defined above as the backwater. Since the normal water surface is usually not observable, the backwater cannot usually be measured. The difference in water level across the embankments Δh can be measured from observations on the actual water surface alone. That difference Δh will be referred to as the fall. The fall includes the drawdown on the downstream side of the embankment. The fall is defined by the BPR (1970, figure 12, p. 21) as the difference between the water level along the banks at section (1) and the water level on the centerline at section (3). The BPR has also published curves for determining the distance to section (1) measured from the water line on the upstream side of the embankment (BPR, 1970, p. 25).

Measurements of the water surface at section (1) may not be easily obtained during floods and the location of section (1) itself may not be certain. A common practice is to mark the water surface at points D, G, H and I (see figure 1.2). Points D and G are taken one half of a bridge width from the abutments. One bridge width is considered a good approximation for the distance to section (1) and the water levels at D and G are considered to be the same as at A. The zone of drawdown near the contraction is approximated as a semicircle of radius one bridge width. The fall is then recorded as the difference between the

average of the upstream water levels marked at D and G and the average of the downstream water levels marked at H and I. It should be noted, however, that the water levels at H and I will usually be lower than the water level on the centerline at section (3). (Kindsvater, Carter and Tracy, 1953, figure 3, p. 4). The procedure described here, however, is the one apparently used by the USGS for measuring the fall at bridge sites. In particular, the technique described was the one used to obtain the measured fall at Tallahala Creek at State Highway 528 near Bay Springs, Mississippi tabulated by the BPR (1970, Table B-2, p. 102).

In summary, there are two common definitions of fall Δh. The first is posed by the BPR (1970, p. 21); it is probably the most useful for the purpose of plotting water-surface profiles; but it involves a centerline water-surface measurement which is difficult to obtain. The second is inspired by field practice; it uses water levels at the abutments of the bridge opening as a measure of water level on the downstream side of the embankment which can usually be obtained from high-water marks or can easily be marked during the flood. Fall defined by the second definition will usually be greater than the fall defined by the first since the water level is usually higher on the centerline of the contracted section than on its edges (Kindsvater, Carter, and Tracy, 1953, figure 3, p. 4). Both definitions are based on the hypothetical water-surface configuration illustrated in figure 1.2 and described above.

1.2.2.3 Prediction of Backwater at Contractions

As mentioned above, there is no reliable method for predicting backwater or fall at contractions. And there has been little investigation into the mechanics of backwater at bridges.

The mechanics of backwater at bridges has most recently been treated by Laursen (1970). Laursen distinguishes four zones in describing flood flow through a contraction (see figure 1.3). Zones I and IV are described by Laursen as zones of gradually varied "accretion" and "abstraction" respectively where water moves between the central channel and the flood plain. Zones II and III are described by Laursen as zones of "rapidly varying" acceleration and deceleration respectively.

Both Laursen (1970) and Kindsvater, Carter, and Tracy (1953) refer to the separation of flow downstream from the contraction. The flow separates as it passes through the opening into a live stream or "jet" and an "eddy zone" just downstream from the contraction; the flow reattaches with the bank some distance downstream (see figure 1.3). Laursen recognizes a loss of kinetic energy due to the rapid deceleration and expansion of the live stream; he computes that loss from formulae recommended by Albertson et. al. (1950). Albertson's formula is based on laboratory experiments with a slot orifice. Neither Laursen (1970) nor Kindsvater, Carter and Tracy (1953) are clear with regard to the degree of stagnation or the mechanism of the "eddy zone".

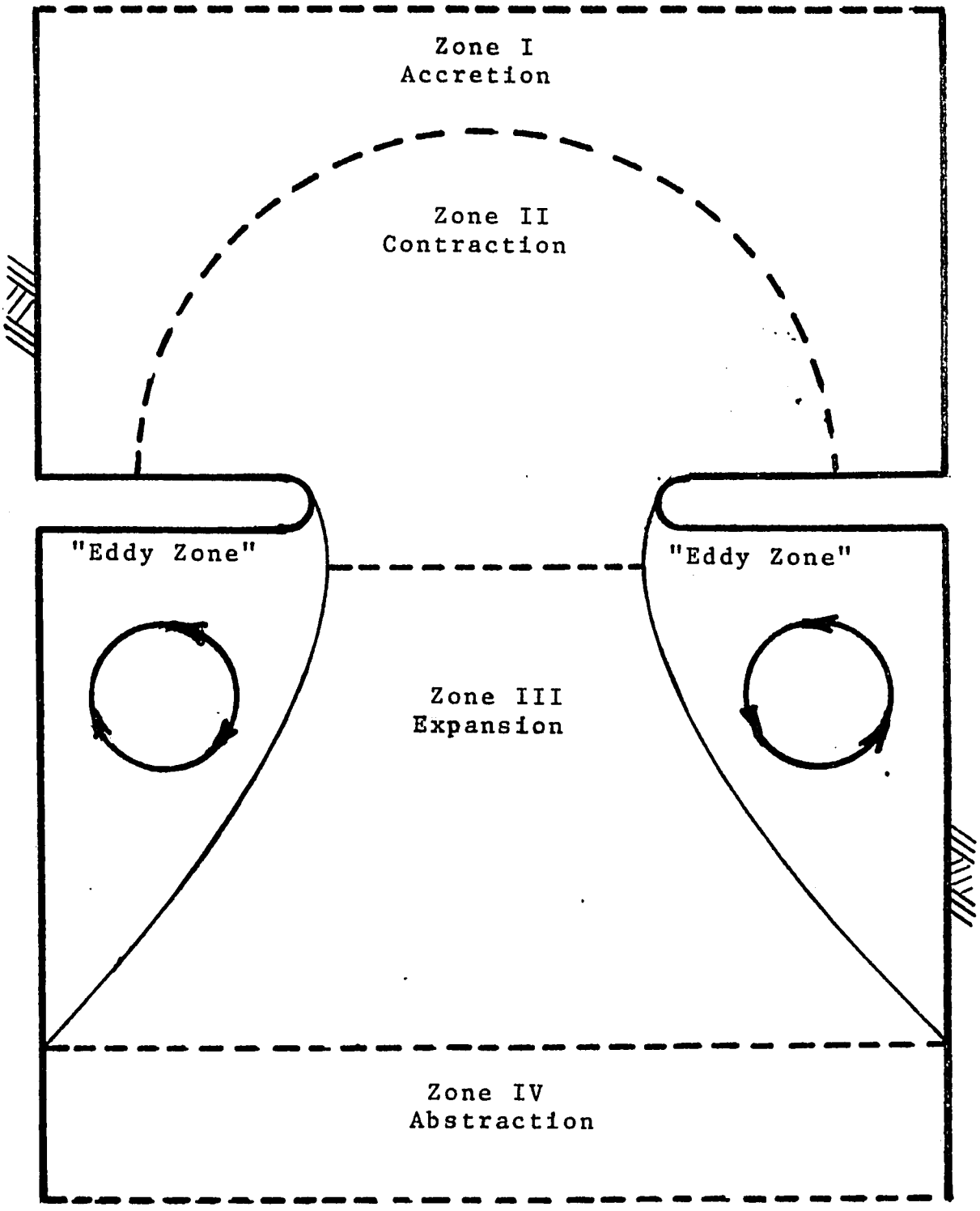

Figure 1.3 -- Schematic Diagram of Zones of Flow near a Contraction

Laursen (1970) has recommended a procedure for calculating the backwater effect of a contraction based on an assumed potential flow distribution and a computed energy loss due to expansion in zone III based on Albertson's work with the slot orifice.

1.3 Problem Definition and Approximations

The problem treated by this work will be limited to that of computing the flow distributions and water-surface elevations for steady turbulent flood flows through single opening contractions in natural channels of mild slope. The total discharge through the contraction and the water surface elevation across a downstream cross section are assumed to be known. The flow distributions at both the upstream and downstream boundaries are to be computed but it is assumed that those cross sections are chosen to be perpendicular to the direction of flow.

It is assumed that the physical problem cam be approximated by a mathematical model which will now be described. It is assumed that the physical flow approximates the following conditions:

1) Steady state -- No time dependency or hydraulic transients.
2) Two-dimensional -- All velocities will be parallel to the ground plane (xy - plane) and all pressure distributions will be hydrostatic. The velocity distribution in the z-direction normal to the xy - plane is uniform; it represents the depth integrated average velocity of the physical problem. The flow is essentially analogous to compressible plane flow with density proportional to the depth of the real fluid. Such flows are described by Landau and Lifshitz (1959, p. 396) under shallow

water theory and are analogous to the one-dimensional gradually varied flow described by Chow (1959, p. 217).

3) Subcritical -- Velocities are smaller in magnitude than the celerity of small gravity waves propagating in a fluid of like density and depth. This assumption will be shown to preclude the existence of discontinuities in velocity along streamlines.

4) Turbulent -- The flow behaves as a fully developed turbulent boundary layer generated by viscous attraction at the channel bottom. These viscous forces dominate any viscous forces or boundary layers developed at any other solid boundaries.

5) Constant mass density -- The mass density ρ is that of water. It is constant throughout.

Consider region R^3 bounded above by the free water surface $Z = Z(x,y)$ and below by the channel bottom $G = G(x,y)$. Let D be its projection in the xy-plane as shown in figure 1.4 and let ∂D be a piecewise smooth curve bounding D in the xy-plane. Also let $d = d(x,y)$ represent the depth of flow on D. Thus,

$$d(x,y) = Z(x,y) - G(x,y) \tag{1.3}$$

Let $\underline{V}(x,y) = u(x,y)\underline{i} + v(x,y)\underline{j}$ represent the two-dimensional depth integrated average velocity field defined on D; $\underline{V}$ is assumed to vary continuously on D. Furthermore, let ∂D be segmented into ∂D_1, ∂D_2, ∂D_3, and ∂D_4 where ∂D_1 and ∂D_2 are projections of boundaries across which there is

no flow (solid boundaries) and ∂D_3 and ∂D_4 are projections of boundaries across which the velocity vector is normal to ∂D (flow boundaries) (see figure 1.4).

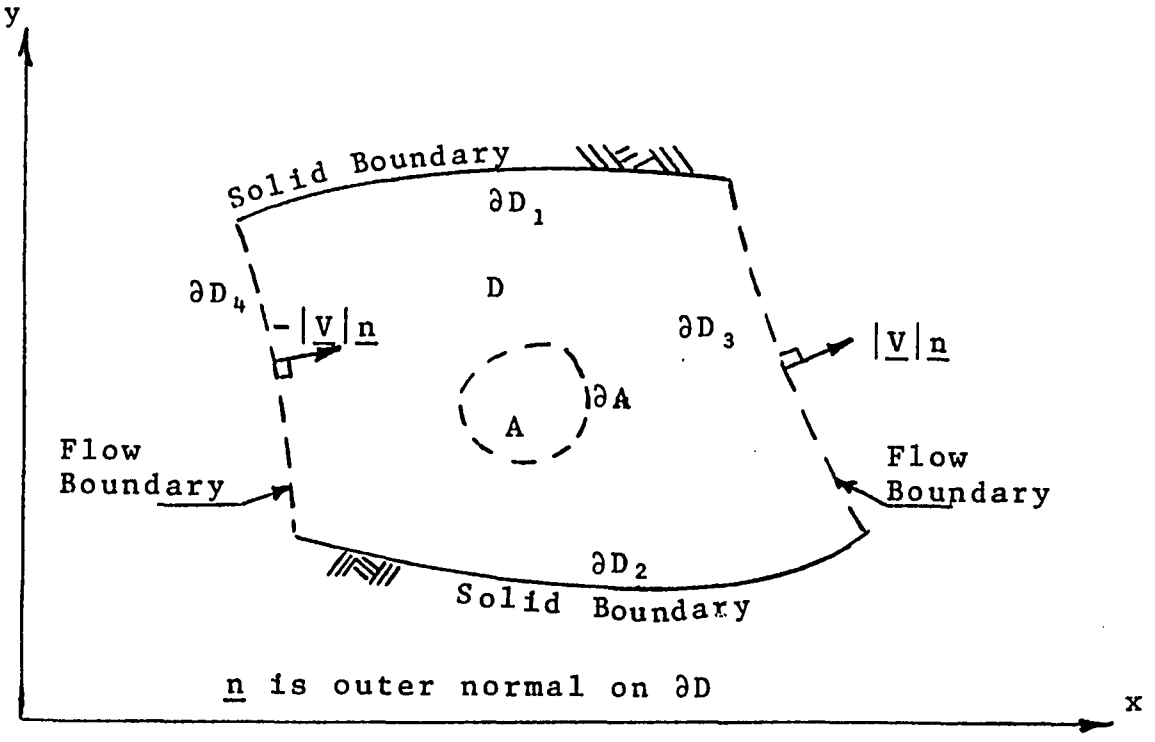

Figure 1.4 -- Schematic Diagram for Problem Definition

Let the viscous shear stress generated at the channel bottom be replaced by a depth integrated average body force $\underline{F} = \underline{F}(x,y)$ defined on D. Its magnitude will be related by uniform flow formulae to the velocity $\underline{V} = \underline{V}(x,y)$, depth of flow $d = d(x,y)$, and Manning roughness $n = n(x,y)$ defined on D. This is consistent with approximations (2) and (4) above.

Let the water-surface elevation Z along the downstream flow boundary ∂D_3 be specified. The water-level control could be specified by a condition on the upstream flow

boundary ∂D_4 but the downstream control is suitable to most physical problems and it will be adopted here.

The flow separation downstream from the contraction forms a velocity discontinuity between adjacent streamlines which will be treated as a free boundary problem. For that problem the boundary geometry ∂D will be variable. Appropriate boundary conditions for the location of the free boundary must be formulated. Once the geometry is fixed, however, the problem definition is identical to that of fixed boundary problems with velocity field varying continuously on D. The mathematical model will be formulated for fixed boundaries ∂D and the procedures for its application to the free boundary problem will then be formulated. All further discussions are based on fixed boundaries ∂D except where otherwise designated.

This dissertation will treat the following problems:

1) Formulation of the equations of motion governing the flow of the mathematical model described above,
2) Formulation of numerical solution algorithms for computing the flow distributions and water-surface elevations on D, and
3) Formulation of procedures for the application of the model to problems where separation is expected downstream from the contraction and a criterion for determining when separation should be expected and when it should not.

The following data will be considered input to the model:

1) Ground-surface elevations $G = G(x,y)$ on D,
2) Manning roughness coefficients $n = n(x,y)$ on D (to be explained in section 2),
3) Total volume rate of flow or discharge Q through D,
4) Downstream water-surface elevations $Z = Z(\xi)$ on ∂D_3,
5) Geometry of all fixed banks ∂D_1 and ∂D_2, and
6) Geometry of upstream and downstream cross sections ∂D_3 and ∂D_4 normal to the velocity field $\underline{V} = \underline{V}(x,y)$.

2. FRICTION FORCES

As stated above (cf. section 1.3), friction force generated by viscous shear stress at the channel bottom on D will be replaced by a depth integrated average body force assumed to act uniformly on the entire thickness of the turbulent boundary layer. This is consistent with approximations (2) and (4) of section 1.3. In vector form the friction body force $\underline{F} = \underline{F}(x,y)$ will be related to the velocity $\underline{V} = \underline{V}(x,y)$, Manning roughness $n = n(x,y)$, and depth of flow $d = d(x,y)$ as follows:

$$\underline{F} = -C_f(n,d)\,|\underline{V}|\,\underline{V} \tag{2.1}$$

where,

$$C_f(n,d) = \left(\frac{n}{1.49}\right)^2 \frac{g}{d^{4/3}} \qquad \text{and}$$

g = acceleration of gravity.

Equation (2.1) will be developed in detail below.

It is not the primary purpose of this work to study friction stress formulae. There is, however, theoretical, empirical, and historical basis for the use of friction formulae of the form (2.1).

Chow (1959, Chapter 8) describes the development of the turbulent boundary layer in open-channel flow. After accelerating from rest and traveling some distance in the channel the velocity distribution becomes stable and constant. The total resistance of viscous shear stress is

then in equilibrium with the componant of gravity force along the channel bottom. Since that viscous stress is proportional to the mass of the fluid it can be treated as a body force. It will be referred to as the friction body force F.

The french engineer, Antoine Chezy, is believed to be the first to express a relationship between the friction force of the channel bottom on such a flow and the velocity and roughness of the channel bed. Chezy's formula was developed and verified by experiments on an earthen canal, the Courpalet Canal, and on the Seine River in late 1769 (Chow, 1959, p. 93). It is thus applicable to prismatic channels of relatively small cross sectional area as compared with alluvial flood plains. Nevertheless, his approach has since been used repeatedly in the development of empirical formulae to explain friction forces in natural channels.

Chezy assumed "that the force resisting flow per unit area of the streambed is proportional to the square of the velocity " (Chow, 1959, p. 93).
Thus,

(2.2) $$f = KV^2$$

where, $V = Q/A$,

Q = total discharge in cubic feet per second, and

A = cross sectional area of channel.

In 1889 the irish engineer, Robert Manning, presented a formula, which was later modified to its present form:

$$Q = KS^{1/2} \tag{2.3}$$

where, $K = \frac{1.49}{n} AR^{2/3}$ = channel conveyance,

Q = total discharge in cubic feet per second,

R = hydraulic radius (cross sectional area divided by wetted perimeter of channel section in feet),

S = slope of energy line for uniform flow,

n = Manning roughness coefficient, and

A = cross sectional area of channel.

The quantity K is the conveyance. It is a measure of the carrying capacity of the channel.

Manning's formula was developed for conditions similar to those stated above for Chezy's work. It is mentioned here because it has become the cornerstone for most practical work since and it is widely used in the United States at this time for computing water-surface profiles in natural channels. The U.S. Geological Survey has developed procedures for estimating Manning's roughness coefficient "n" and has verified its use for flood flows in natural streams under an assortment of conditions (Barnes, 1967).

The slope of the energy line for conditions of uniform flow can be considered equivalent to the friction stress per pound of water. For points on the ground surface in the interior of very wide flood plains, the depth of flow d can be used for the hydraulic radius. We thus obtain the following expression for friction stress on the flood plain making use of Manning's "n" as an index of roughness:

$$f = \left[\left(\frac{n}{1.49}\right)^2 \frac{\gamma_w}{d^{1/3}}\right] V^2 \tag{2.4}$$

where, d = depth,

γ_w = unit weight of water, and

n = Manning's roughness coefficient.

The quantity in brackets can be considered a constant of proportionality between friction stress and the square of velocity for comparison to the Chezy formulation. It is noted that this constant of proportionality is a function of depth. In fact, the roughness coefficient n itself is a function of depth. It thus seems justifiable for purposes of this work to adopt one coefficient which is a function of depth and to follow Chezy's convention to express friction stress by the simple relationship:

$$f = C_f'(n,d)V^2 \tag{2.5}$$

$C_f'(n,d)$ will be a channel resistance which can be computed from Manning's "n" and depth of flow using equation (2.4).

It is a function of hydraulic roughness and depth. The resistance is inversely related to the conveyance.

In order to obtain an expression for the depth integrated average body force used to replace the force of friction on the turbulent boundary layer (cf. section 1.3), the friction stress f must be divided by the mass density per unit area of the boundary layer (ρd):

$$F = \frac{f}{\rho d} = \frac{C_f'}{\rho d} V^2 = C_f V^2 \tag{2.6}$$

where $C_f = C_f'/\rho d$ is a depth dependent resistance characterizing the body force F. The functional dependence of the resistance C_f on the water surface $Z = Z(x,y)$ will be denoted by

$$C_f = C_f[x,y;Z(x,y)] \ . \tag{2.7}$$

It will be understood that the dependence of C_f on x and y includes the dependence on roughness $n = n(x,y)$ and ground-surface elevation $G = G(x,y)$.

The vector form of equation (2.1) can be obtained from equation (2.6) by noting that the friction force of magnitude given by equation (2.6) will be directed opposite to the velocity vector at all points (x,y) on the interior of D.

3. EQUATIONS OF MOTION GOVERNING FLOW DISTRIBUTION

3.1 General

The equations of motion which govern the distribution of flow on D will now be formulated. They are based on the mathematical model and approximations described in section 1.3. The water surface $Z = Z(x,y)$ will be considered a known function throughout this section. The equations which govern the water surface and which define its interdependence with the flow distribution will be discussed in later sections.

3.2 Conservation of Mass and the Stream Function

Consider a control volume the projection of which will be designated $A \subset D$ and which is bounded above and below by Z and G respectively (cf. figure 1.4). Continuity of mass requires the following balance between flow into the control volume and rate of increase of mass in the control volume:

$$\int_{\partial A} (-\underline{v} \cdot \underline{n} \rho d) ds = \frac{\partial}{\partial t} \int_A (\rho d) dA \,. \tag{3.1}$$

For steady state conditions the term on the right vanishes. Gauss' theorum can be used to convert the integral on the left to a volume integral. Constant density ρ can be assumed for water (cf. approximation (5) section 1.3). Thus,

$$\int_A \operatorname{div}(\underline{V} d) = 0 \,. \tag{3.2}$$

Since A was chosen arbitrarily and the integrand is assumed continuous on D (cf. section 1.3), the integrand must vanish. The vollowing differential equation assures conservation of mass for the flow described:

$$\text{div}(\underline{V}d) = 0 \quad . \tag{3.3}$$

Consider now the following integral on an arbitrary closed path ∂A in D:

$$\int_{\partial A} [(-vd)dx + (ud)dy] \quad . \tag{3.4}$$

Equation (3.3) assures that this integral is independent of path on D. The stream function ψ is thus defined:

$$d\psi = (-vd)dx + (ud)dy, \tag{3.5}$$

or

$$\frac{\partial \psi}{\partial x} = -vd \quad \text{and} \quad \frac{\partial \psi}{\partial y} = ud \quad .$$

A streamline is defined as a path along which the velocity field $\underline{V} = \underline{V}(x,y)$ is tangent at all points. The differential equations describing this condition are given by:

$$\frac{dx}{u} = \frac{dy}{v} \quad . \tag{3.6}$$

Dividing both sides by the point depth d and rearranging terms gives:

$$(3.7) \qquad (ud)dy - (vd)dx = 0 \quad .$$

Substituting the expressions for the velocity componants u and v from equations (3.5) results in the following expression on the streamline:

$$(3.8) \qquad d\psi = \frac{\partial \psi}{\partial x}dx + \frac{\partial \psi}{\partial y}dy = 0 \quad .$$

Thus the stream function ψ is constant on a streamline. Streamlines can be located by solving for the level curves of the stream function.

The flow between two two-dimensional streamlines can be obtained by the following integral on a path ∂C between the two streamlines (see figure 3.1):

$$(3.9) \qquad Q = \int_{\partial C} (\underline{V}d)\cdot \underline{n}ds = \int_{\partial C} (ud)dy - (vd)dx = \int_{\partial C} d\psi \quad .$$

Thus the flow between two two-dimensional streamlines is given by the difference of the stream function values on the two streamlines.

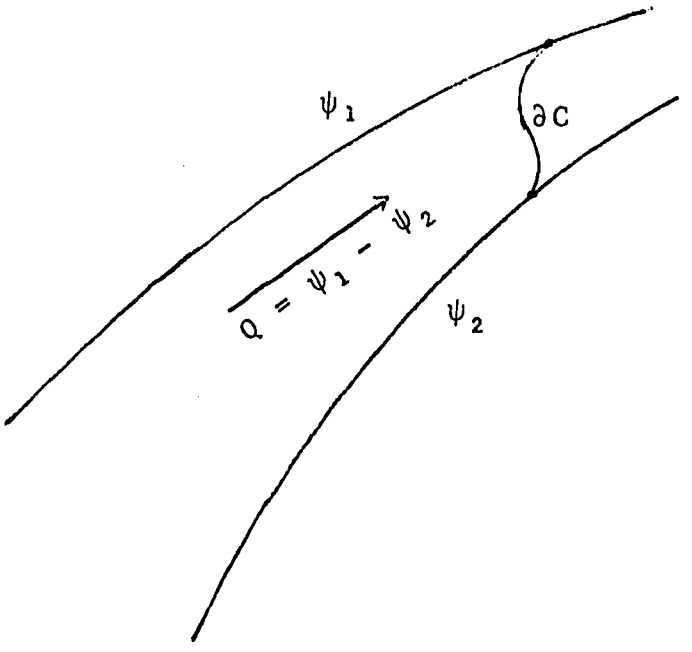

Figure 3.1 -- Discharge between Two Streamlines

3.3 Conservation of Momentum

The Navier-Stokes equation expresses the law of conservation of momentum for the three-dimensional, viscous, incompressible flow of a Newtonian fluid in vector form (Pao, 1967, p. 280):

$$\frac{D\underline{V}_3}{Dt} = \underline{F}_b - \frac{1}{\rho}\nabla p + \nu\nabla^2\underline{V}_3 \tag{3.10}$$

where,

$\underline{F}_b = \underline{F}_b(x,y,z)$ = body force vector field,

$p = p(x,y,z)$ = pressure function,

ν = kinematic viscosity (constant),

$\underline{V}_3 = u(x,y,z)\underline{i} + v(x,y,z)\underline{j} + w(x,y,z)\underline{k}$ = three-dimensional velocity field on R^3, and

$\frac{D\underline{V}_3}{Dt}$ = material derivative of velocity vector.

The pressure $p = p(x,y,z)$ can be eliminated from the above equation by taking the curl of both sides of the equation, noting that the order of operation for the curl, material derivative, and Laplacian operators can be interchanged and that the curl of a gradient vanishes identically. Thus,

$$\frac{D\underline{\omega}}{Dt} = \text{curl } \underline{F}_b + \nu\nabla^2\underline{\omega} \tag{3.11}$$

where,

$\underline{\omega} = \underline{\omega}(x,y,z)$ = three dimensional vorticity vector field.

The vorticity $\underline{\omega}$ is defined as curl $\underline{V}_3$. Its magnitude is equal to twice that of the local angular velocity vector (Pao, 1967, p. 21). For the two-dimensional flow (cf. approximation (2), section 1.3) it has only one non-zero componant which is normal to the xy-plane ($\underline{\omega} = \zeta(x,y)\underline{k}$).

Equation (3.11) can be specialized for the flow described in section 1.3 by the following scalar equation:

$$\frac{D\zeta}{Dt} = \text{curl } \underline{F} + \nu\nabla^2\zeta \quad . \tag{3.12}$$

The last term on the right expresses the force due to viscous surface stresses on the x and y faces of the three-dimensional fluid elements. For very wide flood planes and high Reynolds numbers, these viscous forces are significant only in the boundary layers developed along the solid boundaries ∂D_1 and ∂D_2. Elsewhere they will be dominated by the viscous surface forces generated on the channel bottom G and propagated through the fluid by turbulent mixing (cf. approximation (4), section 1.3). In this model, only those viscous forces represented by the friction body force $\underline{F}$ will be accounted for. The viscous term $\nu\nabla^2\zeta$ of equation (3.12) will be neglected in further analysis.

3.4 Differential Equation Governing Distribution of Flow

Combining equations (2.1), (3.5) and (3.12) and neglecting the viscous term of (3.12) the following equation for two-dimensional flow in the xy-plane is obtained:

$$\frac{D\zeta}{Dt} = \text{curl } \underline{F} = \frac{\partial}{\partial x}(-C_f|\underline{V}|v) + \frac{\partial}{\partial y}(C_f|\underline{V}|u) \tag{3.13}$$

or

$$-\frac{D\zeta}{Dt} = \frac{\partial}{\partial x}\left(\frac{C_f|\underline{V}|}{d}\frac{\partial\psi}{\partial x}\right) + \frac{\partial}{\partial y}\left(\frac{C_f|\underline{V}|}{d}\frac{\partial\psi}{\partial y}\right) \quad .$$

The flow distribution on D will be specified by a stream function $\psi = \psi(x,y)$ which is a solution to (3.13) subject to the following boundary conditions (cf. figure 1.4):

(3.14a) $$\psi(x,y) = \psi_1 \text{ on } \partial D_1,$$

(3.14b) $$\psi(x,y) = \psi_2 \text{ on } \partial D_2, \text{ and}$$

(3.14c) $$\frac{\partial \psi}{\partial n} = 0 \text{ on } \partial D_3 \text{ and } \partial D_4.$$

ψ_1 and ψ_2 are set so that the total discharge Q is expressed by:

(3.15) $$Q = \psi_1 - \psi_2 .$$

Equation (3.13) is a nonlinear partial differential equation. The velocity $\underline{V}$ is related to the derivatives of the stream function ψ by equation (3.5). The vorticity was defined above as curl $\underline{V}$ and, thus, it is also related to ψ. Furthermore, the resistance C_f is related to the water surface $Z = Z(x,y)$ as indicated by equation (2.7); the functional dependence of Z on ψ will be discussed in section 4.

4. EQUATIONS OF MOTION GOVERNING WATER-SURFACE ELEVATION

4.1 Pressure Equation for a Streamline

Equations for determining the water surface $Z = Z(x,y)$ will now be formulated. By approximation (2) (cf. section 1.3) the pressure distribution is hydrostatic. The depth integrated pressure on the fluid layer at a point on D can thus be related to the water surface $Z = Z(x,y)$. It will be assumed throughout this section that the stream function $\psi = \psi(x,y)$ is known on D. The family of streamlines on D can then be found by solving for the level curves of ψ on D.

The two-dimensional depth integrated Euler equation can be obtained by integrating equation (3.10) with respect to z, neglecting the viscous stress term $\nu\nabla^2\underline{V}_3$ as follows:

$$\frac{D\underline{V}}{Dt} = \underline{F} - \frac{1}{\rho d}\nabla P \tag{4.1}$$

where,

$$P = \int_{G(x,y)}^{Z(x,y)} p(x,y,z)\,dz \quad .$$

For hydrostatic conditions (cf. approximation (2), section 1.3):

$$P = \tfrac{1}{2}\,\gamma_w d^2 \quad . \tag{4.2}$$

Let s represent arc length along the two-dimensional streamline. The scalar product of equation (4.1) and the vector $\underline{ds}$ is expressed by:

$$(4.3) \qquad \left[V\frac{\partial V}{\partial s} + \frac{\partial V}{\partial t}\right]ds = Fds - \frac{1}{\rho d}\frac{\partial P}{\partial s}ds \quad .$$

Figure (4.1) shows a differential length of channel ∂S taken along a two-dimensional streamline. The partial derivative can now be computed formally as follows:

$$(4.4) \qquad \frac{\partial P}{\partial s} = \lim_{\Delta s \to o} \frac{P(s + \Delta s) - P(s)}{\Delta s}$$

where,

$$P(s) = \tfrac{1}{2}\,\gamma_w[Z(s) - G(s)]^2$$

and

$$P(s + \Delta s) = \tfrac{1}{2}\,\gamma_\omega[Z(s + \Delta s) - G(s)]^2 \,.$$

Note that variation in depth integrated pressure P is due to variation in water surface Z alone. It is independent of variations in ground surface G. This is attributable to the horizontal componant of force exerted by the sloping channel bottom on the fluid; the expression for $P(s + \Delta s)$ includes the force of the channel bottom G on the fluid ∂S. The expressions for P can now be substituted into the expression for the partial derivative. Combining

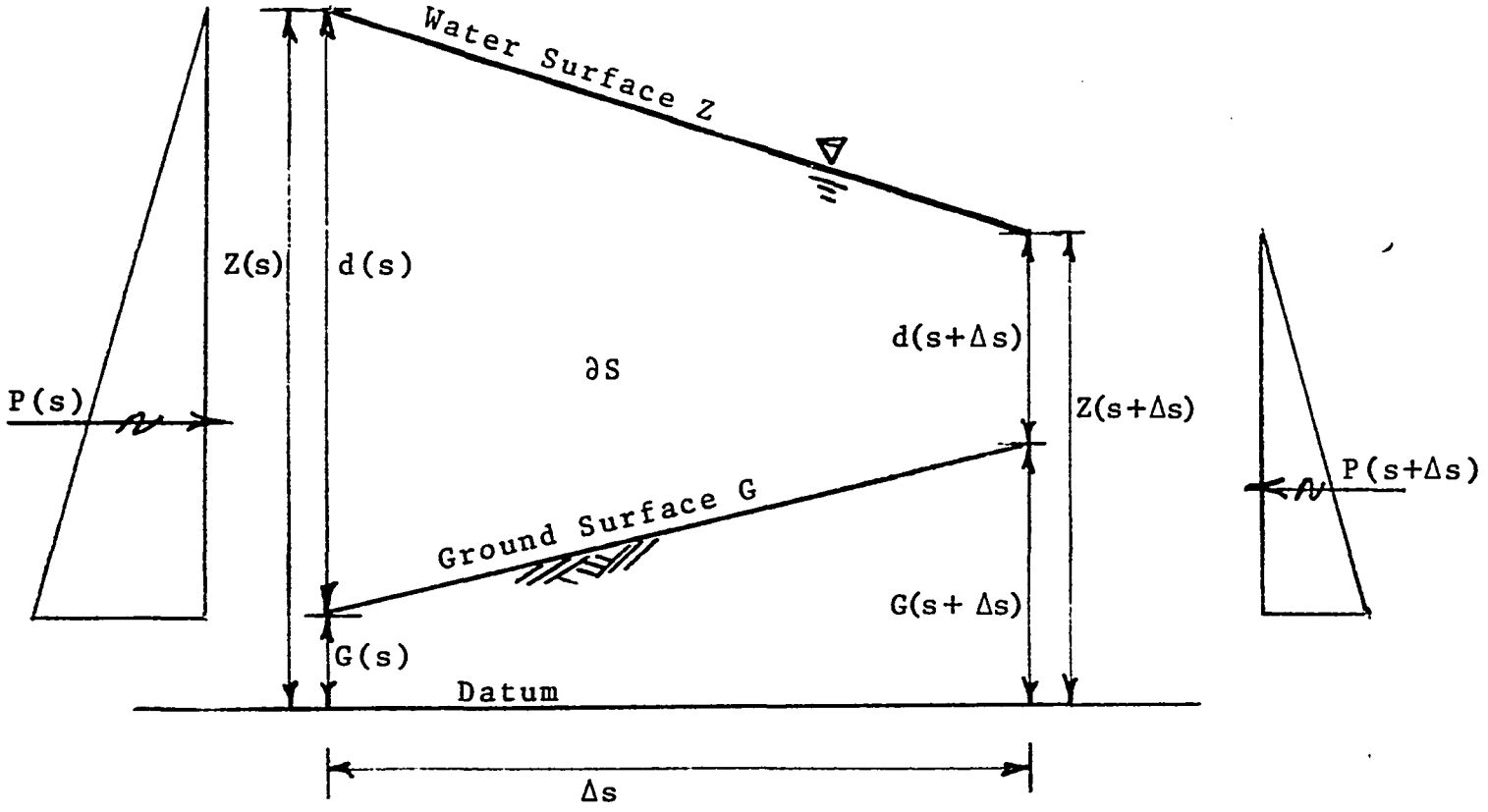

Figure 4.1 -- Pressure Diagram for Channel Segment Along Two-Dimensional Streamline

like terms then results in the following expression:

$$\frac{\partial P}{\partial s} = {}^1/_2\,\gamma_w \lim_{\Delta s \to o}\left[\frac{Z^2(s + \Delta s) - Z^2(s)}{\Delta s}\right] \tag{4.5}$$

$$-\gamma_w G(s) \lim_{\Delta s \to o}\left[\frac{Z(s + \Delta s) - Z(s)}{\Delta s}\right] .$$

The two limits on the right are definitions of partial derivatives for $Z^2(s)$ and $Z(s)$ respectively. Thus,

$$\frac{\partial P}{\partial s} = \gamma_w [Z(s) - G(s)] \frac{\partial Z(s)}{\partial s} \tag{4.6}$$

or

$$\frac{\partial P}{\partial s} = \gamma_w d(s) \frac{\partial Z(s)}{\partial s} .$$

Substituting equation (4.6) into equation (4.3) and specializing for steady state conditions gives:

$$VdV + gdz - Fds = 0 . \tag{4.7}$$

If $V(s)$ is continuous then

$$VdV = d\left(\frac{V^2}{2}\right) . \tag{4.8}$$

and equation (4.7) can be integrated as follows:

$$\frac{V^2}{2g} + Z - \int_0^s \frac{F}{g}\, ds = B(\psi) \quad . \tag{4.9}$$

This is the pressure equation for the flow described in section 1.3. The constant $B(\psi)$ can be determined for each streamline if the velocity head $\frac{V^2}{2g}$ and water surface Z are known at one point on the streamline. $B(\psi)$ will in general be different on each streamline. Since the water surface is assigned on ∂D_3 (cf. section 1.3), and every streamline intersects ∂D_3 perpendicularly, ∂D_3 can be considered as an initial curve and the water surface $Z = Z(x,y)$ on D can be generated by the corresponding one parameter family of solutions to equation (4.9) on the level curves of the stream function $\psi = \psi(x,y)$. The downstream water surface on ∂D_3 will be considered an initial curve to equation (4.9). Thus,

$$Z(x,y) = Z_d(\xi) \quad \text{on } \partial D_3 \quad . \tag{4.10}$$

It will now be shown that the continuity of V(s) is assured by the assumption of subcritical flow (cf. approximation (3) section 1.3).

Landau and Lifshitz (1959, p. 396) discuss an analogy between the variable depth of two-dimensional incompressible free-surface flow and the density of plane compressible flow.

The plane flow pressure density relationship can be expressed in terms of the depth and unit weight of water of the free surface flow by equation (4.2).

The speed of sound for the plane compressible flow corresponds to the critical speed V_c of the free-surface flow. The speed of sound V_s in compressible flow is the speed at which velocity discontinuities in streamlines propagate. Its magnitude can be computed from the pressure-density relationship (Pao, 1967, p. 390):

$$V_s^2 = \frac{dp'}{d\rho'} \tag{4.11}$$

where,

p' = pressure for the plane compressible flow, and

ρ' = density for the plane compressible flow.

Thus, using the pressure density relationship (4.2) the critical speed (V_c) for the free-surface flow can be computed:

$$V_c^2 = \frac{dP}{d(\rho d)} = gd \tag{4.12}$$

or

$$\frac{V_c^2}{2g} = \frac{d}{2} \quad .$$

Critical speed in shallow water is the celerity of small gravity waves. It is the speed at which velocity discontinuities in streamlines propagate. For steady flows, then, a velocity discontinuity in a streamline would be possible

only if the velocity of the channel flow were equal in magnitude to the critical speed. Otherwise the discontinuity would propagate and the flow would become unsteady. In a steady flow where all velocities are subcritical, discontinuities can be formed only by external disturbances. The integration of equation (4.3) is thus valid.

The pressure equation (4.9) derived here is identical in form to the Bernoulli equation for a streamline. The same equation could have been written by simply applying Bernoulli's equation to a three-dimensional streamline formed by the intercept of the free surface with a two-dimensional streamline. It is not known, however, if such a streamline on the free surface remains on the free surface when it passes through a contraction. The above discussion shows that the assumption of such a condition is not necessary. Equation (4.9) is valid on any two-dimensional streamline of the flow specified in section 1.3.

4.2 Energy Variations Normal to Streamlines

An alternate approach is possible which gives an expression for the variation in total energy from one streamline to another. It is based on the following vector identity (Pao, 1967, p. 150):

$$(\underline{V}\cdot\nabla)\underline{V} \equiv \nabla\left(\frac{V^2}{2}\right) - \underline{V} \times \text{curl } \underline{V} \quad . \tag{4.13}$$

This expression can be substituted into the depth integrated Euler equation (4.1) for two-dimensional steady flows as follows:

$$(4.14) \qquad \left[\nabla\left(\frac{V^2}{2}\right) - \underline{V} \times \text{curl}\underline{V}\right] = \underline{F} - \frac{1}{\rho d}\nabla P \quad .$$

Using equation (4.6) and rearranging terms results in the following equation:

$$(4.15) \qquad \nabla\left(\frac{V^2}{2g} + Z\right) = \frac{\underline{F} + \underline{V} \times \text{curl}\ \underline{V}}{g} \quad .$$

The quantity on the left is the gradient of the total energy E. Taking the scalar product of this equation with unit vectors tangent and normal to a streamline at a point on D results in the following expressions:

$$(4.16) \qquad \frac{\partial E}{\partial s} = \frac{F}{g} \quad \text{and} \quad \frac{\partial E}{\partial n} = \frac{\underline{V} \times \text{curl}\ \underline{V}}{g} \quad .$$

The first expression gives the same result as equation (4.9). The second expression shows that variations in total energy along normals to streamlines must be related to vorticity. For irrotational flows there will be no variation and the energy surface and stream function will be orthogonal.

4.3 Water Level Contour Maps

Water level contour maps are prepared by sketching the level curves of the water surface through plotted points of known water level. They are prepared for observed water surfaces from high-water marks or for computed water surfaces from computed point water levels. The point data is frequently scattered; the flow distribution is frequently used as a guide to smoothing the data. If the flow distribution is that of potential flow ($\zeta(x,y) \equiv 0$) the energy surface $E = E(x,y)$ is orthogonal to the stream function (cf. equation 4.16) and the energy-surface contours can be sketched normal to the observed or computed streamlines. Water levels are then obtained by subtracting velocity head from the energy surface (cf. equation 4.9).

In general, however, the flow is rotational ($\zeta \neq 0$) and a more general relationship between the energy surface and water-level contours based on the vorticity field $\zeta = \zeta(x,y)$ is necessary.

Data collected by the USGS in Alabama illustrate the case of rotational flow. Figure 4.2 shows water levels and velocity distributions respectively measured along the downstream embankment of bridges at Buttahatchee River near Henson Springs, Alabama during the flood of December 19, 1967, (McCain, 1970). The water levels shown in figure 4.2 are highest where the velocity head is shown to be greatest. Since the measurements along the embankment are located on a path that is predominantly normal to the

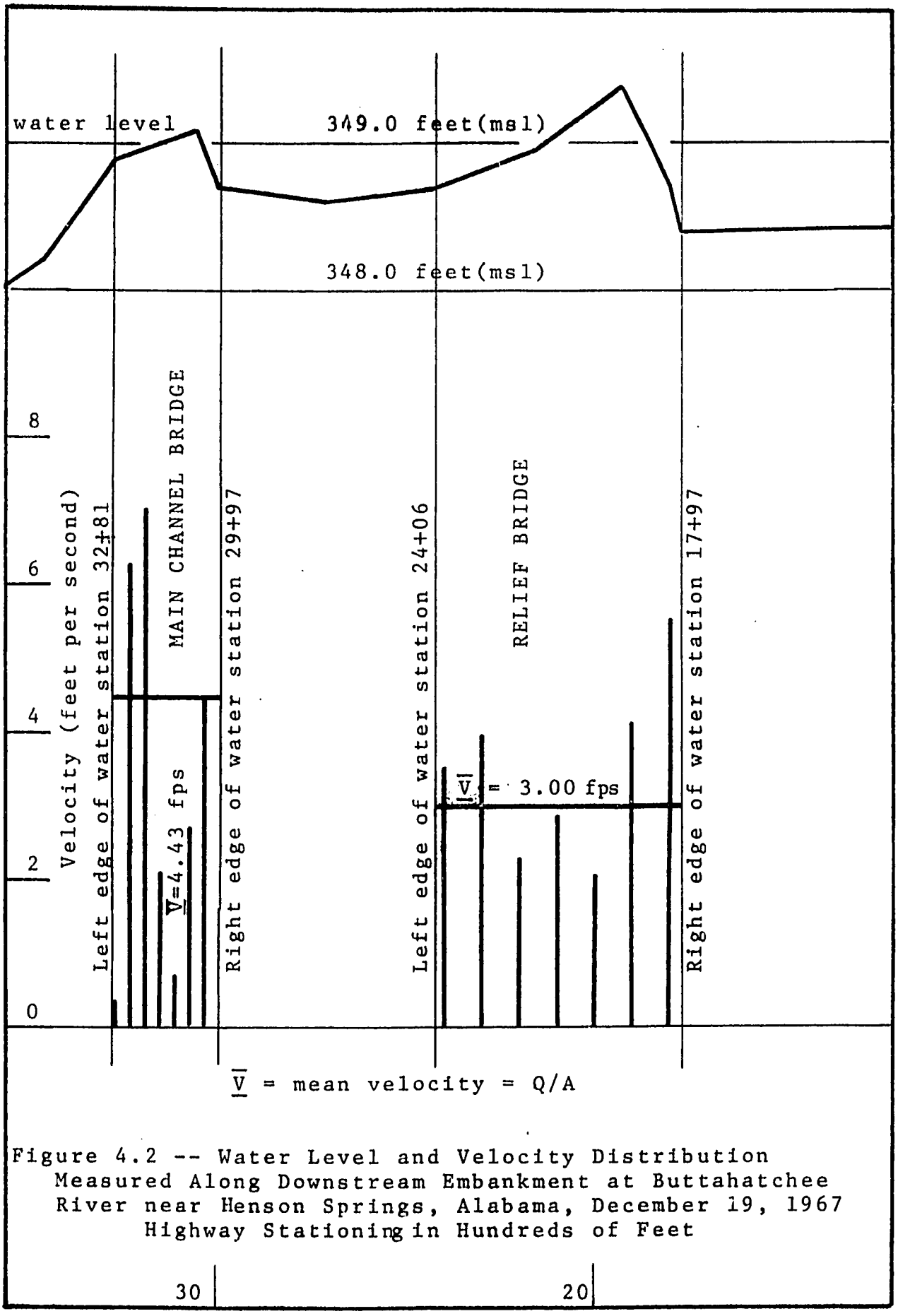

Figure 4.2 -- Water Level and Velocity Distribution Measured Along Downstream Embankment at Buttahatchee River near Henson Springs, Alabama, December 19, 1967 Highway Stationing in Hundreds of Feet

direction of flow, this increase in energy must be related to the vorticity field. Equation (4.16) indicates that such a variation in total energy would be impossible in an irrotational flow.

Figure 4.4 illustrates the situation schematically. The flow emerging from the contraction forms a zone of high velocity bounded by zones of slower velocities. A strip of high vorticity is formed along the boundary between the two zones. The sense of the vorticity vector along these strips is indicated on the diagram. The vector $\frac{\partial E}{\partial n}\underline{n}$ which is computed from the vector product of the velocity $\underline{V}$ with the vorticity vector $\underline{\omega}$ (cf. equation 4.16) is also shown. The energy surface $E = E(x,y)$ must increase in the live stream according to the sense of the vectors shown.

The increase of total energy in the live stream has also been observed in laboratory hydraulic model studies (Kindsvater, Carter and Tracy, 1953, figure 3, p. 4).

The principle can be applied in the preparation of water-level contour maps at bridge sites. Where the vorticity is believed to be small, such as on the open flood plains where velocities are small, the level curves of the energy surface $E = E(x,y)$ should be approximately orthogonal to the streamlines. Where velocity heads are small so that the energy surface $E(x,y)$ approximates the water surface $Z(x,y)$, that approximate orthogonality also applies to the level curves of the water surface $Z = Z(x,y)$. Where the velocity field $\underline{V} = \underline{V}(x,y)$ changes more rapidly, such as

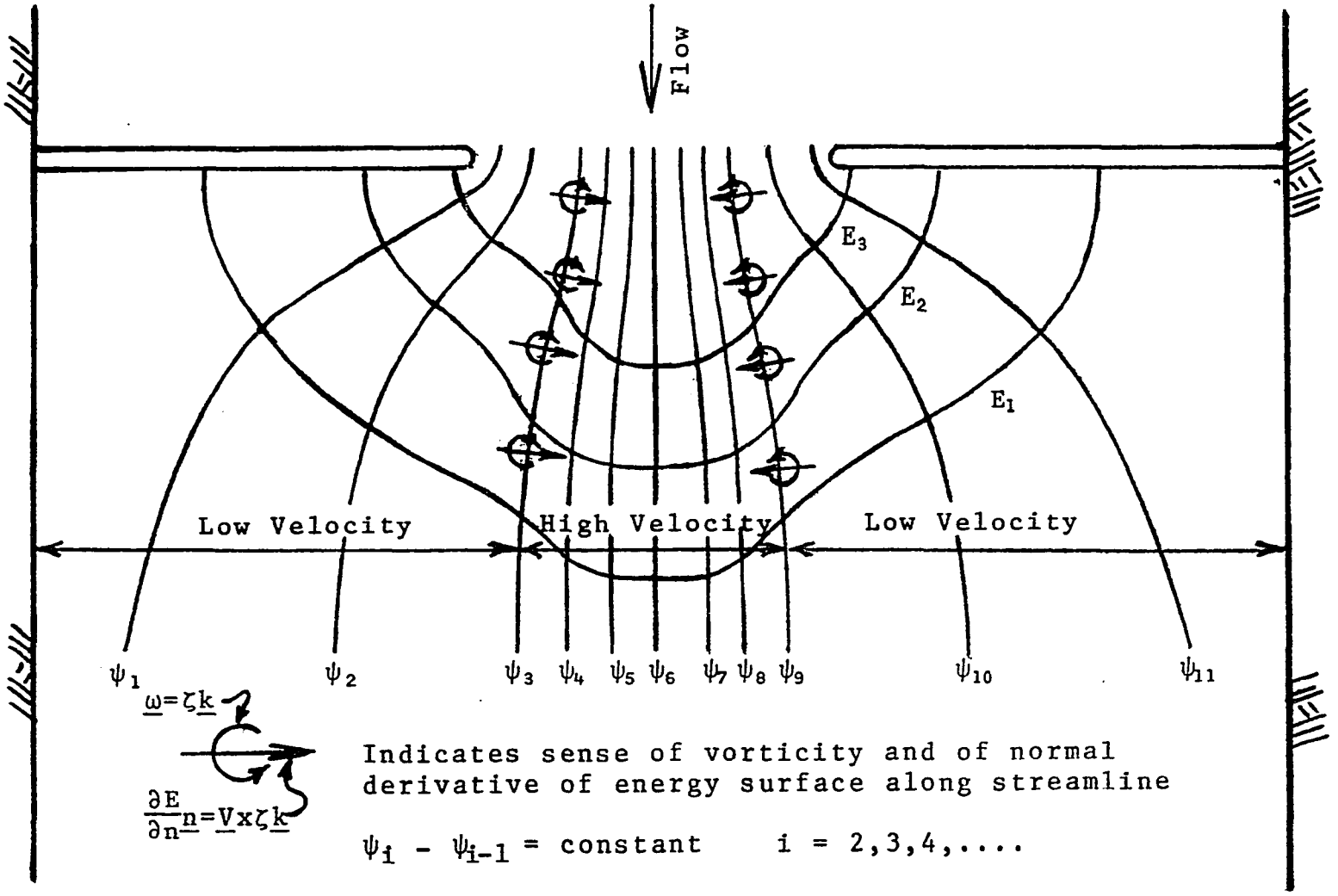

Figure 4.4 -- Relationship of Energy Surface to Flow Distribution

at the edges of a main channel, this approximate orthogonality may not be appropriate and the energy surface should deviate from orthogonality with the stream function in the sense governed by equations (4.16).

It is not the opinion of the writer that the vorticity $\zeta = \zeta(x,y)$ should actually be calculated before level curves are sketched through plotted high-water marks. But there is a common misconception that such level curves must be sketched normal to the direction of flow. Water levels observed from high-water marks or computed by equation (4.9) should be used as the primary guide in sketching water level maps. Equations (4.16) should be used as subjective guides where necessary for the purpose of data interpolation or extrapolation.

5. NUMERICAL SOLUTION

5.1 Solution Algorithm

The functional dependence of the water surface $Z = Z(x,y)$ on the stream function $\psi = \psi(x,y)$ is discussed in section 4. The water surface elevations are generated by solutions to the pressure equation (4.9) along the family of streamlines specified by $\psi(x,y)$. Let that functional dependence be denoted by:

$$Z = Z[x,y;\psi(x,y)] \quad . \tag{5.1}$$

The functional dependence of the stream function $\psi = \psi(x,y)$ on the water surface $Z = Z(x,y)$ is discussed in section 3.4. The resistance $C_f = C_f[x,y;Z(x,y)]$ in equation (3.13) is dependent on the water level $Z = Z(x,y)$ (cf. equation 2.7). Let the functional dependence of ψ on Z be denoted by:

$$\psi = \psi[x,y;Z(x,y)] \quad . \tag{5.2}$$

In order to obtain the stream function ψ when the water surface Z is known it is necessary to solve the nonlinear partial differential equation (3.13), subject to boundary conditions (3.14).

Consider now the following linearization of equation (3.13):

$$(5.3)\qquad \frac{-D\zeta_{(i-1)}}{Dt} = \frac{\partial}{\partial x}\left[\frac{C_{f\,(i-1)}|\underline{V}_{(i-1)}|^{\beta_1}}{d_{(i-1)}}\frac{\partial\psi_{(i)}}{\partial x}\right] + \frac{\partial}{\partial y}\left[\frac{C_{f(i-1)}|\underline{V}_{(i-1)}|^{\beta_i}}{d_{(i-1)}}\frac{\partial\psi_{(i)}}{\partial x}\right]$$

where,

$$C_{f(i)} = C_{f(i)}[x,y;Z_{(i)}(x,y)] ,$$

$$\underline{V}_{(i)} = \frac{1}{d_{(i)}}\frac{\partial\psi_{(i)}}{\partial y}\underline{i} - \frac{1}{d_{(i)}}\frac{\partial\psi_{(i)}}{\partial x}\underline{j} ,$$

$$\zeta_{(i)} = \text{curl}\ \underline{V}_{(i)} ,$$

$$d_{(i)} = d_{(i)}(x,y) = Z_{(i)}(x,y) - G(x,y) ,$$

$$\beta_i = \beta_{i-1} + \Delta\beta_i ,$$

$$\beta_i \leq 1 ,$$

$$\beta_o = \beta_1 = 0 ,$$

$$\Delta\beta_i = \begin{cases} R & i = kj_R \\ 0 & i = \text{other} , \end{cases} \qquad k = 1,2,3....$$

$Z_{(o)} = Z_{(o)}(x,y)$ = assumed water surface,

$\underline{V}_{(o)} = \zeta_{(o)} = 0$, and

$i = 1,2,3.....$.

This is a general linear "quasi-harmonic" partial differential in $\psi_{(i)}$ (Zienkiewicz, 1970, p. 149) if the terms $\frac{D\zeta_{(i-1)}}{Dt}$ and $\frac{C_{f(i-1)}|V_{(i-1)}|^{\beta_i}}{d_{(i-1)}}$ are considered known functions of x and y.

A result of the calculus of variations shows that an equivalent problem to that of solving equation (5.3) on D subject to boundary conditions (3.14) is that of solving the following minimization problem:

$$(5.4) \qquad \min_{\psi_{(i)}} \Phi[\psi_{(i)}(x,y)] =$$

$$\int_D \left[\frac{\frac{1}{2} C_{f(i-1)} |V_{(i-1)}|^{\beta_i}}{d_{(i-1)}} \left\{ \left(\frac{\partial \psi_{(i)}}{\partial x} \right)^2 + \left(\frac{\partial \psi_{(i)}}{\partial y} \right)^2 \right\} - \frac{D\zeta_{(i-1)}}{Dt} \psi_{(i)} \right] dA \ .$$

subject to boundary condition (3.14a) and (3.14b). Boundary condition (3.14c) is a natural boundary condition for the minimization problem and needs no special consideration.

Zienkiewicz (1970 Chapter 10) gives the details for solving the minimization problem by the finite element method. A summary of the numerical procedure is given in section 5.2.

Algorithm (5.1)

Equation (5.3) defines sequences of functions $\{\psi_{(i)} = \psi_{(i)}(x,y)\}$ and $\{Z_{(i)} = Z_{(i)}(x,y)\}$ generated as follows:

1) $Z_{(o)} = Z_{(o)}(x,y)$ is an assumed initial water surface. From $Z_{(o)}$ initial depths $d_{(o)}$ and resistances $C_{f(o)}$ are generated.

2) $\psi_{(1)} = \psi_{(1)}[x,y;Z_{(o)}(x,y)]$ is the stream function which satisfied equation (5.3) subject to boundary conditions (3.14) using the initial resistance $C_{f(o)}$ computed in step 1. $\beta_1 = 0$ so that $\underline{V}_{(o)}$ need not be defined.

3) $Z_{(1)} = Z_{(1)}[x,y;\psi_{(1)}(x,y)]$ is the water surface generated by equation (4.9) subject to boundary condition (4.10) along the family of streamlines specified by $\psi_{(1)}(x,y)$.

4) The other terms are generated recursively as follows:

$$\psi_{(i)} = \psi_{(i)}[x,y;Z_{(i-1)}(x,y,\psi_{(i-1)})],$$

$$Z_{(i)} = Z_{(i)}[x,y;\psi_{(i)}(x,y)], \text{ and}$$

$$i = 2,3,4,\ldots .$$

Each solution of equation (5.3) requires the evaluation of the magnitude of velocity $|\underline{V}_{(i-1)}|$ and material derivative $\frac{D\zeta_{(i-1)}}{Dt}$ based on the previous solution $\psi_{(i-1)}$. The relaxation coefficients R & j_R can be adjusted to improve convergence of the sequence $\{\psi_{(i)}\}$.

If the sequence $\{\psi_{(i)}\}$ converges, then the stream function $\psi = \psi(x,y)$ and water surface $Z = Z(x,y)$ which simultaneously satisfy equations (3.13) and (4.9) subject to boundary conditions (3.14) and (4.10) are given by:

$$\psi(x,y) = \lim_{i\to\infty} \psi_{(i)}(x,y)$$

and

$$Z(x,y) = \lim_{i\to\infty} Z_{(i)}(x,y) \quad .$$

5.2 Finite Element Solution for Flow Distribution

The region D is first subdivided into triangular shaped elements and the nodes are numbered consecutively. Although this subdivision and numbering is in general arbitrary, the adoption of certain conventions will be found convenient and efficient. A division by rows and columns is shown schematically in figure 5.1. Let the number of rows of nodes be designated by N and let the number of columns of nodes be designated by M. Let each node be indexed by its row and column number respectively designated (I,J). In addition to the row-column indexing (I,J) let each node have a unique index k assigned to it; that index will start at node (1,1) and proceed by rows (the index J incrementing more rapidly) from K=1 to k=NM. The coordinates of each node (x_k, y_k) can be assigned for each node under the general constraint that the triangular geometry of each of the elements is maintained. This allows great flexibility in choosing the general geometry of the boundaries and the size of the individual elements. (Figure 5.1) is intended to show the indexing and subdivision shemes only. The specific locations of the nodes is much more general as will be illustrated by example problem later.

Let the elements be designated by the k-indeces of their nodes i,j,m and alternatively by a unique index e analogous to the k-index for the nodes. The total number of elements E will be given by $E = 2(N-1)(M-1)$.

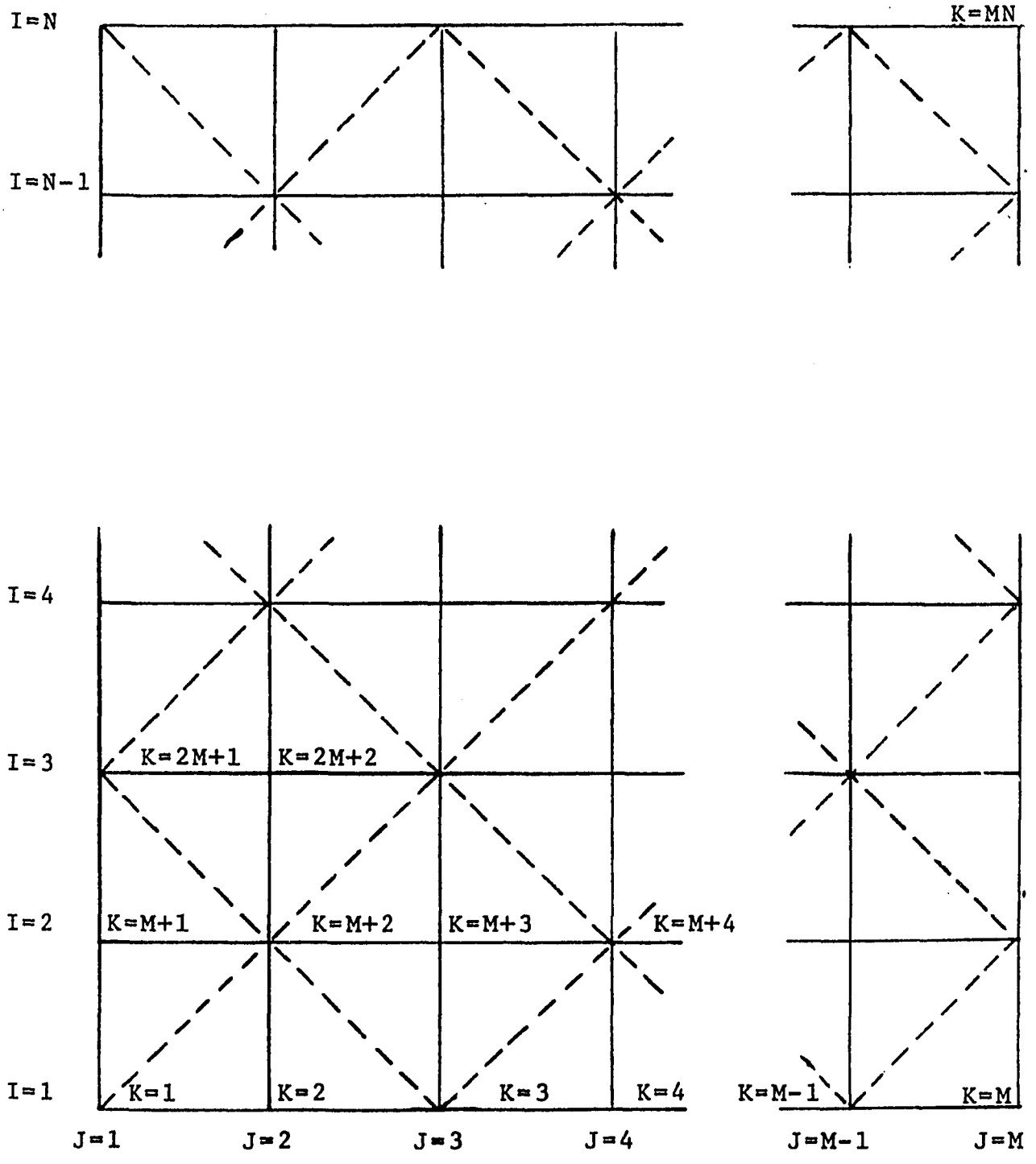

Figure 5.1 -- Indexing Scheme for Finite Element Grid System

Each of the functions $\psi_{(i)}$, $\frac{D\zeta_{(i-1)}}{Dt}$, and $\frac{C_{f(i-1)}|\underline{V}_{(i-1)}|^{\beta_i}}{d_{(i-1)}}$ (cf. equation 5.3) are then approximated by linear functions defined by nodal values at the nodes of the elements and by linear interpolations of the nodal values on the interiors of the elements. For the general function $\phi = \phi(x,y)$ we have on the element e defined by the nodes i, j and m:

$$\phi_e = \alpha_1 + \alpha_2 x + \alpha_3 y \quad . \tag{5.5}$$

Values for α_1, α_2, and α_3 can be obtained by substituting the nodal values ϕ_i , ϕ_j, and ϕ_m along with their respective coordinate values (x_i,y_i) , (x_j,y_j) and (x_m,y_m) individually into equation (5.5). The resulting system of three simultaneous equations can then be solved for α_1, α_2, and α_3. The resulting expression for ϕ_e is given by Zienkiewicz (1970, equation 3.5, p. 27):

$$\phi_e = \frac{1}{2\Delta}\Big[(a_i + b_i x + c_i y)\phi_i + (a_j + b_j x + c_j y)\phi_j + (a_m + b_m x + c_m y)\phi_m\Big] \tag{5.6}$$

where,

$$a_i = x_i y_m - x_m y_i ,$$

$$b_i = y_i - y_m ,$$

$$c_i = x_m - x_j , \text{ and}$$

$$2\Delta = \det \begin{vmatrix} 1 & x_i & y_i \\ 1 & x_j & y_j \\ 1 & x_m & y_m \end{vmatrix} .$$

The other coefficients are obtained by cyclic permutation of the subscripts in the order i, j, m.

Expressions for the gradient and for the partial derivatives of the functional (5.4) with respect to the nodal values ψ_i, ψ_j, and ψ_m are obtained for the element e by direct operation on (5.6). Using the results from Zienkiewicz (and specializing for the present problem):

(5.7)
$$(\nabla\psi)_e = \frac{1}{2\Delta}\begin{bmatrix} b_i & b_j & b_m \\ c_i & c_j & c_m \end{bmatrix}\begin{bmatrix} \psi_i \\ \psi_j \\ \psi_m \end{bmatrix} = (v\underline{i} - u\underline{j})\, d ,$$

and
$$\frac{\partial \Phi_e}{\partial \psi_i} = (h_{ii}, h_{ij}, h_{im})\begin{bmatrix} \psi_i \\ \psi_j \\ \psi_m \end{bmatrix} - \left(\frac{D\zeta}{Dt}\,\frac{|\Delta|}{3}\right)_e ,$$

where,

$$h_{rs} = \left(\frac{C_f|\underline{V}|}{4|\Delta|}\right)_e (b_r b_s + c_r c_s), \text{ and}$$

$$r,s = i,j,m \quad .$$

The subscript e specifies that the quantity is associated with a particular element ijm. $\left(\frac{D\zeta}{Dt}\right)_e$ was here considered constant on the individual element ijm. It may assume different values from one element to another.

The minimization of Φ requires that $\frac{\partial \Phi}{\partial \psi_r}$ vanish for all r. Thus from equation (5.7):

$$(5.8) \qquad \frac{\partial \Phi}{\partial \psi_r} = 0 = \sum_{e}^{E} \sum_{s}^{NxM} h_{rs}\psi_s + \sum_{e}^{E} \left[\frac{D\zeta}{Dt}\frac{|\Delta|}{3}\right]_r , \text{ and}$$

$$r = 1,2,3,.....(NxM) .$$

The index s ranges over all of the nodes and the index e ranges over all of the elements. The subscript r on the last term indicates that only those elements intersecting node r will be included in the summation. Equations (5.8) result in a system of simultaneous equations; there will be one equation for each node and there will be one unknown ψ_s at each node. By proper numbering of the grid elements the coefficient matrix of the resulting system of simultaneous equations will have a banded structure. It will also be symetric since $h_{rs} = h_{sr}$ for all s and all r by equations (5.7).

Boundary conditions (3.14a) and (3.14b) are formally specified by special equations:

$$(5.9) \qquad \psi_r = \psi_1 \text{ on } \partial D_1$$

$$\psi_r = \psi_2 \text{ on } \partial D_2 .$$

These equations then replace the rth equations in system (5.8).

5.3 Numerical Solution of the Pressure Equation

Consider a channel segment ∂S along a two-dimensional streamline limited to one element e of the finite element grid system. Assume that the stream function is a known function of x and y and that the water-surface elevation Z(s) is known at a point s on the streamline. Since ∂S is limited to the element e, the discharge per unit width is constant along ∂S and is given by the magnitude of the gradient of the stream function $|\nabla\psi|$.

The water surface Z = Z(x,y) will be computed through an application of the pressure equation (4.9) on the streamline segment as follows:

$$\frac{V^2(s)}{2g} + Z(s) = \frac{V^2(s + \Delta s)}{2g} + Z(s + \Delta s) + h_f \tag{5.10}$$

where the head loss due to friction h_f is given by:

$$h_f = \int_s^{s+\Delta s} \frac{F}{g} ds \quad .$$

The values of the terms on the left are known. The left side of the equation represents the total energy at s which will be denoted by E(s).

An application of the mean value theorum for integrals can be used to evaluate h_f as follows:

$$h_f = \frac{F^*}{g} \Delta s \tag{5.11}$$

where F^* is a value of F(s) on the closed interval [s,s+Δs]. A convenient approximation for F^* is the geometric mean of F(s) and F(s+Δs),

$$F^* = \sqrt{F(s)\ F(s+\Delta s)} \quad .$$

Using equation (2.1) to compute the magnitude of friction force F, the above geometric mean results in the following expression for head loss due to friction:

$$h_f = \left[\frac{n(s)}{1.49\ d^{5/3}(s)}\right]\left[\frac{n(s+\Delta s)}{1.49\ d^{5/3}(s+\Delta s)}\right] (\nabla\psi)^2 \tag{5.12}$$

or

$$h_f = \frac{A_f}{d^{5/3}(s+\Delta s)}$$

where A_f is a constant defined in terms of known quantities n(s), n(s+Δs), d(s+Δs) and $|\nabla\psi|$ as follows:

$$A_f = \frac{n(s)n(s+\Delta s)}{(1.49)^2 d^{5/3}(s)} (\nabla\psi)^2 \quad .$$

The velocity head at $(s+\Delta s)$ can also be expressed as a function of $d(s+\Delta s)$:

$$h_v(s+\Delta s) = \frac{(\nabla\psi)^2}{2gd^2(s+\Delta s)} \tag{5.13}$$

or

$$h_v(s+\Delta s) = \frac{B_v}{d^2(s+\Delta s)}$$

where the constant B_v is defined in terms of known quantities as follows:

$$B_v = \frac{(\nabla\psi)^2}{2g} \quad .$$

Finally the water surface at $(s+\Delta s)$ can be expressed as a function of depth by the equation:

$$Z(s+\Delta s) = G(s+\Delta s) + d(s+\Delta s) \tag{5.14}$$

where the ground surface $G(s+\Delta s)$ is given data. Substituting into equation (5.10) and rearranging terms results in the following equation:

$$d(s+\Delta s) = E(s) - \frac{A_f}{d^{5/3}(s+\Delta s)} - \frac{B_v}{d^2(s+\Delta s)} \tag{5.15}$$

This algebraic equation can be solved for $d(s+\Delta s)$. The water surface at $(s+\Delta s)$ can then be computed from equation (5.14).

5.4 Computed Vorticity on Finite Element Grid

The vorticity ζ is related to the stream function as follows:

$$\zeta = \text{curl } \underline{V} = \text{curl}\left[\frac{1}{d}\left(\frac{\partial \psi}{\partial y}, -\frac{\partial \psi}{\partial x}\right)\right] \tag{5.16}$$

$$= \frac{-\nabla^2 \psi}{d} + \nabla\left(\frac{1}{d}\right) \times \underline{V} d \quad .$$

A convenient expression for the Laplacian of the stream function can be obtained by applying Gauss' theorum to the vector $\psi \nabla \psi$ as follows:

$$\int_{\partial A} \psi \nabla \psi \cdot \underline{n} ds = \int_A [(\nabla \psi)^2 + \psi \nabla^2 \psi] dA \quad . \tag{5.17}$$

Rearranging terms results in the following expression:

$$\int_A \psi \nabla^2 \psi dA = \int_{\partial A} \psi \frac{\partial \psi}{\partial n} ds - \int_A (\nabla \psi)^2 dA \quad . \tag{5.18}$$

The above form is particularly useful for calculating the Laplacian on an element of a linear finite element grid. The terms on the right involve only first order derivatives

which can be evaluated by equation (5.7).

The average vorticity ζ_e on the element e can now be expressed as follows:

$$\zeta_e = \left[\frac{(\nabla\psi)^2 |\Delta| - \int_{\partial e} \psi \frac{\partial \psi}{\partial n} ds}{\overline{\psi} |\Delta| d} \right]_e + \left[\nabla \left(\frac{1}{d}\right) x \underline{V} d \right]_e = \text{constant} \tag{5.19}$$

where,

$$\overline{\psi} = (\psi_i + \psi_j + \psi_m)/3 \ .$$

6. SEPARATION

6.1 General

Separation refers to a discontinuity in the velocity field $\underline{V} = \underline{V}(x,y)$ between two dajacent streamlines. Such discontinuities along streamlines do not propagate since no velocity componants are formed. The velocity $\underline{V} = \underline{V}(x,y)$ along all streamlines in the velocity field may still be continuous.

Separation frequently occurs just downstream from a contraction forming a live stream (sometimes referred to in th e literature as a "jet" (Laursen, 1970, p. 1021)) and a stagnation zone (sometimes referred to as an "eddy zone" since the fluid mass rotates very slowly in the form of a large eddy (Kindsvater, Carter and Tracy, 1953, p. 5)).

Figure 6.1 illustrates such a separation. The region D discussed in section 1.3 above is here subdivided into a live stream zone L and a stagnation zone S. The line of separation between them is designated $\partial S_f = \partial L \cap \partial S$. The velocity field on S is taken as zero. No fluid crosses the boundary of the stagnation zone ∂S. The live stream zone L can be considered analagous to the original zone D of section 1.3 with ∂S_f a solid boundary. The differences between zone L of the present discussion and zone D are: 1) the location of ∂S_f is not known in advance, and 2) the non-solid boundary ∂S_f will not support a discontinuity in pressure between zones S and L.

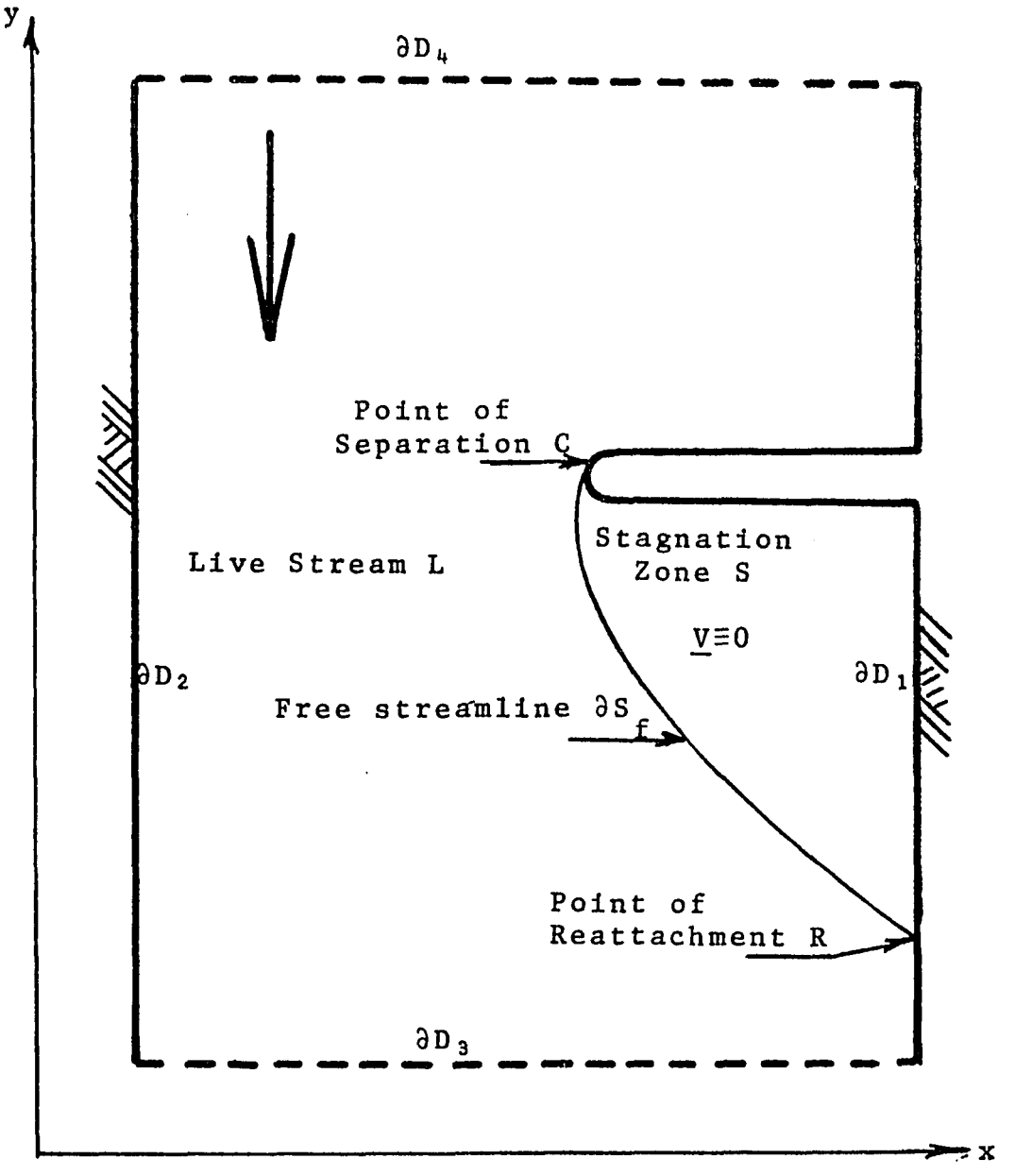

Figure 6.1 -- Schematic Diagram for Free Boundary Problem on Flow Separation

If such a condition existed in a physical problem the velocity discontinuity would generate large viscous forces along the line of separation. These viscous forces would impart some small momentum to the fluid in the stagnation zone causing the latter to move slowly in a rotational pattern. There would be no interchange of fluid between zones L and S, however, and the average velocity of the center of mass of the fluid in zone S would be zero.

The viscous forces referred to above that would cause the rotational motion of zone S have been neglected throughout the formulation of this mathematical model (cf. approximation (4) section 1.3). The fluid in S will, therefore, be considered stagnant in further discussions.

The depth integrated average pressure field $P = P(x,y)$ (cf. equation 4.2) cannot be discontinuous at a non-solid boundary. Such a discontinuity would require external forces to maintain the conservation of momentum stated by equation 3.10. Since the fluid in zone S is stagnant, the depth integrated average pressure gradient ∇P of equation 4.1 must vanish. It follows that the water surface $Z = Z(x,y)$ on S must be constant. (Even in the physical problem the stationarity of the center of mass of the fluid S leads to the conclusion that the water-surface elevations on S are approximately constant).

Since there can be no discontinuity in pressure on ∂S_f and the pressure on S is constant, there can be no pressure variation on the non-solid boundary ∂S_f. This provides the following additional boundary condition necessary to locate ∂S_f:

$$Z(x,y) = Z_s \qquad \text{on } \partial S_f \cup S \tag{6.1}$$

where,

Z_s = constant water-surface elevation on S.

Consider now the effect of a small perturbation in a free streamline ∂S_f which initially satisfies condition (6.1). Let any pressure differential generated along ∂S_f be supported by a hypothetical thin solid barrier along ∂S_f. Such a barrier would have no effect on the initial condition since the pressure would be the same on both of its faces and there is no flow between zones S and L across ∂S_f. Let the perturbations be small enough that they do not significantly change the flow distribution or velocity field on L.

Consider first perturbing ∂S_f by moving R toward the embankment along the solid boundary as shown in figure (6.2). Such a perturbation would cause an increase in water level on S since R would be further upstream along the streamline on the solid boundary and the friction loss along that streamline between R and the downstream water-level control (cf. equation 4.10) would be increased. The increase in

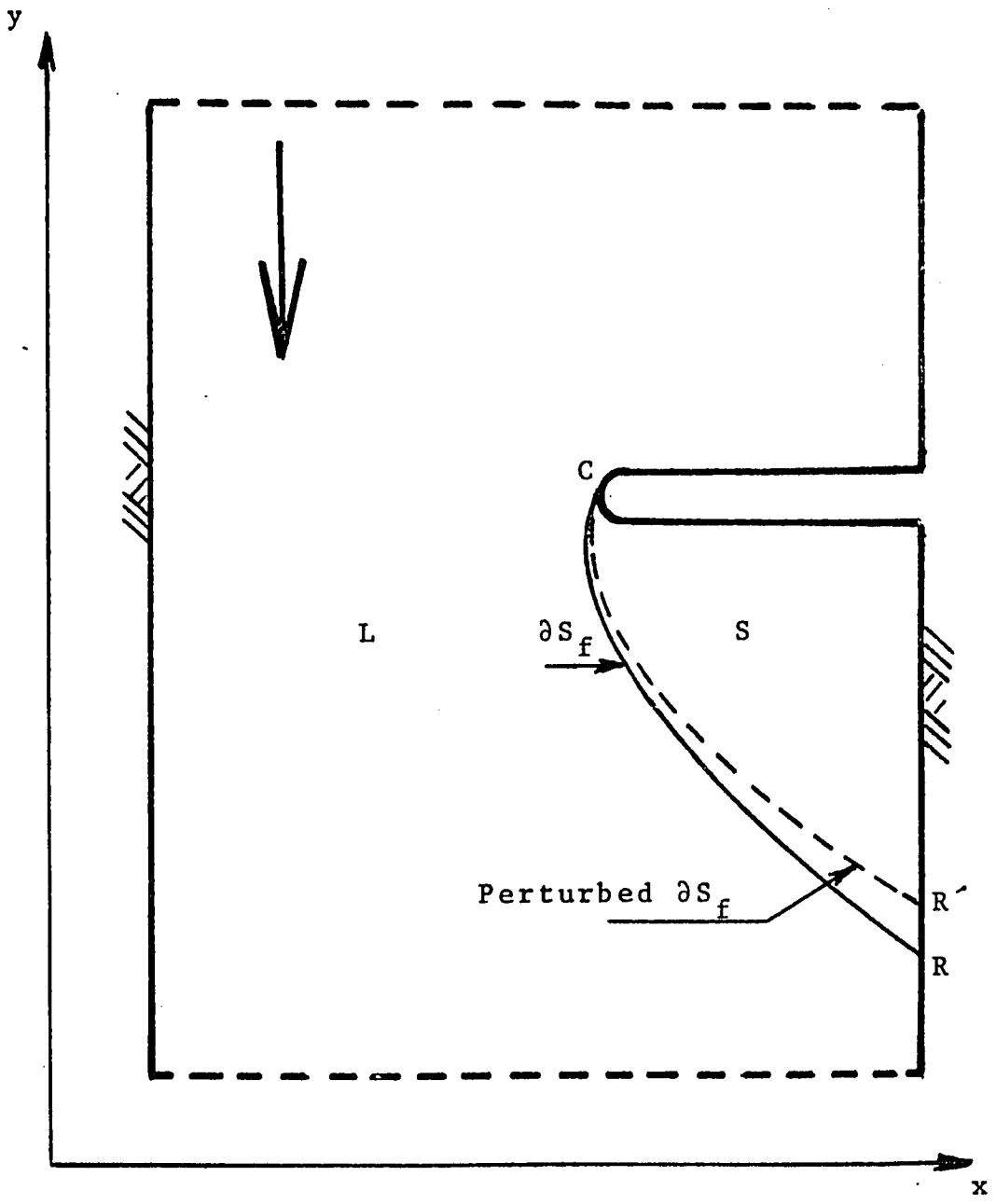

Figure 6.2 -- Schematic Diagram Showing
Perturbation of Free Boundary

water level on S would cause a differential pressure force on the solid barrier that would tend to move it toward its initial position. If the barrier were moved in the opposite direction the water level would decrease on S causing a pressure force on the barrier that would tend to move it toward its initial position. The barrier will, therefore, be in stable equilibrium when it is on ∂S_f.

This argument implies that the path ∂S_f is a one parameter function of the position of R on the solid boundary ∂D; the question of uniqueness for general shapes of ∂S_f is not easily resolved particularly for rotational flows affected by friction.

6.2 Necessary Condition for Existence of Separation

Condition (6.1) provides a basis for the formulation of a necessary condition for the existence of separation. Since the water surface on ∂S_f cannot vary, equation (4.9) reduces to the following expression:

$$(6.2)\quad \frac{V^2}{2g} - \int_o^s \frac{F}{g} ds = B(\psi) - Z_s = \text{constant on } \partial S_f .$$

Equation (6.2) specifies that any change in velocity head between any two points on ∂S_f must be balanced by the head loss due to friction on ∂S_f between the two points. This condition can be applied to the two points C and R on ∂S_f which represent the abutment of the bridge opening and the

point of reattachment respectively (see figure 6.1 as follows:

$$(6.3) \qquad \left(\Delta\frac{V^2}{2g}\right)_{CR} = \int_C^R \frac{F}{g} ds$$

or

$$\left(\Delta h_v\right)_{CR} = \left(h_f\right)_{CR} .$$

The term on the left will be referred to as the kinetic energy excess since it represents the quantity of kinetic energy that will be dissipated by friction loss on the free streamline.

Equation (6.3) implies a necessary condition for the existence of separation downstream from a bridge abutment: the kinetic energy excess in the two-dimensional streamline at the abutment must exceed the head loss due to friction on that streamline between the point of separation C and the point of reattachment R.

If the kinetic energy excess at C is less than the head loss due to friction on ∂S_f then the water-surface elevation at C must exceed the water-surface elevation Z_s on S. This follows from the pressure equation (4.9). If such a condition characterizes every choice of the free streamline ∂S_f then there will be no separation. The streamline passing through the point C at the abutment will follow the downstream side of the embankment and continue

along the solid bank ∂D_1 or ∂D_2.

Separation will not occur if the channel resistance C_f is very large in the expansion region just downstream from the contracted section. In such cases the head loss due to friction will be large along all possible choices for ∂S_f. There will be little possibility for the kinetic energy excess $(\Delta h)_{CR}$ to be greater than $(h_f)_{CR}$. Even if the discharge Q is increased, the basic relationship between kinetic energy excess and head loss due to friction will be unchanged since both are proportional to velocity head (cf. equation 2.1). Only if the discharge is increased to the extent that the channel resistance $C_f = C_f[x,y;Z(x,y)]$ (cf. equation 2.7) is affected through a change in water level $Z = Z(x,y)$ on D will conditions necessary to the existance of separation be changed. Channel resistance C_f will usually be the determing factor.

7. EXAMPLE PROBLEMS

7.1 The Computer Program

Algorithm 5.1 has been programmed for the IBM 360 model 65 computer at Louisiana State University.

The finite element grid described in section 5.2 (cf. figure 5.1) is defined by the x and y coordinates of each node. The nodes are indexed by the row-column index designation (I, J) described in section 5.2. The k-index is assigned and used internally.

The ground-surface elevation G and Manning roughness coefficient n for each node are input to the program. The grid nodes J = 1 are placed on the solid boundary ∂D_2 of the region D described in section 1.3 (cf. figure 1.4). Likewise, the grid nodes J = M are placed on the solid boundary ∂D_1 and the grid nodes I = 1 and I = N are assumed to lie on the downstream and upstream flow boundaries ∂D_3 and ∂D_4 respectively. The stream function values at the nodes J = 1 are set to ψ_2 and those at nodes J = M are set to ψ_1 (cf. equations 5.9). The values of ψ_1 and ψ_2 specify the total discharge Q (cf. equation 3.15). Downstream water-surface elevations (cf. equation 4.10) are specified at nodes I = 1.

Algorithm 5.1 is then executed with these input data.

7.2 Flow Through an Expansion -- Example Free Streamline Problem

Flow through an expansion with separation as shown in figure 7.1 is an example of a free streamline problem. The flow separates at the corner C into a live stream zone L and a stagnation zone S where the common boundary $\partial S_f = \partial L \cap \partial S$ is the free streamline (cf. section 6.1).

The geometry of the free streamline is specified as a one parameter function of the location of the point of reattachment R. The point of reattachment R is then adjusted until the necessary condition (6.3) for separation is satisfied.

The expansion dimensions are parameterized as follows (see figure 7.1):

1) y_R = distance of point of reattachment R measured from expansion,
2) x_e = the difference between the width of the expanded section and the width of the contracted section, and
3) n = hydraulic roughness (constant over entire region).

The results of the model study are summarized in table 7.1. After each of the trial computer runs the head loss due to friction on the free streamline $(h_f)_{CR}$ is compared to the kinetic energy excess on the free streamline $(\Delta h_v)_{CR}$. If the head loss due to friction on ∂S_f is found to exceed

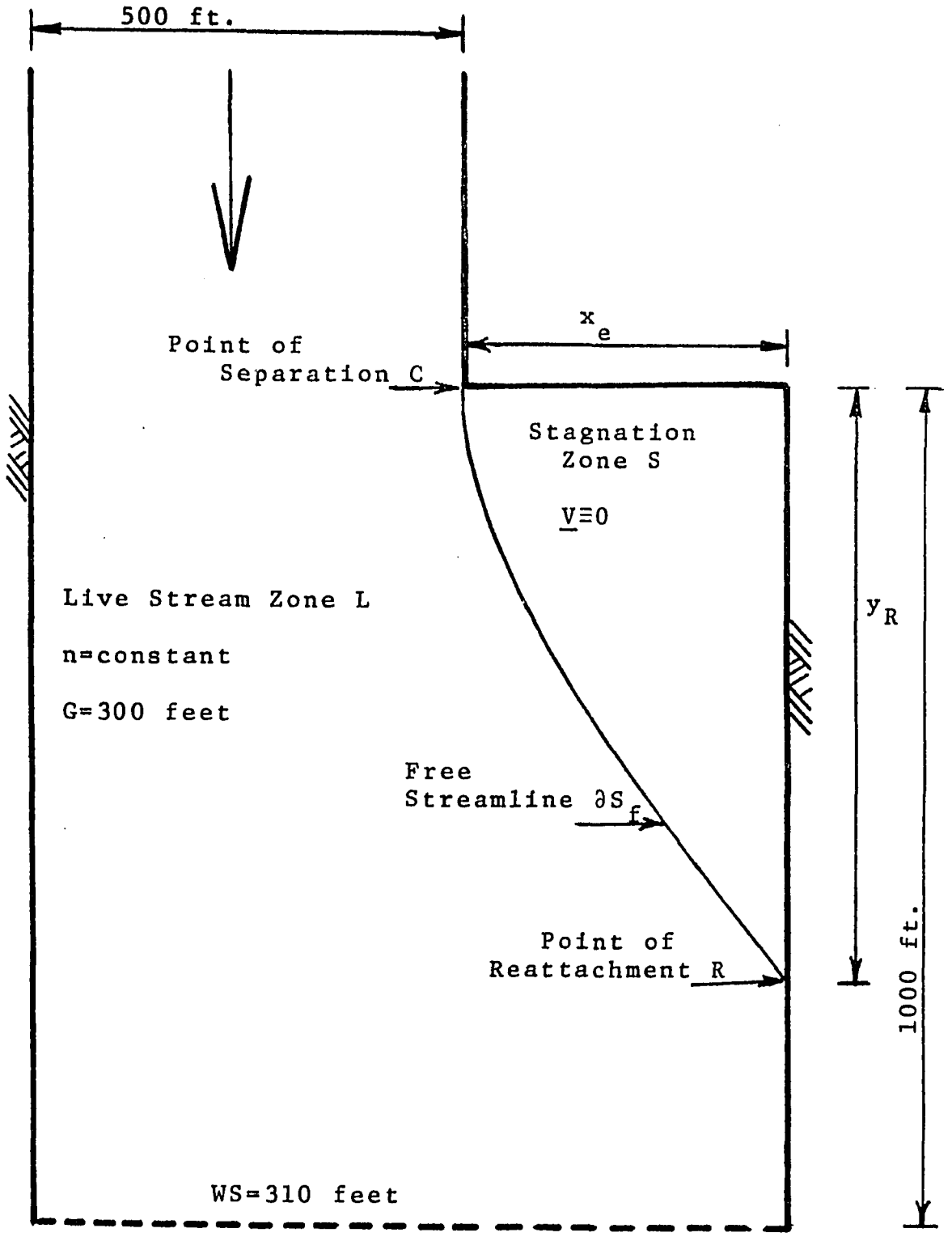

Figure 7.1 -- Schematic Diagram for Flow through an Expansion

Table 7.1

Flow through Expansion -- Example Problem
Summary of Results

Case No.	x_e	n	y_R	$(\Delta h_v)_{CR}$	$(h_f)_{CR}$	$\lvert \partial S_f \rvert$	Comments
1	300	0.05	400	.097	.115	516	Long
2	300	0.05	350	.103	.106	477	OK
3	300	0.05	300	.111	.096	440	Short
4	500	0.05	450	.111	.133	787	Long
5	500	0.05	400	.111	.128	685	Long
6	500	0.05	350	.121	.112	629	Short
7	500	0.05	250	.130	.121	590	Short
8	1000	0.05	300	.281	.113	1079	Short
9	1000	0.05	600	.164	.125	1209	Short
10	500	.125	150	.144	.579	538	Long

the kinetic energy excess on ∂S_f the entry in table 7.1 is marked "long" and the length of the free streamline $|\partial S_f|$ is decreased on the next computer run by decreasing y_R, thereby moving the point of reattachment R farther upstream. If the kinetic energy excess is found to exceed the head loss due to friction, the entry is marked "short" and $|\partial S_f|$ is increased on the next run by increasing y_R, thereby moving R farther downstream. The trial and error process is terminated when condition (6.3) is approximated.

Cases 1, 2, and 3 represent a ratio of expanded section to contracted section of 8/5 (x_e = 300 feet). The head loss due to friction is greater than the kinetic energy excess for case 1; the length of the free streamline $|\partial S_f|$ is consequently designated as too "long" and y_R is changed to 300 feet (case 3). For y_R = 300 feet the length of the free streamline $|\partial S_f|$ is decreased from 516 feet (case 1) to 440 feet (case 3); the kinetic energy excess is found to exceed the head loss due to friction for case 3 and $|\partial S_f|$ is marked too "short". Finally an intermediate value for y_R(350 feet) is chosen (case 2) and the head loss due to friction on ∂S_f is found to be approximately equal to the kinetic energy excess on ∂S_f. Condition (6.3) is approximated and case 2 for which the length of the free streamline is 477 feet is marked "OK" for an expansion ratio of 8/5 (x_e = 300 feet). The

procedure is, therefore, terminated.

In order to investigate the hypothesis that the channel resistance is the determining factor for the existance of separation, the width of the expanded section was increased while holding the hydraulic roughness constant.

Cases 4, 5, 6, and 7 represent an expansion ratio of 2 ($x_e = 500$ feet). Condition (6.3) is approximated for $y_R \simeq 375$ feet (cases 5 and 6). Thus separation can exist for expansion ratios of 8/5 and 2 when the hydraulic roughness is held to n = 0.05.

Even when the expansion ratio is increased to 3 (x_e = 1000 feet) the kinetic energy excess can still dominate the head loss due to friction on the free streamline (cases 8 and 9).

Only by increasing the hydraulic roughness (case 10) can a case be found for which head loss due to friction exceeds the kinetic energy excess for all choices of the free streamline ∂S_f. It is, therefore, concluded that hydraulic roughness is an important parameter in determining existance of separation. More generally the channel resistance C_f (or conveyance) is probably the most important parameter since variations in the channel depth could also change the relationship between velocity head and friction stress along the free streamline (cf. equation 2.1).

7.3 Bridge Site Analysis for Tallahala Creek at State Highway 528 Near Bay Springs, Mississippi

7.3.1 Flood of April 14, 1969

The computer program described above (section 7.1) was used to simulate the flood of April 14, 1969, at Tallahala Creek at State Highway 528 near Bay Springs, Mississippi. The site is a USGS gaging station; a site map is shown in figure 7.2. A discharge measurement was made at a gage height of 311.28 feet above mean sea level; the measured discharge was 9,780 cubic feet per second (cfs). The flood crested at a gage height of 311.97 feet above mean sea level and the peak discharge was determined from the station rating to be 12,500 cfs.

The values of predicted fall Δh and predicted backwater for the flood were calculated by the writer according to the USGS technique (USGS, 1955) and the BPR technique (BPR, 1970). For the USGS technique the predicted backwater would be 0.240 feet and the predicted fall Δh would be 0.460 feet. For the BPR method the predicted backwater would be 0.299 feet and the predicted fall would be 0.510 feet. Figure 7.3 shows a backwater of 1.5 feet and a fall Δh of 0.90 feet. The normal water surface profile shown on figure 7.3 was determined by step backwater calculations (Anderson and Anderson, 1964); the cross sections that would have existed in the natural channel had the embankment not been in place were estimated.

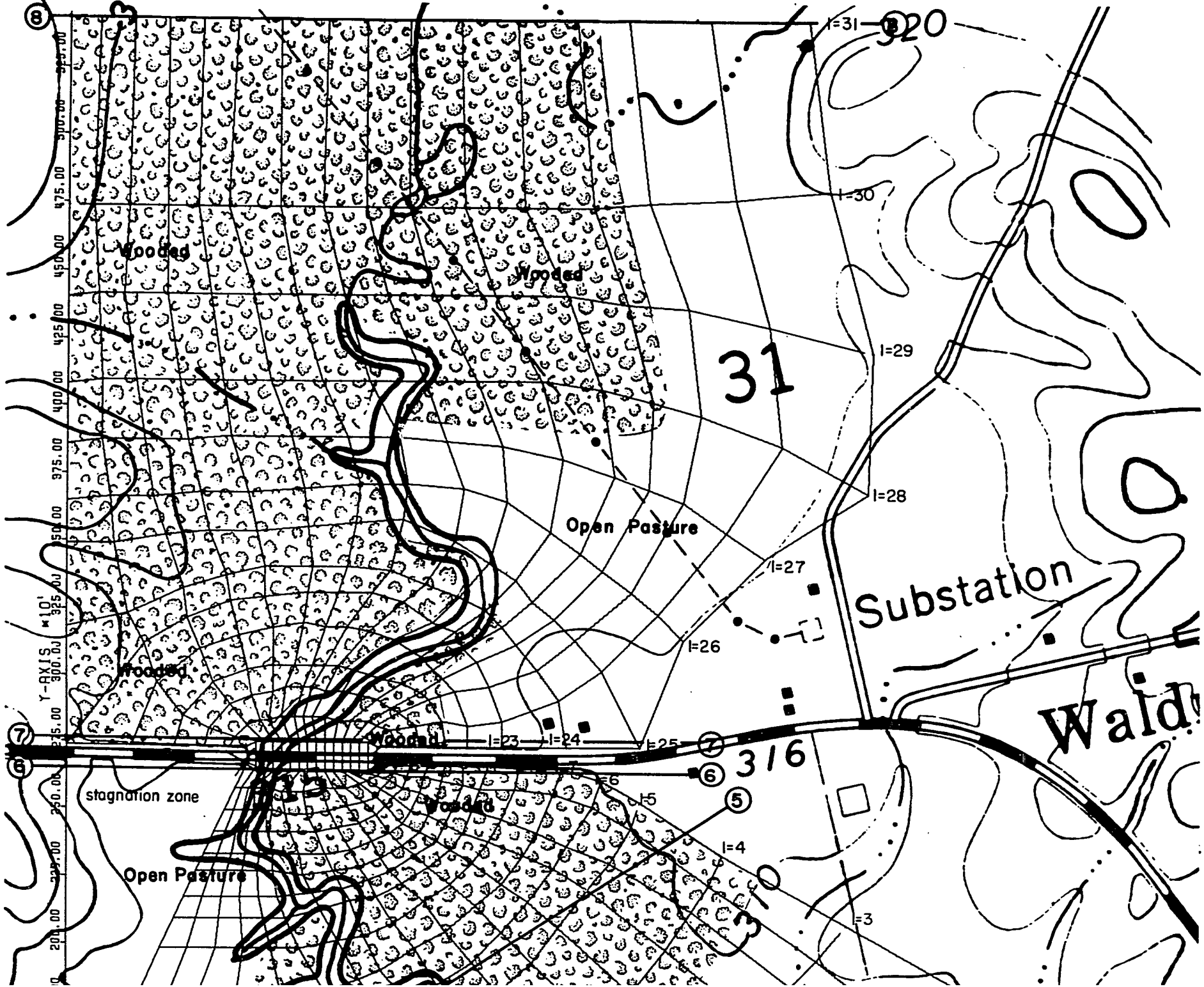
I=31
320
I=30
Wooded
Wooded
31
I=29
I=28
Open Pasture
I=27
Substation
I=26
Wooded
Wooded
I=23
I=24
I=25
316
stagnation zone
Wooded
I=4
Open Pasture
I=3
Y-AXIS *10'
300.00
325.00
350.00
375.00
400.00
425.00
450.00
475.00
200.00
225.00
250.00

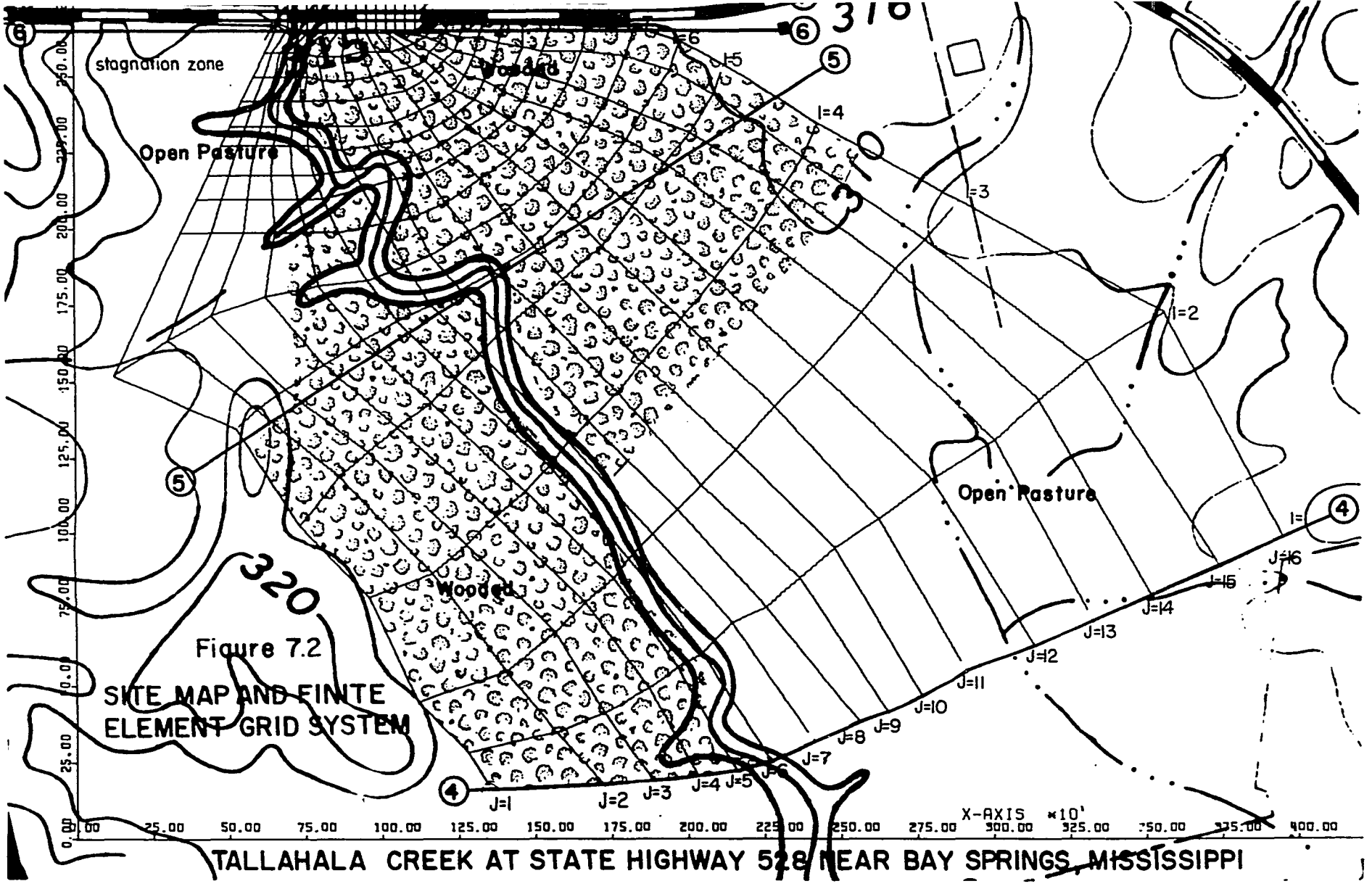

Figure 7.2

SITE MAP AND FINITE ELEMENT GRID SYSTEM

TALLAHALA CREEK AT STATE HIGHWAY 528 NEAR BAY SPRINGS, MISSISSIPPI

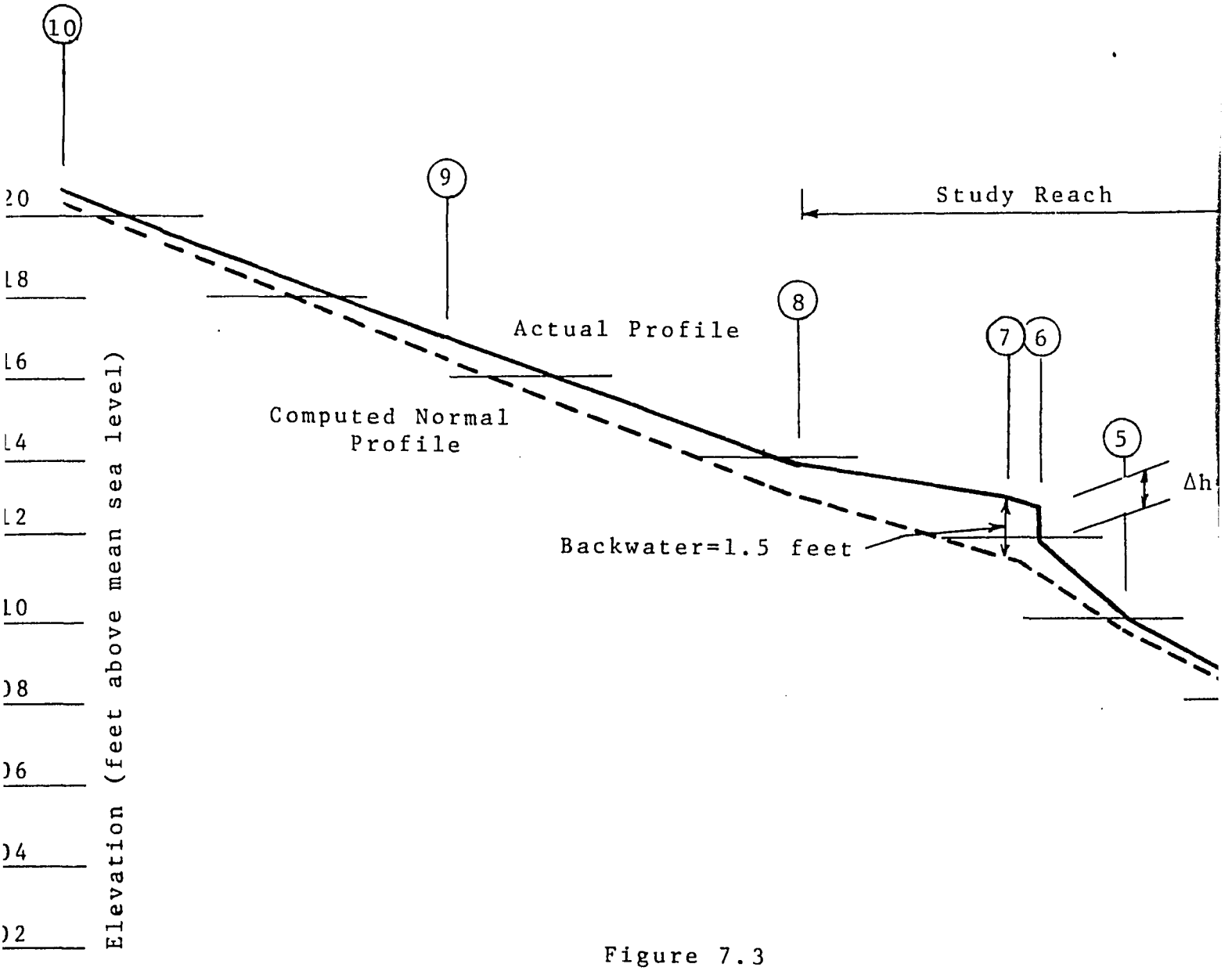

Figure 7.3
Water Surface Profiles
East Tallahala Creek at State Highway 528 near Bay Springs, Mississi
Flood of April 14, 1969

Distance in Thousands of Feet along Channel Centerline

24 23 22 21 20 19 18 17 16 15 14 13 12 11 10

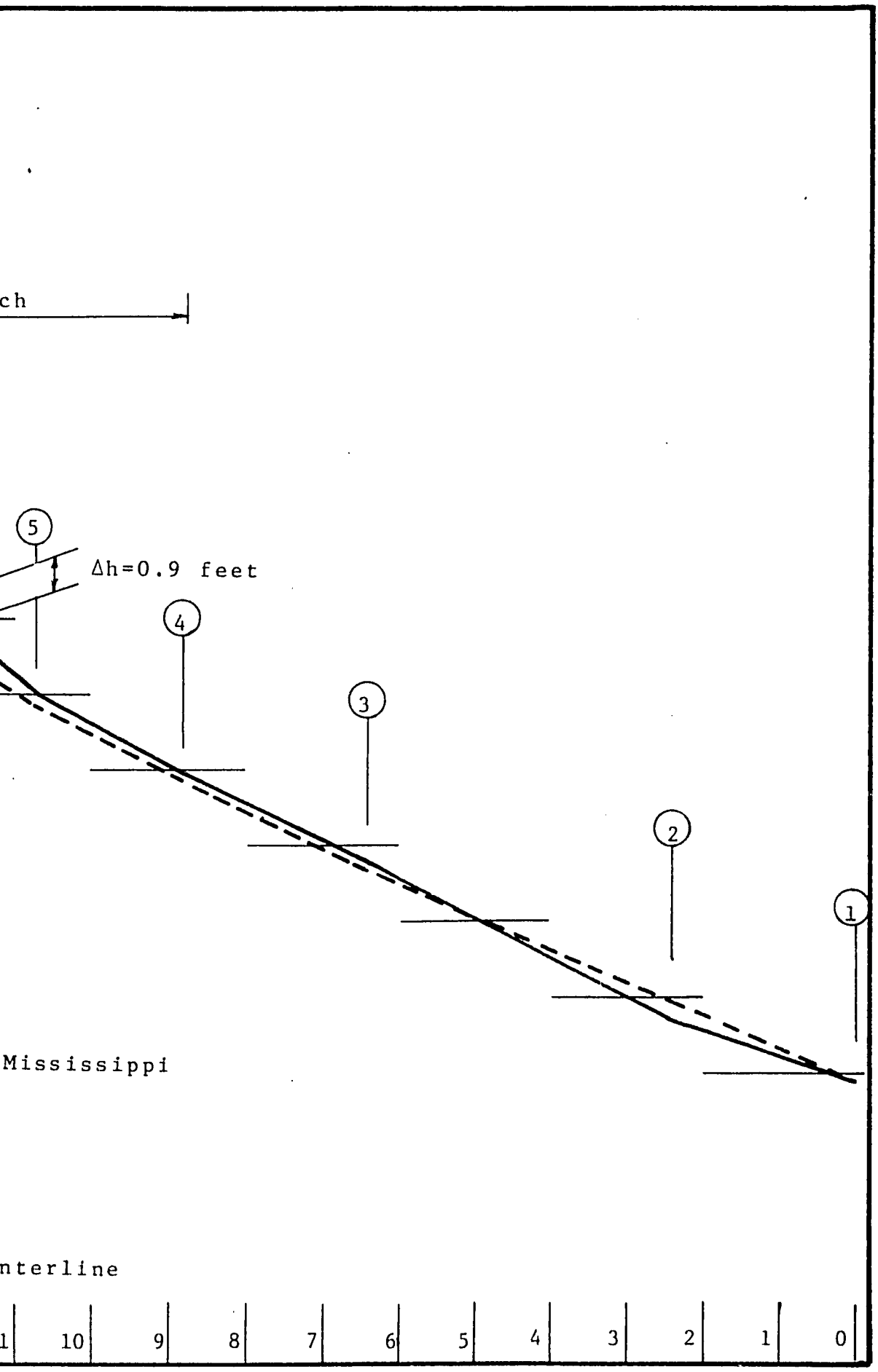
ch
5
Δh=0.9 feet
4
3
2
1
Mississippi
nterline
11
10
9
8
7
6
5
4
3
2
1
0

Neither the normal water-surface profile nor the backwater can be measured objectively; only the fall Δh is subject to objective measurement (cf. section 1.2.2).

The values of predicted backwater are smaller than the values for predicted fall. This condition will always exist since currently used empirical techniques are based on weir formulae for prismatic channels. Such one-dimensional mathematical models can lead only to the conclusion that water levels will be above normal upstream from the weir and below normal downstream from the weir; a weir in a one-dimensional flow field cannot raise downstream water levels.

Figure 7.3 shows above normal water levels downstream from the contraction as well as a value for backwater that is greater than the value for fall Δh. Increased velocities and increased lengths of streamlines in the expansion zone just downstream from the contraction can cause this above normal water level downstream from the contraction at least along the channel centerline. This is true particularly for heavily vegetated flood plains where separation does not exist (cf. section 6.2) and the streamlines are greatly lengthened by the contraction. Head loss due to friction along the longer streamlines with higher velocities and high hydraulic roughness will cause great friction loss in the expansion zone.

The USGS surveyed high-water marks and ground elevations at ten cross sections of the valley after the flood. The locations of the surveyed cross sections are indicated on the water-level profiles in figure 7.3. The USGS field party also made estimates of the hydraulic roughness (Manning n-values) (cf. section 2).

The surveyed data is not detailed enough for the present study. Only five cross sections were taken in the study reach (see figure 7.3). The data was extended on the basis of USGS topographic maps and aerial photographs to obtain roughness coefficients and ground elevations for the entire study region. These estimates as well as the field estimates of roughness are very sensitive to human judgement.

Since the data are incomplete, the results of this analysis are inconclusive for purposes of field verification of the theory set forth in this dissertation. The USGS is currently collecting flood data at bridge sites in Louisiana, Mississippi, and Alabama in cooperation with State Highway Departments and the Bureau of Public Roads for the purpose of such verification. It is anticipated that the USGS will use this model for verification and calibration in conjunction with the data collection program.

Figure 7.2 shows the site and the finite element grid system that was fitted to it. Each of the quadrilateral

elements shown were divided into two triangular elements according to the scheme discussed in section 5.2 and illustrated in figure 5.1. The row and column (I,J) indexing are shown on figure 7.2. The major roughness patterns are also indicated on figure 7.2. The hydraulic roughness of the wooded areas shown were assigned Manning n-values ranging from n = 0.125 to n = 0.250 by the survey party. The highest hydraulic roughness that was field calibrated by Barnes (1967) is n = 0.075; the writer knows of no field calibration of hydraulic roughness in the range n = 0.125 to n = 0.250. Ground-surface elevations can be read from the contours of the site map in figure 7.2.

Detailed ground elevations determined at each of the grid nodes by using the topographic map, aerial photographs, and the surveyed cross sections are tabulated in table 7.2. The tabulated values may be located on figure 7.2 by the row and column (I,J) indeces.

Values for hydraulic roughness were increased by ten percent at the nodes corresponding to the solid boundaries ∂D_1 and ∂D_2 (cf. figure 1.4) in order to account for the increased wetted perimeter at the edges of the region D. The hydraulic roughness at nodes (I=18, J=1) and (I=18, J=16) were set to 10.000 in order to simulate the effects of spur dikes located on the upstream side of the embankment.

Preliminary calculations using values of hydraulic

TABLE 7.2

TALLAHALA CREEK AT STATE HIGHWAY 528 NEAR BAY SPRINGS, MISSISSIPPI
GROUND SURFACE ELEVATIONS
(FEET ABOVE MEAN SEA LEVEL)

I	J=1	J=2	J=3	J=4	J=5	J=6	J=7	J=8	J=9	J=10	J=11	J=12	J=13	J=14	J=15	J=16
31	309.40	309.40	309.10	309.20	309.20	309.20	309.60	308.40	308.40	308.40	308.60	308.60	309.00	309.20	310.00	310.20
30	309.40	309.40	309.10	309.20	309.20	309.20	309.60	308.40	308.40	308.40	308.60	308.60	309.10	309.40	310.00	310.20
29	309.00	309.00	309.00	309.00	309.00	309.00	308.40	308.40	308.40	308.60	308.80	309.00	309.00	309.50	309.50	309.50
28	309.00	309.00	309.00	309.00	309.00	309.00	308.40	308.40	300.00	308.80	309.00	309.00	309.00	309.50	309.50	309.50
27	309.00	309.00	309.00	309.00	309.00	308.40	308.40	300.00	308.40	308.40	309.00	309.00	309.00	309.50	309.50	309.50
26	308.60	308.60	308.60	308.60	308.60	308.60	308.40	300.00	309.00	309.00	309.00	309.00	309.00	309.50	310.00	310.00
25	308.40	308.40	308.40	308.40	308.40	308.40	308.40	300.00	300.00	300.00	308.00	308.00	308.80	308.80	309.40	310.00
24	308.40	308.40	308.40	308.40	308.40	308.40	308.40	308.40	307.00	300.00	300.00	307.00	307.80	307.80	308.80	308.80
23	308.40	308.40	308.40	308.40	308.40	308.40	308.40	308.40	305.60	305.60	300.00	300.00	306.80	306.80	306.80	306.80
22	310.00	308.40	308.40	308.40	308.40	308.40	308.40	308.40	308.40	308.40	300.00	300.00	305.60	305.60	306.20	306.20
21	308.00	308.00	306.40	304.00	304.00	304.00	304.00	304.00	304.00	304.00	300.00	300.00	304.40	305.60	305.60	305.60
20	306.00	306.00	306.00	306.00	306.00	306.00	306.00	304.30	304.30	304.30	300.00	300.00	304.30	304.30	304.60	304.70
19	306.00	306.00	304.40	300.00	300.00	300.00	300.00	298.00	298.00	300.00	300.00	304.40	304.40	304.40	304.70	304.70
18	300.00	298.00	298.00	300.00	300.00	300.00	300.00	304.40	304.40	304.40	304.40	304.40	304.40	304.40	304.60	304.60
17	302.00	300.00	298.00	298.00	298.00	302.00	306.00	306.00	306.00	306.00	306.00	306.00	306.00	306.00	306.00	306.00
16	300.00	300.00	298.00	298.00	298.00	300.00	300.00	300.00	304.40	304.40	304.40	304.40	304.40	304.40	304.40	304.40
15	299.90	299.90	299.90	299.90	299.90	299.90	299.90	304.40	304.40	304.40	304.40	304.40	304.40	304.40	304.40	304.40
14	306.00	298.00	298.00	298.00	298.00	298.00	305.00	305.00	304.50	304.50	304.40	306.00	307.50	307.80	308.00	308.00
13	306.80	297.90	297.90	297.90	297.95	305.00	305.00	305.40	305.00	304.50	304.50	304.50	308.00	308.00	307.80	307.80
12	308.80	302.00	302.00	302.00	302.00	297.80	301.00	304.50	304.50	304.50	305.00	308.00	306.00	306.00	306.00	306.00
11	308.80	305.70	305.70	305.70	305.50	297.80	301.00	302.00	304.50	304.70	308.00	306.00	306.00	306.00	305.80	305.80
10	308.80	305.60	305.60	305.60	305.40	305.20	305.00	304.60	304.60	308.00	306.00	306.30	306.30	306.00	306.00	306.00
9	308.80	305.50	305.50	305.50	305.25	303.00	303.00	303.00	303.00	308.00	306.30	306.30	306.30	306.30	306.40	306.40

TABLE 7.2 CONTINUED

TALLAHALA CREEK AT STATE HIGHWAY 528 NEAR BAY SPRINGS, MISSISSIPPI
GROUND SURFACE ELEVATIONS
(FEET ABOVE MEAN SEA LEVEL)

I	J=1	J=2	J=3	J=4	J=5	J=6	J=7	J=8	J=9	J=10	J=11	J=12	J=13	J=14	J=15	J=16
8	308.80	304.75	304.75	304.75	304.63	304.50	301.00	301.00	303.00	305.20	306.00	306.30	306.30	306.30	306.80	306.80
7	308.80	308.80	306.80	304.50	304.50	304.50	305.50	305.50	305.50	305.50	306.00	306.20	306.30	306.30	308.00	308.00
6	305.20	304.40	304.20	304.00	304.50	306.00	305.50	305.50	300.00	305.50	305.50	306.00	307.20	307.80	308.20	308.60
5	304.00	304.00	304.00	305.00	305.00	305.50	305.50	300.00	305.50	305.50	305.50	307.20	307.20	307.20	307.20	307.20
4	305.00	305.00	305.00	305.00	305.00	305.00	300.00	305.00	305.00	305.00	305.00	305.00	306.40	306.40	306.40	306.40
3	306.00	306.00	305.00	305.30	305.00	300.00	305.00	305.00	305.00	305.00	305.00	305.70	306.40	306.40	306.40	306.40
2	306.50	306.00	306.00	306.00	305.00	300.00	305.00	305.00	305.00	304.20	304.00	304.00	304.00	304.00	305.20	306.40
1	305.50	305.50	305.50	306.00	305.50	300.00	304.50	304.40	304.40	304.40	304.00	304.00	304.00	303.80	304.50	305.00

roughness based on the estimates of the survey party resulted in an average computed water level at cross section 8 of 314.3. The actual water-surface profile in figure 7.3 shows a water level of 313.9 at cross section 8. It was found that by multiplying all of the roughness coefficients by 0.80 the correct water level at cross section 8 could be computed. The adjusted roughness coefficients were used for all further calculations; they are tabulated for each node of the finite element grid in table 7.3. The tabulated values can be located on the site map of figure 7.2 by the row and column (I,J) indeces.

The computed results are tabulated for the nodes of the finite element grid system in tables 7.4 and 7.5. The computed water levels are tabulated in table 7.5 and the computed normalized stream function values are tabulated in table 7.4. The actual stream function values are obtained by multiplying the tabulated values by the total discharge 12,500 cfs. The normalized values are convenient for studying the distribution of flow since they can be read directly as fractions of the total discharge.

Figure 7.4 shows the computed two-dimensional flow distribution and a water-level contour map prepared from the computed water levels tabulated in table 7.5. The water-level contours were sketched according to the procedure discussed in section 4.3. Where the flow distribution is approximately irrotational the contours were

TABLE 7.3

TALLAHALA CREEK AT STATE HIGHWAY 528 NEAR BAY SPRINGS, MISSISSIPPI
FLOOD OF APRIL 14, 1969
HYDRAULIC ROUGHNESS COEFFICIENTS
(MANNING N-VALUES)

I	J=1	J=2	J=3	J=4	J=5	J=6	J=7	J=8	J=9	J=10	J=11	J=12	J=13	J=14	J=15	J=16
31	0.176	0.160	0.160	0.160	0.160	0.160	0.160	0.096	0.096	0.096	0.120	0.120	0.144	0.160	0.032	0.035
30	0.176	0.160	0.160	0.160	0.160	0.160	0.160	0.096	0.096	0.096	0.120	0.144	0.144	0.160	0.032	0.035
29	0.176	0.160	0.160	0.160	0.160	0.160	0.160	0.096	0.096	0.120	0.120	0.144	0.160	0.160	0.032	0.035
28	0.176	0.160	0.160	0.160	0.160	0.160	0.096	0.096	0.096	0.120	0.144	0.144	0.160	0.032	0.032	0.035
27	0.176	0.160	0.160	0.160	0.160	0.160	0.096	0.096	0.120	0.064	0.032	0.032	0.032	0.032	0.032	0.035
26	0.132	0.120	0.120	0.120	0.120	0.120	0.120	0.032	0.032	0.032	0.032	0.032	0.032	0.032	0.032	0.035
25	0.132	0.120	0.120	0.120	0.120	0.120	0.120	0.048	0.048	0.048	0.032	0.032	0.032	0.032	0.032	0.035
24	0.132	0.120	0.120	0.120	0.120	0.120	0.120	0.120	0.120	0.048	0.048	0.032	0.032	0.032	0.032	0.035
23	0.132	0.120	0.120	0.120	0.120	0.120	0.120	0.120	0.120	0.120	0.120	0.120	0.120	0.120	0.120	0.132
22	0.132	0.120	0.120	0.120	0.120	0.120	0.120	0.120	0.120	0.120	0.120	0.120	0.120	0.120	0.120	0.132
21	0.132	0.120	0.120	0.120	0.120	0.120	0.120	0.120	0.120	0.120	0.120	0.120	0.120	0.120	0.120	0.132
20	0.132	0.120	0.120	0.120	0.120	0.120	0.120	0.120	0.120	0.120	0.120	0.120	0.120	0.120	0.120	0.132
19	10.000	0.120	0.120	0.048	0.048	0.048	0.048	0.048	0.048	0.080	0.080	0.080	0.080	0.080	0.120	10.000
18	0.034	0.031	0.031	0.031	0.031	0.031	0.031	0.031	0.031	0.031	0.031	0.031	0.031	0.031	0.031	0.034
17	0.038	0.035	0.035	0.035	0.035	0.035	0.035	0.035	0.035	0.035	0.035	0.035	0.035	0.035	0.035	0.038
16	0.038	0.035	0.035	0.035	0.035	0.035	0.035	0.035	0.035	0.035	0.035	0.035	0.035	0.035	0.035	0.038
15	0.035	0.040	0.040	0.040	0.040	0.056	0.056	0.160	0.160	0.160	0.160	0.160	0.160	0.160	0.160	0.176
14	0.035	0.040	0.040	0.040	0.040	0.056	0.160	0.160	0.160	0.160	0.160	0.160	0.160	0.160	0.160	0.176
13	0.035	0.040	0.040	0.040	0.040	0.056	0.056	0.056	0.160	0.160	0.160	0.160	0.160	0.160	0.160	0.176
12	0.035	0.040	0.040	0.040	0.040	0.056	0.056	0.160	0.160	0.160	0.160	0.160	0.160	0.160	0.160	0.176
11	0.035	0.040	0.040	0.040	0.040	0.056	0.056	0.056	0.160	0.160	0.160	0.160	0.160	0.160	0.160	0.176
10	0.035	0.040	0.040	0.040	0.040	0.071	0.071	0.160	0.160	0.160	0.160	0.160	0.160	0.160	0.160	0.176
9	0.035	0.040	0.040	0.040	0.040	0.120	0.120	0.160	0.160	0.160	0.160	0.160	0.160	0.160	0.200	0.220

TABLE 7.3 CONTINUED

TALLAHALA CREEK AT STATE HIGHWAY 528 NEAR BAY SPRINGS, MISSISSIPPI
FLOOD OF APRIL 14, 1969
HYDRAULIC ROUGHNESS COEFFICIENTS
(MANNING N-VALUES)

I	J=1	J=2	J=3	J=4	J=5	J=6	J=7	J=8	J=9	J=10	J=11	J=12	J=13	J=14	J=15	J=16
8	0.035	0.040	0.040	0.040	0.040	0.120	0.106	0.106	0.160	0.160	0.160	0.160	0.160	0.200	0.200	0.220
7	0.035	0.032	0.032	0.032	0.160	0.120	0.120	0.160	0.160	0.160	0.160	0.160	0.177	0.200	0.200	0.220
6	0.078	0.035	0.032	0.160	0.120	0.120	0.120	0.120	0.120	0.160	0.160	0.160	0.200	0.200	0.200	0.132
5	0.088	0.080	0.160	0.160	0.120	0.120	0.120	0.120	0.160	0.160	0.160	0.177	0.200	0.200	0.120	0.132
4	0.101	0.142	0.160	0.160	0.120	0.120	0.120	0.160	0.160	0.160	0.160	0.200	0.200	0.142	0.120	0.132
3	0.106	0.200	0.200	0.191	0.144	0.056	0.036	0.036	0.036	0.036	0.036	0.036	0.036	0.036	0.036	0.040
2	0.106	0.200	0.200	0.144	0.144	0.048	0.036	0.036	0.036	0.036	0.036	0.036	0.036	0.036	0.036	0.040
1	0.106	0.096	0.200	0.144	0.144	0.048	0.048	0.036	0.036	0.036	0.036	0.036	0.036	0.036	0.036	0.040

TABLE 7.4

TALLAHALA CREEK AT STATE HIGHWAY 528 NEAR BAY SPRINGS, MISSISSIPPI
FLOOD OF APRIL 14, 1969
COMPUTED FLOW DISTRIBUTION
(COMPUTED NORMALIZED STREAM FUNCTION)

I	J=1	J=2	J=3	J=4	J=5	J=6	J=7	J=8	J=9	J=10	J=11	J=12	J=13	J=14	J=15	J=16
31	0.000	0.023	0.050	0.079	0.108	0.137	0.171	0.230	0.302	0.383	0.472	0.543	0.615	0.659	0.735	1.000
30	0.000	0.019	0.048	0.082	0.108	0.134	0.176	0.215	0.299	0.383	0.469	0.548	0.618	0.664	0.759	1.000
29	0.000	0.024	0.046	0.083	0.120	0.156	0.195	0.265	0.347	0.424	0.511	0.592	0.651	0.701	0.778	1.000
28	0.000	0.029	0.059	0.097	0.134	0.174	0.230	0.301	0.413	0.493	0.568	0.630	0.673	0.711	0.864	1.000
27	0.000	0.030	0.069	0.108	0.146	0.202	0.261	0.360	0.444	0.521	0.608	0.679	0.724	0.806	0.918	1.000
26	0.000	0.039	0.081	0.127	0.176	0.231	0.295	0.362	0.475	0.547	0.671	0.754	0.813	0.887	0.944	1.000
25	0.000	0.045	0.099	0.145	0.199	0.256	0.306	0.361	0.451	0.597	0.688	0.757	0.817	0.874	0.937	1.000
24	0.000	0.051	0.117	0.171	0.220	0.285	0.327	0.382	0.438	0.513	0.660	0.766	0.812	0.879	0.938	1.000
23	-0.000	0.060	0.117	0.176	0.228	0.290	0.336	0.380	0.435	0.531	0.592	0.738	0.801	0.867	0.950	1.000
22	0.000	0.044	0.116	0.181	0.242	0.297	0.338	0.378	0.420	0.477	0.565	0.739	0.785	0.843	0.945	1.000
21	0.000	0.027	0.098	0.175	0.239	0.293	0.339	0.372	0.408	0.455	0.542	0.695	0.805	0.845	0.924	1.000
20	0.000	0.031	0.086	0.147	0.220	0.269	0.327	0.362	0.425	0.499	0.585	0.740	0.833	0.882	0.934	1.000
19	0.000	0.001	0.057	0.119	0.164	0.234	0.305	0.365	0.428	0.511	0.620	0.713	0.829	0.902	0.997	1.000
18	0.000	0.000	0.060	0.106	0.277	0.422	0.512	0.575	0.622	0.668	0.711	0.755	0.811	0.872	0.924	1.000
17	0.000	0.079	0.184	0.288	0.416	0.530	0.590	0.638	0.680	0.722	0.761	0.803	0.847	0.896	0.947	1.000
16	0.000	0.145	0.307	0.426	0.535	0.631	0.685	0.746	0.769	0.795	0.823	0.853	0.882	0.915	0.938	1.000
15	0.000	0.095	0.192	0.306	0.427	0.529	0.700	0.755	0.794	0.827	0.866	0.904	0.934	0.955	0.973	1.000
14	0.000	0.043	0.198	0.353	0.526	0.683	0.715	0.763	0.808	0.851	0.895	0.929	0.944	0.964	0.982	1.000
13	0.000	0.048	0.182	0.349	0.531	0.624	0.717	0.771	0.814	0.856	0.902	0.922	0.939	0.956	0.979	1.000
12	0.000	0.036	0.180	0.309	0.449	0.592	0.711	0.762	0.810	0.854	0.879	0.898	0.920	0.953	0.981	1.000
11	0.000	0.045	0.154	0.284	0.409	0.518	0.660	0.746	0.803	0.834	0.865	0.891	0.919	0.943	0.976	1.000
10	0.000	0.028	0.144	0.267	0.406	0.521	0.645	0.730	0.801	0.827	0.860	0.889	0.918	0.945	0.975	1.000
9	0.000	0.032	0.135	0.271	0.417	0.509	0.629	0.726	0.794	0.821	0.850	0.889	0.919	0.950	0.976	1.000

TABLE 7.4 CONTINUED

TALLAHALA CREEK AT STATE HIGHWAY 528 NEAR BAY SPRINGS, MISSISSIPPI
FLOOD OF APRIL 14, 1969
COMPUTED FLOW DISTRIBUTION
(COMPUTED NORMALIZED STREAM FUNCTION)

I	J=1	J=2	J=3	J=4	J=5	J=6	J=7	J=8	J=9	J=10	J=11	J=12	J=13	J=14	J=15	J=16
8	0.000	0.022	0.128	0.270	0.380	0.482	0.576	0.653	0.734	0.806	0.849	0.891	0.928	0.959	0.983	1.000
7	0.000	0.034	0.086	0.258	0.384	0.468	0.556	0.610	0.704	0.770	0.839	0.889	0.938	0.958	0.986	1.000
6	0.000	0.047	0.178	0.298	0.393	0.466	0.529	0.593	0.671	0.753	0.830	0.895	0.938	0.958	0.986	1.000
5	0.000	0.155	0.239	0.301	0.373	0.443	0.512	0.591	0.668	0.732	0.824	0.881	0.928	0.951	0.981	1.000
4	0.000	0.107	0.169	0.228	0.289	0.359	0.454	0.522	0.596	0.667	0.771	0.851	0.899	0.935	0.966	1.000
3	0.000	0.062	0.107	0.143	0.175	0.221	0.341	0.423	0.500	0.601	0.717	0.796	0.880	0.928	0.962	1.000
2	0.000	0.059	0.083	0.103	0.119	0.135	0.238	0.304	0.390	0.477	0.587	0.716	0.815	0.889	0.952	1.000
1	0.000	0.074	0.092	0.105	0.115	0.132	0.245	0.323	0.375	0.442	0.535	0.664	0.765	0.863	0.960	1.000

TABLE 7.5

TALLAHALA CREEK AT STATE HIGHWAY 528 NEAR BAY SPRINGS, MISSISSIPPI
FLOOD OF APRIL 14, 1969
COMPUTED WATER LEVELS
(FEET ABOVE MEAN SEA LEVEL)

I	J=1	J=2	J=3	J=4	J=5	J=6	J=7	J=8	J=9	J=10	J=11	J=12	J=13	J=14	J=15	J=16
31	314.09	313.85	313.89	313.93	313.98	313.91	313.98	313.96	313.98	313.70	313.93	313.63	313.92	313.89	313.41	314.05
30	313.68	313.41	313.45	313.50	313.55	313.53	313.47	313.55	313.51	313.17	313.50	313.06	313.48	313.42	313.16	313.63
29	313.47	313.10	313.19	313.25	313.34	313.29	313.32	313.26	312.95	312.86	313.04	313.05	313.14	313.01	313.27	313.35
28	313.21	312.78	312.98	312.96	313.05	312.99	313.02	312.92	312.53	312.72	312.48	312.87	312.74	312.82	313.23	313.13
27	312.99	312.47	312.72	312.81	312.81	312.86	312.89	312.61	312.55	312.44	312.63	312.56	312.80	313.10	313.22	312.94
26	312.80	312.28	312.48	312.66	312.52	312.77	312.77	312.59	312.54	311.82	312.44	312.73	313.00	312.99	313.15	312.69
25	312.70	312.18	312.34	312.43	312.54	312.63	312.69	312.60	312.51	312.48	312.52	312.71	312.98	312.94	313.05	312.59
24	312.53	311.95	312.32	312.21	312.41	312.43	312.52	312.67	312.47	312.47	312.61	312.78	312.93	312.92	313.04	312.57
23	312.24	311.99	312.19	312.02	312.27	312.22	312.42	312.46	312.39	312.10	312.42	312.76	312.96	312.86	313.01	312.46
22	311.92	311.77	311.98	311.79	311.99	311.96	312.00	312.06	312.04	312.19	312.14	312.64	312.81	312.70	312.90	312.36
21	311.71	311.15	311.54	311.58	311.89	311.71	311.88	311.73	311.81	311.86	311.87	312.28	312.61	312.56	312.82	312.25
20	311.56	311.74	311.36	311.44	311.61	311.64	311.64	311.63	311.64	311.77	311.57	312.39	312.27	312.54	312.68	312.14
19	311.52	311.55	311.07	311.57	311.47	311.68	311.59	311.66	311.65	311.88	311.66	311.67	312.12	312.14	312.18	312.08
18	311.52	311.60	311.26	311.22	311.62	311.57	311.88	311.28	311.45	311.28	311.57	311.96	311.89	312.02	312.04	312.06
17	311.43	311.17	311.49	311.72	311.66	311.47	310.91	311.29	311.13	311.53	311.85	311.76	311.71	311.88	311.96	311.99
16	311.54	311.43	311.68	311.65	311.58	311.61	311.47	311.87	311.91	311.94	311.96	311.76	311.93	311.98	311.90	312.04
15	311.53	311.11	311.38	311.54	311.51	311.57	311.53	311.91	311.92	311.90	311.92	311.95	311.86	311.98	311.85	312.03
14	311.49	311.04	311.45	311.77	311.66	311.44	311.59	311.80	311.66	311.59	311.78	311.78	311.90	311.72	311.83	311.76
13	311.38	311.13	311.32	311.76	311.54	311.44	311.55	311.77	311.66	311.60	311.77	311.73	311.64	311.59	311.49	311.51
12	311.24	310.86	311.23	311.44	311.47	311.33	311.55	311.74	311.52	311.47	311.66	311.51	311.52	311.45	311.40	311.34
11	311.07	310.82	311.06	311.39	311.23	311.81	311.40	311.70	311.50	311.50	311.46	311.40	311.43	311.36	311.26	311.27
10	311.00	310.43	311.05	311.35	311.19	311.66	311.40	311.56	311.43	311.51	311.29	311.35	311.35	311.29	311.19	311.26
9	310.91	310.55	311.06	311.33	311.19	311.60	311.36	311.45	311.51	311.42	311.11	311.28	311.26	311.25	311.11	311.11

TABLE 7.5 CONTINUED

TALLAHALA CREEK AT STATE HIGHWAY 528 NEAR BAY SPRINGS, MISSISSIPPI
FLOOD OF APRIL 14, 1969
COMPUTED WATER LEVELS
(FEET ABOVE MEAN SEA LEVEL)

I	J=1	J=2	J=3	J=4	J=5	J=6	J=7	J=8	J=9	J=10	J=11	J=12	J=13	J=14	J=15	J=16
8	310.89	310.37	311.07	311.31	311.17	311.23	311.03	311.24	311.35	311.30	310.98	311.10	311.17	310.97	311.16	310.95
7	310.86	310.38	310.58	311.27	311.03	311.06	310.84	311.01	310.96	311.10	310.85	310.93	310.90	310.85	310.82	310.76
6	310.17	310.50	310.68	310.90	310.74	310.83	310.85	310.49	310.74	310.92	310.71	310.72	310.67	310.70	310.36	310.34
5	310.01	310.52	310.74	310.56	310.40	310.26	310.88	310.37	310.60	310.57	310.53	310.24	310.28	310.15	310.10	309.77
4	309.79	309.58	309.82	310.01	309.58	309.62	309.47	309.47	309.49	309.25	309.28	309.22	309.22	309.10	309.17	309.15
3	308.99	309.43	309.35	308.79	308.22	308.45	308.63	308.56	308.44	308.43	308.40	308.28	308.34	308.27	308.21	308.63
2	308.39	308.59	308.55	308.30	308.24	308.03	308.43	308.19	308.25	308.19	308.18	308.15	308.11	308.11	308.13	308.16
1	308.00	308.00	308.00	308.00	308.00	308.00	308.00	308.00	308.00	308.00	308.00	308.00	308.00	308.00	308.00	308.00

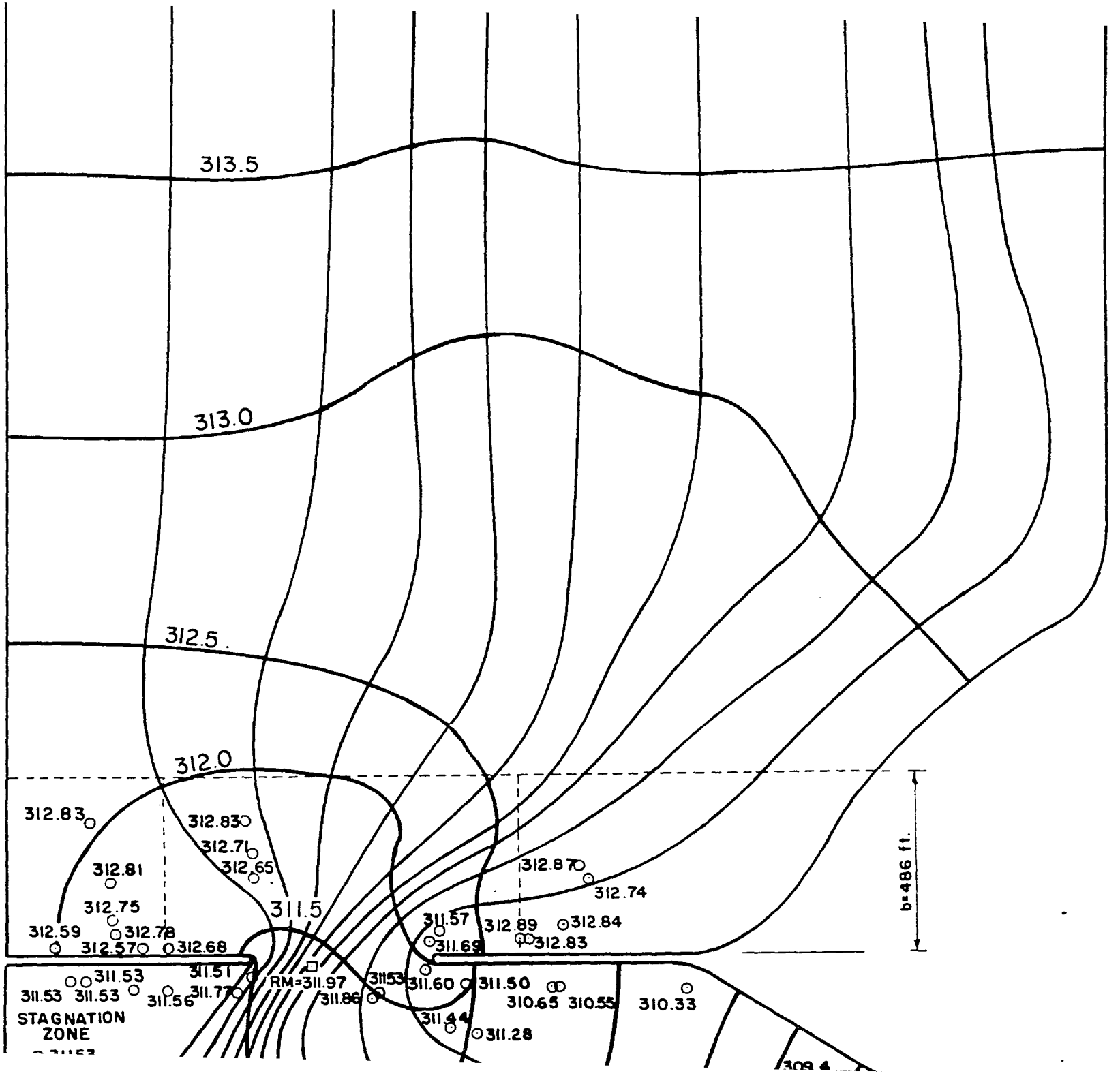
313.5
313.0
312.5
312.0
311.5
312.83
312.83
312.71
312.65
312.81
312.75
312.59
312.78
312.57
312.68
312.87
312.74
311.57
312.89
312.84
311.69
312.83
311.53
311.53
311.53
311.56
311.51
311.77
RM=311.97
311.86
311.53
311.60
311.50
310.65
310.55
310.33
311.44
311.28
STAGNATION ZONE
b=486 ft.

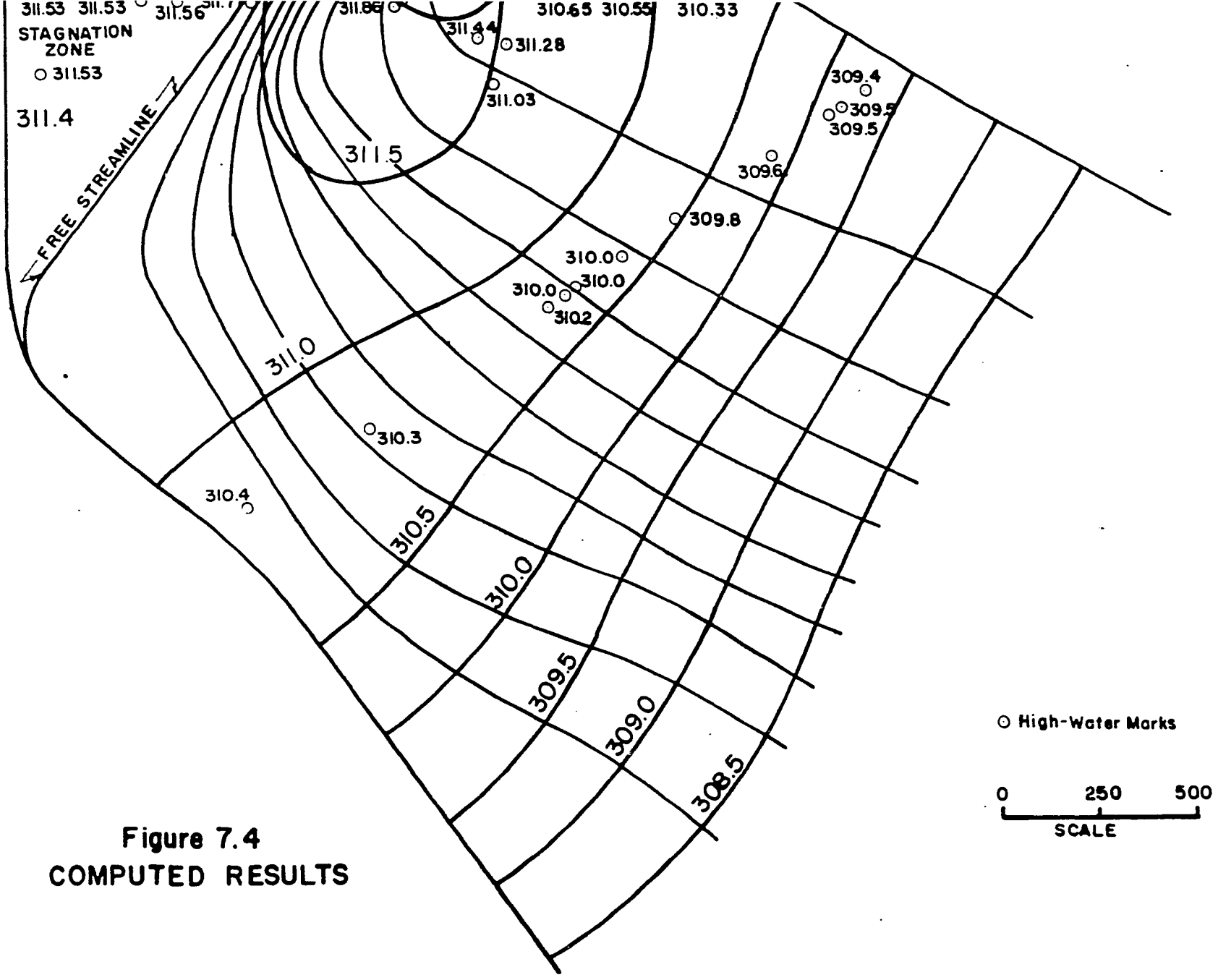

Figure 7.4
COMPUTED RESULTS

TALLAHALA CREEK AT STATE HIGHWAY 528 NEAR BAY SPRINGS, MISS.
Flood of April 14, 1969

sketched normal to the computed streamlines; where the flow is concentrated in the main channel the water level is allowed to increase (cf. figure 4.4). In every case the average computed water level (from table 7.5) on the sketched contours is the level shown on figure 7.4. Surveyed high-water marks are plotted on figure 7.4 for comparison with the computed results.

A stagnation zone is indicated in figure 7.4 downstream from the left embankment. The kinetic energy excess was computed as .54 feet while the head loss due to friction along the free streamline was computed as .57 feet. The necessary condition (6.3) for separation is thus approximated. Note that the stagnation zone is in open pasture (n = 0.04) (cf. figure 7.2). The data supports the possibility of a stagnation zone downstream from the right embankment; all high-water marks shown in the stagnation zone on figure 7.4 are of approximately the same elevation (313.53 feet). The computed water level in the stagnation zone is shown on figure 7.4 as 311.4 feet. That figure was obtained from the water-surface contours. The water-surface elevation in the stagnation zone must be constant.

Figure 7.5 compares computed and measured flow distributions at the bridge. The observed values were obtained from the discharge measurement. The cumulative percentage at a selected point on the contracted section is obtained by dividing the discharge between the right abutment and

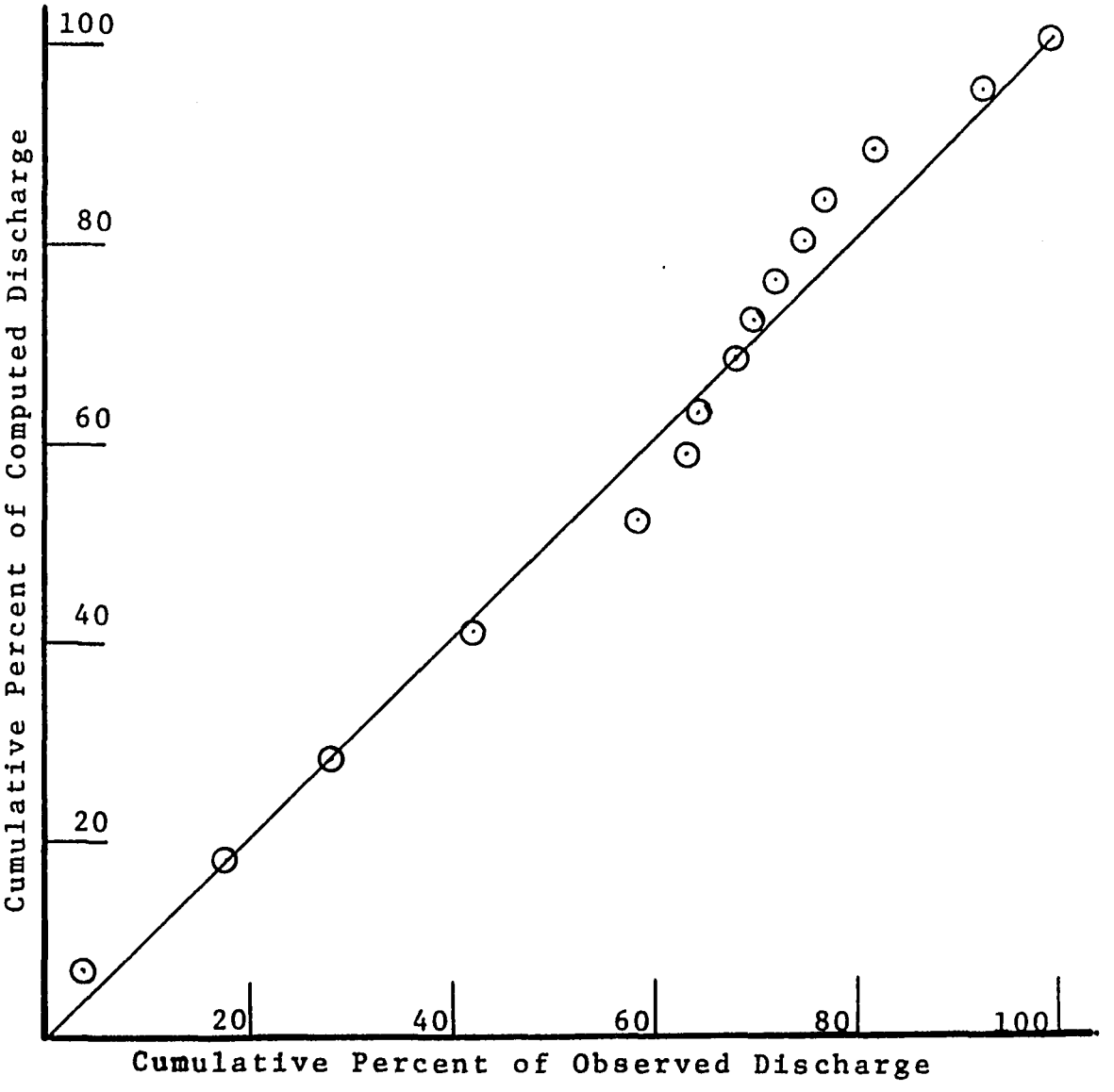

Figure 7.5 -- Comparison of Computed and Observed Flow Distributions at Tallahala Creek at State Highway 528 near Bay Springs, Mississippi, April 14, 1964

the selected point by the total discharge. That calculation is repeated for both the computed stream function and the actual discharge measured for several points on the contracted section.

7.3.2 Flood of April 6, 1964

A higher flood at Tallahala Creek at State Highway 528 near Bay Springs, Mississippi, was recorded on April 6, 1964. That flood overtopped the roadway of the left embankment. The USGS made a discharge measurement during the flood and surveyed high-water marks near the bridge after the flood.

The discharge measurement was made after the flood crested, 0.17 feet below the peak; the total measured discharge was 20015 cfs. Of the total discharge, ten percent was measured crossing the left embankment. The total discharge at the peak (22,000 cfs) was obtained from the station rating, and ten percent of that total (2,200 cfs) was assumed to cross the left embankment.

The stream function values at grid nodes adjacent to the left embankment were set by boundary condition in order to set the flow distribution on the overtopped embankment. Ten percent of the computed flow was forced to cross the embankment.

The hydraulic roughness coefficients used are tabulated in table 7.6. They are the same as those used for the flood of April 14, 1969, except for the value at node (I=18, J=16). Since the spur dike on the upstream side of the left embankment was not in place at the time of the earlier flood, it was not necessary to increase the roughness at that point. The ground-surface elevations used are the same as those for the flood of April 14, 1969 (cf. table 7.2).

The computed results are tabulated in tables 7.7 and

TABLE 7.6

TALLAHALA CREEK AT STATE HIGHWAY 528 NEAR BAY SPRINGS, MISSISSIPPI
FLOOD OF APRIL 6, 1964
HYDRAULIC ROUGHNESS COEFFICIENTS
(MANNING N-VALUES)

I	J=1	J=2	J=3	J=4	J=5	J=6	J=7	J=8	J=9	J=10	J=11	J=12	J=13	J=14	J=15	J=16
31	0.176	0.160	0.160	0.160	0.160	0.160	0.160	0.096	0.096	0.096	0.120	0.120	0.144	0.160	0.032	0.035
30	0.176	0.160	0.160	0.160	0.160	0.160	0.160	0.096	0.096	0.096	0.120	0.144	0.144	0.160	0.032	0.035
29	0.176	0.160	0.160	0.160	0.160	0.160	0.160	0.096	0.096	0.120	0.120	0.144	0.160	0.160	0.032	0.035
28	0.176	0.160	0.160	0.160	0.160	0.160	0.096	0.096	0.096	0.120	0.144	0.144	0.160	0.032	0.032	0.035
27	0.176	0.160	0.160	0.160	0.160	0.160	0.096	0.096	0.120	0.064	0.032	0.032	0.032	0.032	0.032	0.035
26	0.132	0.120	0.120	0.120	0.120	0.120	0.120	0.032	0.032	0.032	0.032	0.032	0.032	0.032	0.032	0.035
25	0.132	0.120	0.120	0.120	0.120	0.120	0.120	0.048	0.048	0.048	0.032	0.032	0.032	0.032	0.032	0.035
24	0.132	0.120	0.120	0.120	0.120	0.120	0.120	0.120	0.120	0.048	0.048	0.032	0.032	0.032	0.032	0.035
23	0.132	0.120	0.120	0.120	0.120	0.120	0.120	0.120	0.120	0.120	0.120	0.120	0.120	0.120	0.120	0.132
22	0.132	0.120	0.120	0.120	0.120	0.120	0.120	0.120	0.120	0.120	0.120	0.120	0.120	0.120	0.120	0.132
21	0.132	0.120	0.120	0.120	0.120	0.120	0.120	0.120	0.120	0.120	0.120	0.120	0.120	0.120	0.120	0.132
20	0.132	0.120	0.120	0.120	0.120	0.120	0.120	0.120	0.120	0.120	0.120	0.120	0.120	0.120	0.120	0.132
19	10.000	0.120	0.120	0.048	0.048	0.048	0.048	0.048	0.048	0.080	0.080	0.080	0.080	0.080	0.120	0.035
18	0.034	0.031	0.031	0.031	0.031	0.031	0.031	0.031	0.031	0.031	0.031	0.031	0.031	0.031	0.031	0.034
17	0.038	0.035	0.035	0.035	0.035	0.035	0.035	0.035	0.035	0.035	0.035	0.035	0.035	0.035	0.035	0.038
16	0.038	0.035	0.035	0.035	0.035	0.035	0.035	0.035	0.035	0.035	0.035	0.035	0.035	0.035	0.035	0.038
15	0.035	0.040	0.040	0.040	0.040	0.056	0.056	0.160	0.160	0.160	0.160	0.160	0.160	0.160	0.160	0.176
14	0.035	0.040	0.040	0.040	0.040	0.056	0.160	0.160	0.160	0.160	0.160	0.160	0.160	0.160	0.160	0.176
13	0.035	0.040	0.040	0.040	0.040	0.056	0.056	0.056	0.160	0.160	0.160	0.160	0.160	0.160	0.160	0.176
12	0.035	0.040	0.040	0.040	0.040	0.056	0.056	0.160	0.160	0.160	0.160	0.160	0.160	0.160	0.160	0.176
11	0.035	0.040	0.040	0.040	0.040	0.056	0.056	0.056	0.160	0.160	0.160	0.160	0.160	0.160	0.160	0.176
10	0.035	0.040	0.040	0.040	0.040	0.071	0.071	0.160	0.160	0.160	0.160	0.160	0.160	0.160	0.160	0.176
9	0.035	0.040	0.040	0.040	0.040	0.120	0.120	0.160	0.160	0.160	0.160	0.160	0.160	0.160	0.200	0.220

TABLE 7.6 CONTINUED

TALLAHALA CREEK AT STATE HIGHWAY 528 NEAR BAY SPRINGS, MISSISSIPPI
FLOOD OF APRIL 6, 1964
HYDRAULIC ROUGHNESS COEFFICIENTS
(MANNING N-VALUES)

I	J=1	J=2	J=3	J=4	J=5	J=6	J=7	J=8	J=9	J=10	J=11	J=12	J=13	J=14	J=15	J=16
8	0.035	0.040	0.040	0.040	0.040	0.120	0.106	0.106	0.160	0.160	0.160	0.160	0.160	0.200	0.200	0.220
7	0.035	0.032	0.032	0.032	0.160	0.120	0.120	0.160	0.160	0.160	0.160	0.160	0.177	0.200	0.200	0.220
6	0.078	0.035	0.032	0.160	0.120	0.120	0.120	0.120	0.120	0.160	0.160	0.160	0.200	0.200	0.200	0.132
5	0.088	0.080	0.160	0.160	0.120	0.120	0.120	0.120	0.160	0.160	0.160	0.177	0.200	0.200	0.120	0.132
4	0.101	0.142	0.160	0.160	0.120	0.120	0.120	0.160	0.160	0.160	0.160	0.200	0.200	0.142	0.120	0.132
3	0.106	0.200	0.200	0.191	0.144	0.056	0.036	0.036	0.036	0.036	0.036	0.036	0.036	0.036	0.036	0.040
2	0.106	0.200	0.200	0.144	0.144	0.048	0.036	0.036	0.036	0.036	0.036	0.036	0.036	0.036	0.036	0.040
1	0.106	0.096	0.200	0.144	0.144	0.048	0.048	0.036	0.036	0.036	0.036	0.036	0.036	0.036	0.036	0.040

7.8. Table 7.7 tabulates values of the computed normalized stream function and table 7.8 tabulates computed water levels. The values are tabulated for the nodes of the finite element grid which can be located by reference to figure 7.2.

Since the flow over the left embankment can be expected to be critical, the pressure equation (4.9) cannot be applied on computed streamlines that cross the embankment. Additional approximations are thus necessary for the application of algorithm 5.1 to the higher flood. Water levels were not computed for grid nodes in the region upstream from the left embankment that were on computed streamlines that crossed the embankment; water levels at those nodes were approximated by extrapolating the computed water levels at neighboring nodes on the water-level contour map (figure 7.6). The numerical entries are not tabulated in table 7.8 for those nodes. The water levels on figure 7.6 are to gage datum (265.43 feet above mean sea level).

The fall was measured by the USGS at the time of the discharge measurement (0.17 feet below flood peak). The water levels were marked at the downstream side of the abutments and on the upstream side of the embankment one bridge width from the abutments according to the field procedure discussed in section 1.2.2. That measured fall is reported by the BPR (1970, table B-2, p. 102) as 1.62 feet. The fall at the flood peak can be expected to be somewhat greater.

TABLE 7.7

TALLAHALA CREEK AT STATE HIGHWAY 528 NEAR BAY SPRINGS, MISSISSIPPI
FLOOD OF APRIL 6, 1964
COMPUTED FLOW DISTRIBUTION
(COMPUTED NORMALIZED STREAM FUNCTION)

I	J=1	J=2	J=3	J=4	J=5	J=6	J=7	J=8	J=9	J=10	J=11	J=12	J=13	J=14	J=15	J=16
31	0.000	0.023	0.050	0.079	0.108	0.136	0.171	0.229	0.302	0.382	0.472	0.543	0.615	0.658	0.735	1.000
30	0.000	0.019	0.048	0.082	0.108	0.134	0.175	0.215	0.299	0.382	0.468	0.547	0.617	0.663	0.759	1.000
29	0.000	0.024	0.046	0.082	0.119	0.155	0.194	0.264	0.346	0.423	0.510	0.591	0.650	0.700	0.778	1.000
28	0.000	0.028	0.058	0.095	0.132	0.172	0.228	0.299	0.407	0.491	0.566	0.629	0.672	0.710	0.864	1.000
27	0.000	0.029	0.067	0.106	0.143	0.198	0.257	0.356	0.440	0.518	0.606	0.678	0.723	0.805	0.917	1.000
26	0.000	0.037	0.078	0.123	0.170	0.224	0.288	0.356	0.470	0.542	0.667	0.750	0.810	0.885	0.943	1.000
25	0.000	0.043	0.095	0.139	0.191	0.246	0.295	0.349	0.438	0.586	0.677	0.746	0.808	0.866	0.931	1.000
24	0.000	0.048	0.111	0.163	0.210	0.271	0.312	0.365	0.420	0.493	0.640	0.743	0.790	0.857	0.921	1.000
23	-0.000	0.056	0.111	0.167	0.216	0.275	0.319	0.362	0.414	0.506	0.566	0.708	0.770	0.836	0.920	1.000
22	0.000	0.041	0.110	0.171	0.228	0.280	0.319	0.357	0.397	0.451	0.535	0.701	0.746	0.803	0.904	1.000
21	0.000	0.026	0.092	0.164	0.224	0.274	0.317	0.348	0.382	0.426	0.506	0.650	0.755	0.794	0.871	1.000
20	0.000	0.001	0.082	0.137	0.205	0.250	0.303	0.335	0.393	0.461	0.540	0.680	0.766	0.811	0.866	1.000
19	0.000	0.000	0.053	0.110	0.152	0.217	0.281	0.336	0.394	0.468	0.566	0.651	0.756	0.822	0.908	1.000
18	0.000	0.000	0.056	0.098	0.256	0.390	0.473	0.530	0.572	0.612	0.649	0.686	0.735	0.789	0.835	1.000
17	0.000	0.074	0.171	0.267	0.386	0.491	0.545	0.589	0.627	0.664	0.698	0.734	0.771	0.813	0.955	1.000
16	0.000	0.135	0.286	0.396	0.497	0.586	0.636	0.692	0.713	0.736	0.760	0.786	0.811	0.838	0.859	1.000
15	0.000	0.089	0.179	0.286	0.398	0.493	0.653	0.703	0.738	0.768	0.802	0.835	0.861	0.879	0.891	1.000
14	0.000	0.040	0.185	0.330	0.492	0.638	0.668	0.713	0.755	0.793	0.834	0.864	0.876	0.893	0.906	1.000
13	0.000	0.045	0.171	0.328	0.498	0.585	0.671	0.724	0.764	0.804	0.846	0.863	0.878	0.892	0.910	1.000
12	0.000	0.034	0.171	0.293	0.424	0.558	0.671	0.720	0.767	0.809	0.833	0.850	0.869	0.896	0.921	1.000
11	0.000	0.043	0.147	0.270	0.389	0.492	0.627	0.709	0.766	0.796	0.825	0.850	0.876	0.900	0.928	1.000
10	0.000	0.027	0.138	0.255	0.388	0.497	0.616	0.698	0.767	0.792	0.825	0.857	0.884	0.911	0.940	1.000
9	0.000	0.031	0.129	0.260	0.400	0.488	0.603	0.696	0.762	0.790	0.821	0.862	0.894	0.923	0.948	1.000

TABLE 7.7 CONTINUED

TALLAHALA CREEK AT STATE HIGHWAY 528 NEAR BAY SPRINGS, MISSISSIPPI
FLOOD OF APRIL 6, 1964
COMPUTED FLOW DISTRIBUTION
(COMPUTED NORMALIZED STREAM FUNCTION)

I	J=1	J=2	J=3	J=4	J=5	J=6	J=7	J=8	J=9	J=10	J=11	J=12	J=13	J=14	J=15	J=16
8	0.000	0.021	0.123	0.260	0.366	0.465	0.557	0.632	0.711	0.783	0.828	0.872	0.910	0.941	0.966	1.000
7	0.000	0.033	0.084	0.251	0.373	0.456	0.543	0.595	0.689	0.755	0.826	0.878	0.929	0.950	0.978	1.000
6	0.000	0.046	0.174	0.291	0.385	0.457	0.519	0.582	0.661	0.744	0.822	0.889	0.933	0.953	0.983	1.000
5	0.000	0.153	0.236	0.297	0.368	0.438	0.506	0.584	0.661	0.726	0.818	0.876	0.924	0.948	0.980	1.000
4	0.000	0.106	0.168	0.226	0.288	0.357	0.452	0.519	0.594	0.664	0.768	0.848	0.897	0.934	0.966	1.000
3	0.000	0.062	0.108	0.143	0.176	0.222	0.342	0.424	0.501	0.601	0.718	0.797	0.880	0.928	0.962	1.000
2	0.000	0.060	0.084	0.106	0.123	0.143	0.258	0.328	0.413	0.500	0.609	0.737	0.830	0.899	0.957	1.000
1	0.000	0.072	0.091	0.105	0.116	0.143	0.275	0.350	0.398	0.467	0.560	0.684	0.780	0.872	0.969	1.000

TABLE 7.8

TALLAHALA CREEK AT STATE HIGHWAY 528 NEAR BAY SPRINGS, MISSISSIPPI
FLOOD OF APRIL 6, 1964
COMPUTED WATER LEVELS
(FEET ABOVE MEAN SEA LEVEL)

I	J=1	J=2	J=3	J=4	J=5	J=6	J=7	J=8	J=9	J=10	J=11	J=12	J=13	J=14	J=15	J=16
31	315.62	315.36	315.52	315.61	315.71	315.63	315.73	315.90	315.92	315.56	315.86	315.75	316.07	316.06	315.49	323.79
30	315.13	314.86	315.02	315.15	315.28	315.24	315.26	315.42	315.44	314.99	315.42	315.28	315.69	315.60	315.55	323.79
29	314.88	314.51	314.74	314.90	315.08	315.02	315.14	315.16	314.88	314.92	315.09	315.44	315.56	315.22	315.29	323.80
28	314.57	314.18	314.59	314.61	314.77	314.79	314.88	314.82	314.64	314.67	315.12	315.23	315.13	314.96	315.23	323.83
27	314.31	313.88	314.37	314.34	314.58	314.69	314.76	314.65	314.60	314.68	315.13	315.02	314.99	315.07	319.27	323.86
26	314.10	313.76	314.18	314.48	314.40	314.64	314.67	314.65	314.50	314.55	315.00	315.33	314.99	315.89	320.43	323.87
25	313.98	313.76	314.08	314.27	314.41	314.52	314.58	314.67	314.57	315.11	314.96	315.30	314.95	315.04	319.82	320.44
24	313.75	313.59	314.25	314.12	314.34	314.43	314.47	314.59	314.50	314.44	315.26	315.24	315.01	315.72	319.39	323.86
23	313.43	313.70	314.13	314.00	314.25	314.29	314.37	314.46	314.42	314.50	315.04	314.96	315.05	314.87	319.32	323.85
22	313.23	313.39	313.98	313.85	314.06	314.13	314.09	314.24	314.17	314.20	314.60	314.84	315.08	314.76	317.51	323.82
21	313.09	312.76	313.52	313.72	313.97	313.96	314.00	314.10	313.95	313.96	314.38	314.70	314.94	314.67	315.09	320.36
20	312.82	313.19	313.33	313.55	313.71	313.81	313.78	313.85	313.78	313.82	313.66	314.33	314.43	314.48	314.63	320.29
19	312.76	312.90	312.84	313.65	313.62	313.77	313.80	313.91	313.80	313.75	313.51	313.60	314.24	313.93	317.87	320.17
18	312.75	312.98	313.16	313.17	313.81	313.67	313.71	313.39	313.19	313.39	313.48	313.66	314.08	313.88	313.70	318.52
17	312.69	313.07	313.64	314.07	313.82	313.51	312.81	313.08	313.21	313.21	313.65	313.95	313.78	313.72	313.61	318.25
16	312.98	313.53	313.93	313.79	313.85	313.51	313.60	313.75	313.81	314.00	314.03	313.79	313.76	313.62	313.61	318.46
15	312.90	313.07	313.34	313.70	313.54	313.65	313.56	313.77	313.98	313.80	313.70	313.59	313.59	313.49	313.48	318.33
14	312.79	312.78	313.46	313.81	313.68	313.59	313.41	313.69	313.91	313.66	313.49	313.37	313.38	313.34	313.34	316.86
13	312.65	312.96	313.34	313.78	313.70	313.25	313.37	313.71	313.79	313.52	313.30	313.35	313.24	313.19	313.20	315.87
12	312.50	312.45	313.22	313.48	313.44	313.34	313.42	313.64	313.64	313.44	313.32	313.15	313.20	313.09	313.09	314.65
11	312.39	312.47	313.01	313.52	313.19	313.60	313.47	313.56	313.59	313.41	313.24	313.04	313.06	312.99	312.95	314.22
10	312.35	312.09	312.99	313.46	313.14	313.49	313.36	313.49	313.48	313.36	313.18	313.01	312.89	312.91	312.75	313.67
9	312.30	312.19	313.00	313.45	313.15	313.40	313.22	313.39	313.48	313.25	313.16	312.93	312.77	312.83	312.55	313.34

TABLE 7.8 CONTINUED

TALLAHALA CREEK AT STATE HIGHWAY 528 NEAR BAY SPRINGS, MISSISSIPPI
FLOOD OF APRIL 6, 1964
COMPUTED WATER LEVELS
(FEET ABOVE MEAN SEA LEVEL)

I	J=1	J=2	J=3	J=4	J=5	J=6	J=7	J=8	J=9	J=10	J=11	J=12	J=13	J=14	J=15	J=16
8	312.29	312.02	313.05	313.44	313.22	313.18	312.97	313.22	313.18	313.17	312.91	312.76	312.65	312.40	312.28	312.63
7	312.27	312.06	312.37	313.37	313.04	312.93	312.76	312.83	312.85	313.01	312.74	312.38	312.29	312.29	312.12	312.20
6	311.75	312.18	312.62	312.88	312.66	312.70	312.94	312.34	312.68	312.77	312.54	312.13	311.95	312.01	311.63	311.49
5	311.54	312.38	312.64	312.45	312.26	312.11	312.72	312.22	312.46	312.34	312.27	311.68	311.56	311.47	311.37	311.05
4	311.24	310.95	311.56	311.78	311.40	311.37	311.26	311.15	311.20	310.95	310.95	310.71	310.59	310.48	310.51	310.47
3	310.40	310.88	310.78	310.45	310.17	310.33	310.33	310.32	310.23	310.23	310.21	310.07	310.09	310.05	310.00	310.12
2	310.06	310.21	310.22	310.04	310.14	309.91	310.27	310.03	310.08	310.06	310.05	310.02	309.98	309.99	309.98	309.94
1	309.90	309.90	309.90	309.90	309.90	309.90	309.90	309.90	309.90	309.90	309.90	309.90	309.90	309.90	309.90	309.90

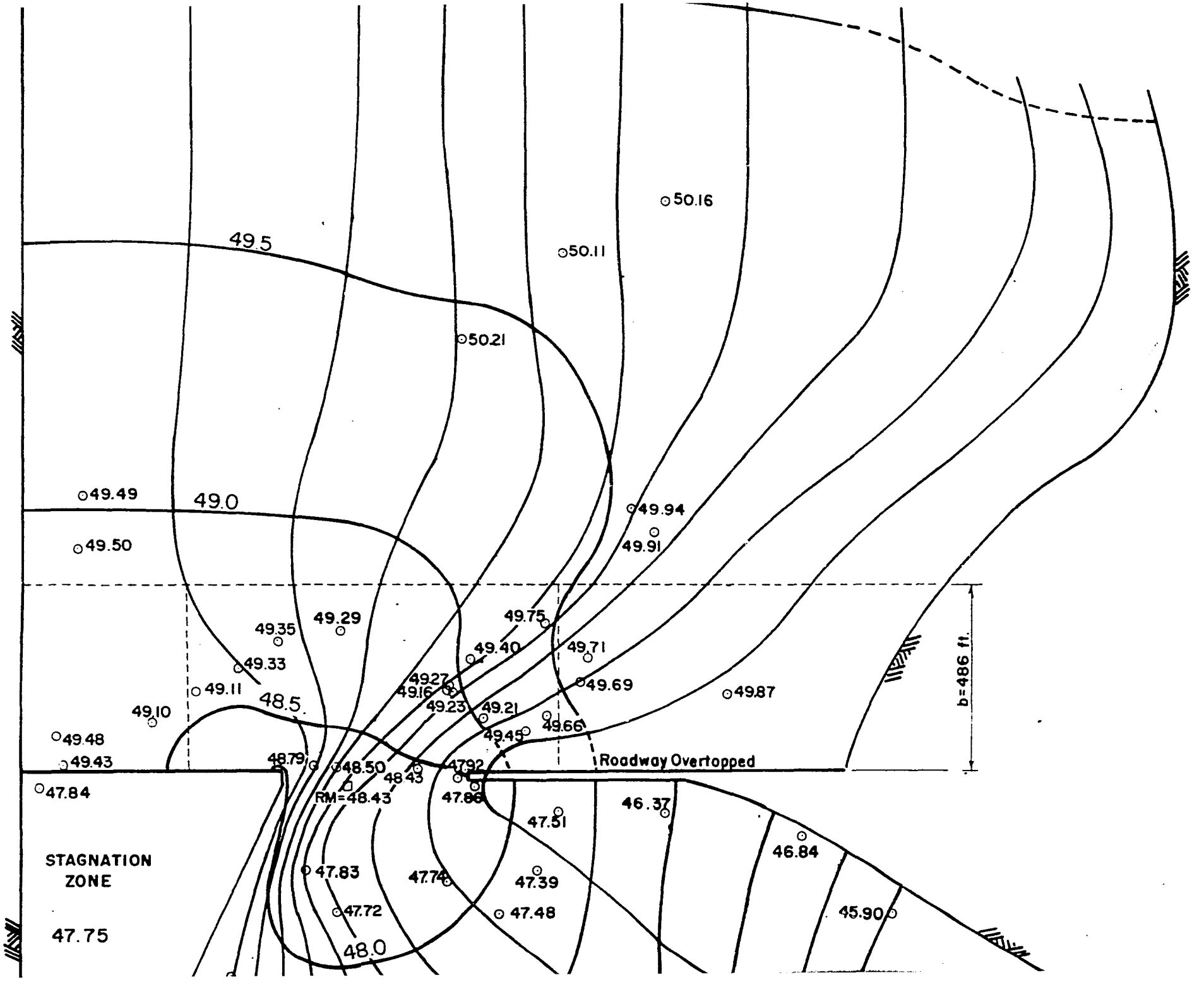
50.16
49.5
50.11
50.21
49.49
49.0
49.94
49.50
49.91
49.29
49.75
49.35
49.40
49.71
49.33
49.27
49.69
49.87
49.11
48.5
49.16
49.23
49.21
49.10
49.66
49.45
49.48
49.43
48.79
48.50
47.92
Roadway Overtopped
48.43
47.84
RM=48.43
47.86
46.37
47.51
46.84
STAGNATION
ZONE
47.83
47.74
47.39
47.72
47.48
45.90
47.75
48.0
b=486 ft.

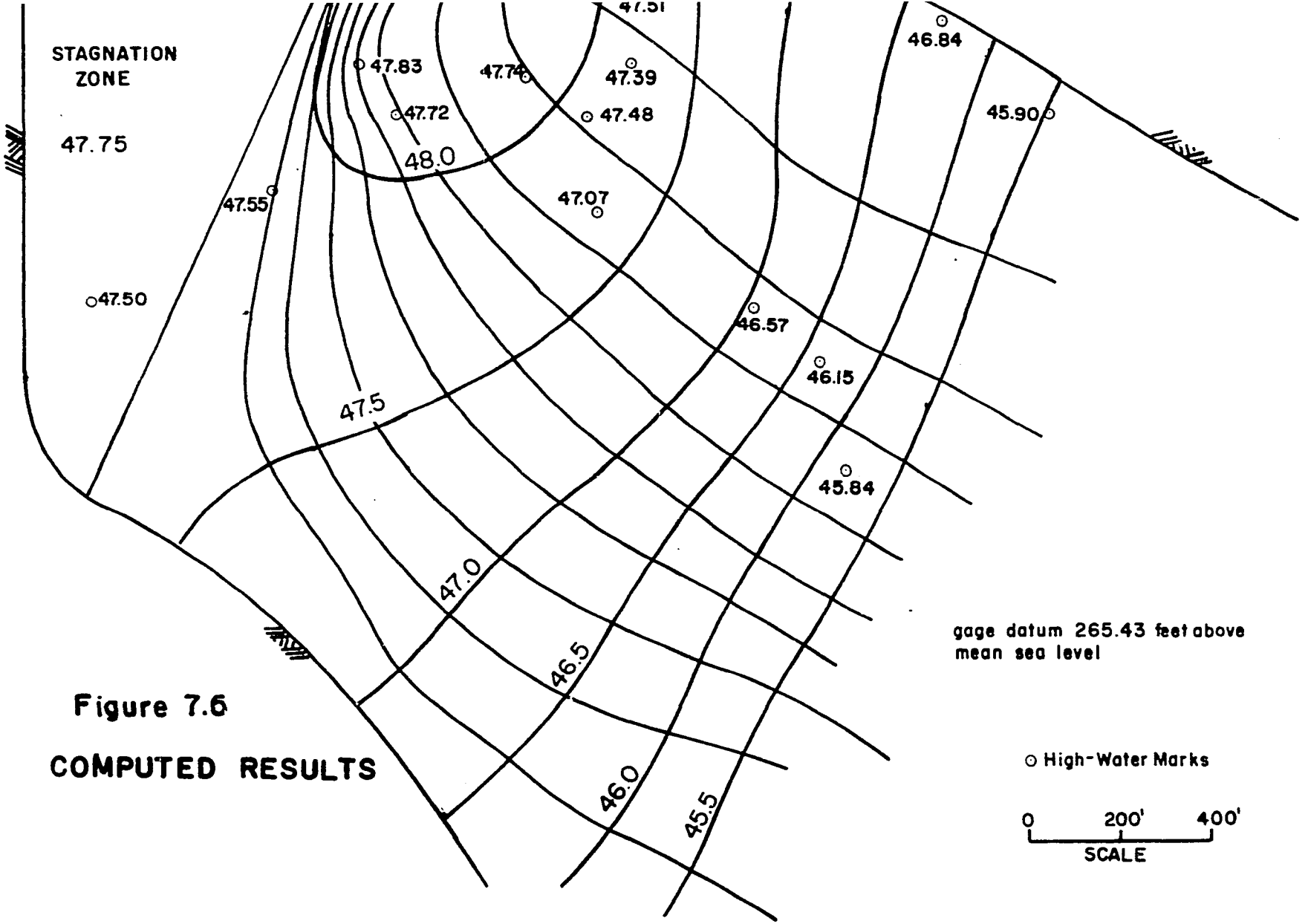

Figure 7.6

COMPUTED RESULTS

TALLAHALA CREEK AT STATE HIGHWAY 528 NEAR BAY SPRINGS, MISSISSIPPI
Flood of April 6, 1964

The high-water marks shown on figure 7.6 support the higher computed water levels upstream from the left embankment as compared with the levels upstream from right embankment (see figure 7.6). That configuration is also typical of the computed water levels shown on figure 7.4 for the flood of April 14, 1969; the high-water marks for that flood do not support that water-level differential.

7.3.3 Computed Fall (Δh)

The difference in water level across the approach embankment Δh was defined in section 1.2.2.2 and its importance as an objective index for verification work was discussed. Two different definitions were given. The first was that used by the BPR and was based on the water level at the channel centerline on section (3) (cf. figure 1.2) as a measure of water level on the downstream side of the embankment. The second was based on the field procedure for measuring fall during floods; it used the average of the water levels at the abutments of the bridge as a measure of downstream water level.

The computed water surface shown in figures 7.4 and 7.6 are not characterized by the descriptions of typical water-surface configuration of the BPR (1970, p. 25) or of Kindsvater, Carter and Tracy (1953, p. 4) (cf. section 1.2.2). Referring to the schematic diagram of figure 1.2, the average computed water level on the region AEFG is not the same as the average computed water level on the region ABCD; the computed water levels are not constant on those

two regions as postulated in section 1.2.2; there is no stagnation zone or corresponding pool water level downstream from the left embankment; and the computed flow distribution indicates a significant angle of flow with the contracted section.

The writer suggests that an appropriate value to assign to the computed fall for comparison with observed fall on the basis of the field practice definition would be the difference between the average computed water level on the region ABCD (cf. figure 1.2) upstream from the left embankment and the computed stagnation water level downstream from the right embankment. The comparison of a computed water level on the region upstream from the left embankment with the stagnation water level downstream from the right embankment is justified by the eccentricity of the computed flow distribution. Those two regions are the only regions where the pool water levels emphasized in the definitions of fall (cf. section 1.2.2) are approximated. The calculations are summarized in table 7.9.

Another value for the computed fall appropriate to the BPR definition could be obtained by comparing the average water level on the approach section (1) with the centerline water level on the contracted section (3) (cf. figure 1.2). That value might seem more objective since it more nearly represents the nominal fall postulated by the BPR definition (BPR, 1970) (cf. section 1.2.2) even though it is based on a computed water surface that is not characteristic

Table 7.9
Comparison of Computed and Observed
Fall Based on the Field Practice Definition

April 14, 1969

Water Level	Computed	Observed
Upstream from left embankment.....	312.6	312.85
Stagnation zone downstream from right embankment.....	311.4	311.54
Average of left and right abutments.....	____	311.55
Fall (Δh)	1.2	1.3

April 6, 1964

Upstream from left embankment.....	49.6	49.5
Stagnation zone downstream from right embankment.....	47.75	47.8
Fall (Δh).....	1.85	1.7
Fall measured during flood 0.17 feet below crest.....		1.62

of the BPR typical water-surface configuration as discussed above. The calculations are summarized in table 7.10.

Table 7.10

Comparison of Computed and Observed
Fall Based on BPR Definition

April 14, 1969

Water Level	Computed	Observed
Average at section (1).....	312.3	312.85
Reference Mark (RM).....		311.97
Centerline Section (3).....	311.5	———
Fall (Δh).....	0.8	0.88

April 6, 1964

Average at section (1).....	49.15	49.7
Reference Mark.....		48.43
Centerline.....	48.2	———
Fall (Δh).....	0.95	1.3

7.4 Computed Vorticity

The calculations were all performed with the material derivative of vorticity $D\zeta/Dt$ (cf. equation 5.12) assumed to be zero. The vorticity was then computed on each element of the finite element grid system using equation (5.19). The values for computed vorticity did not differ significantly from zero.

The material derivative $D\zeta/Dt$ represents changes in angular velocity of the fluid elements. Since the rotational motion of the fluid is caused by viscous forces generated at the channel bottom G and solid boundaries ∂D_1 and ∂D_2, it is not surprising that angular momentum of the fluid is dominated by the surface forces that generate it. Indeed the classical argument for the symmetry of the viscous stress tensor is based on the dominance of surface forces over body forces. Surface area of a fluid element is related to the square of a characteristic dimension for the element while volume is related to the cube of the characteristic dimension. As the characteristic dimension approaches zero the body forces which are related to the volume of the element are dominated by surface forces which are related to surface area (Pao, 1967, p. 37).

For these reasons the material derivative $D\zeta/Dt$ will probably always be approximately zero. Equation (3.13) could then be represented by the homogeneous relationship:

$$\text{Curl } \underline{F} \simeq 0 \tag{7.1}$$

The vorticity should always be computed, however, to check on the assumption.

Even though the vorticity is small, the conclusion that it is zero should be avoided. The computed flow distribution shown in figures 7.4 and 7.6 are very different from the potential flow distribution. To assume a potential flow distribution would be a serious error. A significant change in flow distribution can be associated with a very small vorticity. The angular momentum associated with that small vorticity can be insignificant.

8. CONCLUSIONS

For the steady gradually varied subcritical flow of a fully developed turbulent boundary layer, the Bernoulli equation on a two-dimensional streamline equation (4.9) is an itegral identity of the Euler momentum equation; it is valid even along streamlines that pass through the contraction. Hydrostatic pressure distribution is specified by the definition of gradually varied flow.

Techniques for computing water levels in natural channels by the numerical solution of the Bernoulli equation are currently available (e.g., step backwater). For two-dimensional flow, however, the two-dimensional streamlines must be accurately located before the water levels can be computed. The Bernoulli equation is not independent of path in a rotational flow field; it can only be used among points that lie on the same streamline.

The finite element technique developed by Zienkiewicz (1970) for computing the deflections of an elastic membrane can be used to locate the two-dimensional streamlines. The stream function specifies the two-dimensional flow distribution and the level curves (contours) of the stream function are the two-dimensional streamlines along which the Bernoulli equation can be applied. The differential equation of motion which governs the flow distribution has a form similar to that of the unloaded elastic membrane

equation (cf. equation 3.13) (i.e., the homogeneous "quasi-harmonic" partial differential equation). The values of the stream function correspond to the membrane deflections, and a coefficient which is a function of channel conveyance and magnitude of velocity corresponds to the membrane stiffness coefficient in the membrane analogy. The boundary conditions are specified as forced deflections at the edges of the membrane.

Field data collected by the USGS at Tallahala Creek at State Highway 528 near Bay Springs, Mississippi, are characterized as follows: 1) above normal water levels downstream from the contracted section; 2) the absence of separation downstream from the left approach embankment; and 3) estimated backwater five times as great as the value that would be predicted by empirical techniques currently used by the USGS and the BPR. The mathematical model developed in this dissertation can explain each.

The contraction causes increased velocities and increased lengths of streamlines in both the regions upstream and downstream from the contracted section; head loss due to friction along those streamlines is increased accordingly (cf. equation 4.9). Unless the flow is critical at some point on a streamline, the increased friction losses will result in above normal water levels both upstream and downstream from the contracted section.

A necessary condition for separation is that the

velocity head at the point of separation exceed the total head loss due to friction along the free streamline (cf. equation 6.3). If the velocity head on the free streamline is not sufficient to balance head loss due to friction on the free streamline then the Bernoulli equation on the free streamline (cf. equation 4.9) requires a change in water level somewhere on the free streamline. But the free streamline is the boundary of the stagnation zone and the water level must be constant on the stagnation zone. Such water level fluctuations on the free streamline would thus result in discontinuities in the hydrostatic pressure distribution (cf. equation 4.2). Such discontinuities would result in forces that could not be supported by the fluid.

The necessary condition for separation can be used to predict the absence of separation. The absence of separation is associated with a flow distribution that can damage the downstream side of an earthen highway embankment. The necessary condition for separation thus provides important design information. Where hydraulic roughness is large in the expansion zone downstream from a contraction and friction loss is expected to be great, separation should not be expected.

Comparison of computed and measured values of fall Δh (cf. tables 7.9 and 7.10) indicate that the finite element model can predict the large contraction losses that

currently used empirical techniques seriously underestimate.

Additional data is needed to completely verify that algorithm 5.1 computes the proper flow distribution over the entire two-dimensional region near the contracted section. High-water marks and ground-surface elevations are needed over a region subtended by one valley width upstream and one valley width downstream of the contracted section.

The writer suggests that the testing of equations 4.9 and 7.1 (equation 4.9) under conditions of steady gradually varied turbulent flow might be valid subjects for laboratory hydraulic model studies. Once verified the equations would become the basis for an extension of the theory to field prototypes. This approach would be more valid than the presently used approach of comparing the field prototypes directly to small scale models. The latter exagerates the effects of viscosity (cf. section 1.1) while the suggested approach merely tests a general hypothesis which when verified could be applied generally through mechanics.

There has been no experimental investigation of the two-dimensional nature of hydraulic roughness. Low values of roughness are usually assigned in main channels passing through wooded areas. But if the flow at flood stage is not directed along the channel then the low value is not

justified. Zienkiewicz's (1970) general linear "quasi-harmonic" partial differential equation admits an anisotropic conductance which could easily be adopted to an anisotropic channel resistance C_f in equation (5.3). More extensive field surveys would be required, however, and the added effort would have to be justified economically.

The accuracy of the finite element solution procedure used by algorithm 5.1 can be improved by the use of quadratic elements; the form of the interpolating function (5.5) can be changed to one of the following:

$$\phi_e = \alpha_1 x + \alpha_2 y + \alpha_3 xy + \alpha_4 \tag{8.2a}$$

$$\phi_e = \alpha_1 x + \alpha_2 y + \alpha_3 x^2 + \alpha_4 y^2 + \alpha_5 \tag{8.2b}$$

$$\phi_e = \alpha_1 x + \alpha_2 y + \alpha_3 xy + \alpha_4 x^2 + \alpha_5 y^2 + \alpha_6 \tag{8.2c}$$

The forms (8.2) are associated with elements that have four, five, and six degrees of freedom respectively; the linear form (5.5) has three degrees of freedom. There must be one information node for each degree of freedom associated with each element. The increased number of parameters would increase the order of equations (5.8), but larger quadratic elements would make the same accuracy obtainable with a smaller number of elements as

compared with the linear elements. Zienkiewicz (1970) suggests an element based on equation (8.2c) with six information nodes chosen at the vertices and midpoints.

BIBLIOGRAPHY

Albertson, M. L. et. al., 1950, Diffusion of Submerged Jets, Transactions, ASCE, Vol. 115, p. 639.

Anderson, D. G., and Anderson, W. C., 1964, Computation of Water-Surface Profiles in Open Channels, U.S. Geological Survey, Surface-Water Techniques, Book 1, Chapter 1.

Barnes, Harry H., Jr. 1967, Roughness Characteristics of Natural Channels, U.S. Geological Survey Water-Supply Paper 1849, Washington, D. C., U.S. Government Printing Office.

Bureau of Public Roads, 1970, Hydraulics of Bridge Waterways, reported by Joseph H. Bradley, Hydraulic Design Series No. 1, Washington, D. C., U.S. Government Printing Office, 111 pp.

Chow, Ven Te, 1959, Open Channel Hydraulics, New York, McGraw Hill.

Dennis, S. C. and Chang, Cav-Zu, 1969, Numerical Integration of the Navier-Stokes Equations in Two-Dimensions, University of Wisconsin, Mathematics Research Center, Madison, Wisconsin.

Eichert, Bill S., 1970, Survey of Programs for Water-Surface Profiles, Journal of the Hydraulics Division, ASCE, Vol. 96, No. HY2, Proc. Paper 7098, p. 547-563.

Janssen, Earl, 1956, I. An Analogue Model for Solving the Hydrodynamic Equations for Two Dimensional Viscous Flow. II. Application of the Method to the Case of Flow Past a Flat Plate, University of California, Los Angeles dissertation, Los Angeles, California.

Kindsvater, C. E., and Carter, R. W., 1955, Tranquil Flow Through Open Channel Constrictions, Transactions, ASCE, Vol. 120, p. 955.

Kindsvater, C. E., Carter, R. W., and Tracy, H. F., 1953, Computation of Peak Discharge at Contractions, U.S. Geological Survey Circular 284, Washington, D. C., 35 p.

Landau, L. D. and Lifshitz, E. M., 1959, Fluid Mechanics, Reading Massachusetts, Addison-Wesley Publishing Company, Inc. p. 396-398.

Laursen, E. M., 1970, Bridge Backwater in Wide Valleys, Journal of the Hydraulics Division, ASCE, Vol. 96, No. HY4, Proc. Paper 7246.

Macagno, E. O., and Hung, Tin-Kan, 1970, Computational Study of Accelerated Flow in a Two-Dimensional Conduit Expansion, University of Iowa, Iowa City, Iowa.

McCain, J. F., 1970, Study of Hydraulic Computation Methods for Bridge Sites, Buttahatchee River near Henson Springs, Alabama, U.S. Geological Survey Administrative Report, University, Alabama.

Pao, Richard H. F., 1967, Fluid Dynamics, Columbus, Ohio, Charles E. Merrill Books, Inc.

Tracy, H. J. and Carter, R. W., 1955, Backwater Effects of Open-Channel Constrictions, Transactions, ASCE, Vol. 120, p. 793.

U.S. Geological Survey, 1955, Computation of Backwater at Open-Channel Constrictions, Open File Report.

Zienkiewicz, O. C., 1970, The Finite Element Method in Structural and Continuum Mechanics, New York, McGraw-Hill, Chapters 3 and 10.

Vita

John Thomas Franques, Jr. was born in Baton Rouge, Louisiana on March 16, 1942. He received the Bachelor of Science degree in Civil Engineering at Louisiana State University in 1965. He worked with the Louisiana Department of Highways while completing his undergraduate work.

Shortly after graduation in 1966 he joined the U.S. Geological Survey, Water Resources Division, in Baton Rouge, Louisiana. There he received formal and practical training in the three hydrologic disciplines: surface water hydrology, ground water hydrology, and quality of water hydrology. While with the USGS he attended graduate school at Louisiana State University at night.

In 1968 he received the Master of Science degree in Civil Engineering at Louisiana State University. He then returned to graduate school on a full time basis to complete doctoral course work. His pre-doctoral research was supported by graduate research assistantships under contract between Louisiana State University and the Air Force Armament Laboratory, Eglin Air Force Base, Florida.

In 1970 he completed course work and began dissertation research under the sponsorship of the U.S. Geological Survey through the Water Resources Division thesis and dissertation support program. Dr. R. A. Baltzer, Arlington, Virginia served as Division Scientific Advisor. The USGS sponsorship was prompted by a practical need for a reliable

technique for predicting backwater at highway bridges in the wide valleys of the southern states.

EXAMINATION AND THESIS REPORT

Candidate: John Thomas Franques, Jr.

Major Field: Civil Engineering

Title of Thesis: A Finite Element Model for Two-Dimensional Steady Flow Through Contractions in Natural Channels.

Approved:

Major Professor and Chairman

Dean of the Graduate School

EXAMINING COMMITTEE:

Date of Examination:

September 21, 1971